

2022 IUEP Theory Meeting for Future Colliders
2022. 1. 8.

New Physics **@ ep collider**

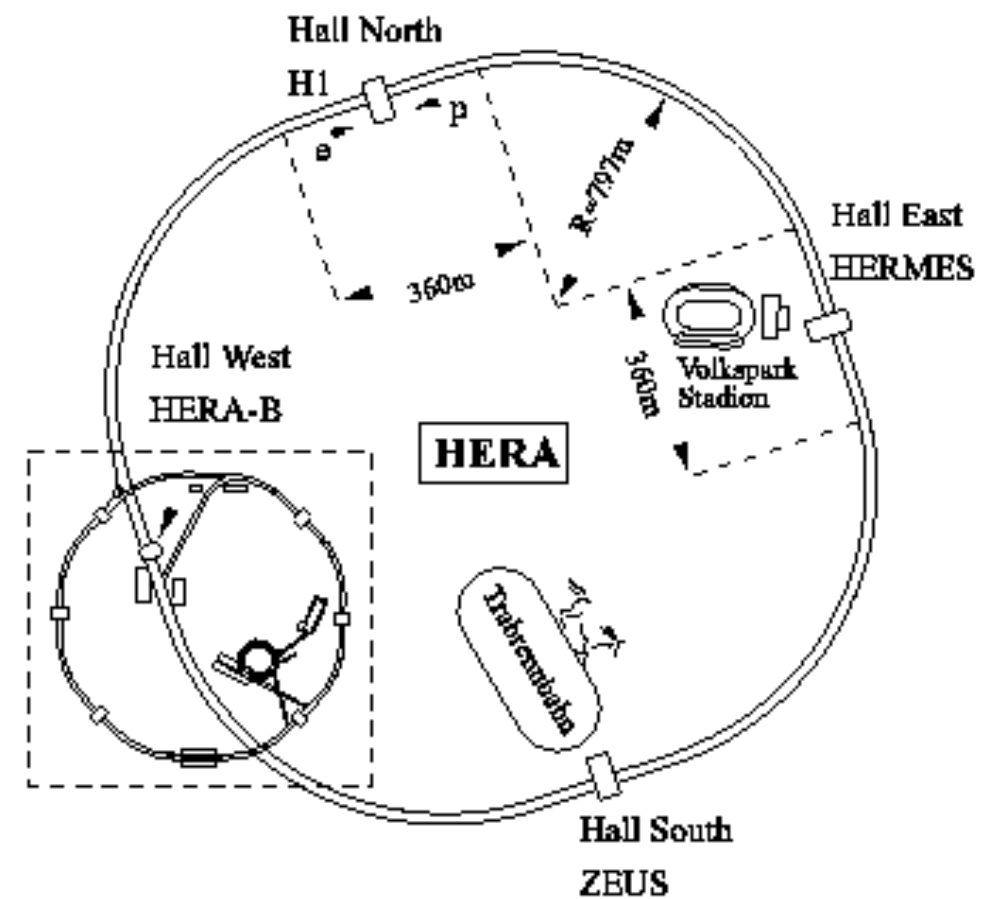
Jeonghyeon Song
(Konkuk University, Korea)

w/ A. Jueid, J. Kim, S. Lee, PLB 819 (2021) 136417

**1. LHeC, very possible in
the near future**

e-p collider: proton substructure

HERA (construction from 1984 to 1992)



- $E_e = 27.5 \text{ GeV}$, $E_p = 920 \text{ GeV} \implies \sqrt{s} \simeq 0.3 \text{ TeV}$

Next ep collider design?

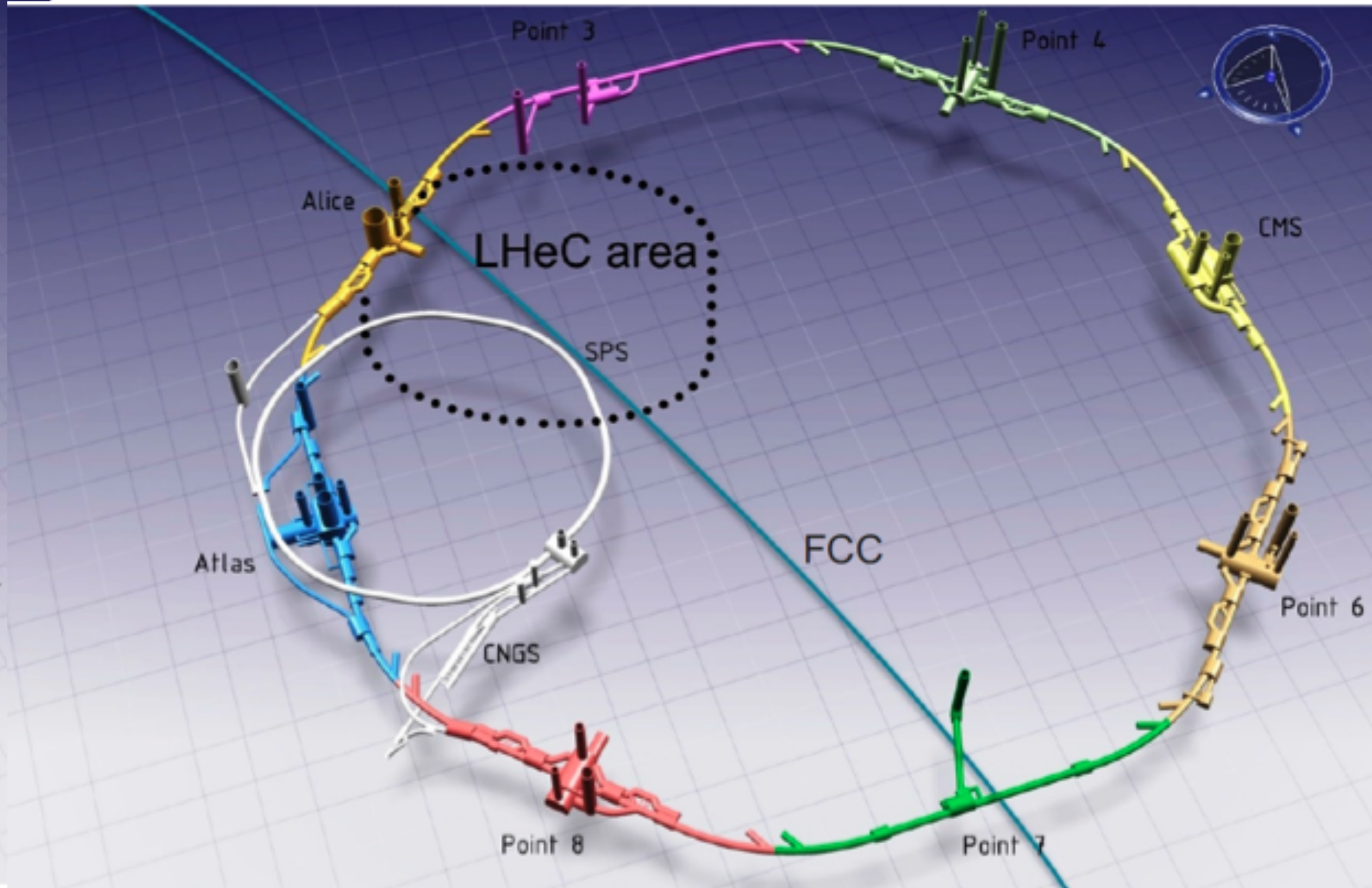
- the need for higher energy
- the need for much higher luminosity

Next ep collider design?

- the need for higher energy
- the need for much higher luminosity

LHeC: the most feasible!

1. LHeC



First CDR in 2012

CERN-OPEN-2012-015
LHeC-Note-2012-002 GEN
Geneva, June 13, 2012



A Large Hadron Electron Collider at CERN

Report on the Physics and Design
Concepts for Machine and Detector

LHeC Study Group

CDR in 2020 : 2007.14491

CERN-ACC-Note-2020-0002
Geneva, July 28, 2020

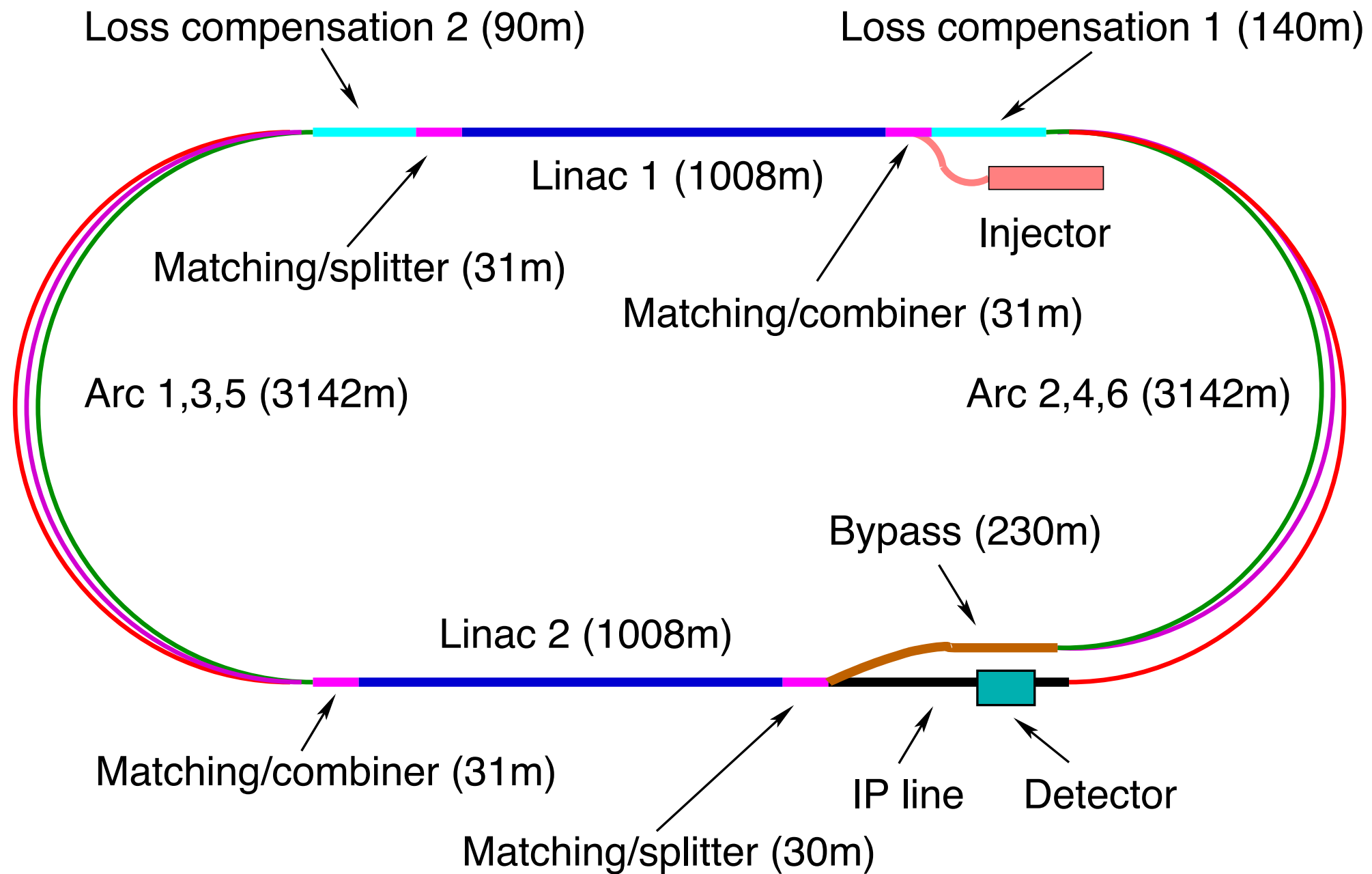


The Large Hadron-Electron Collider at the HL-LHC

LHeC and FCC-he Study Group

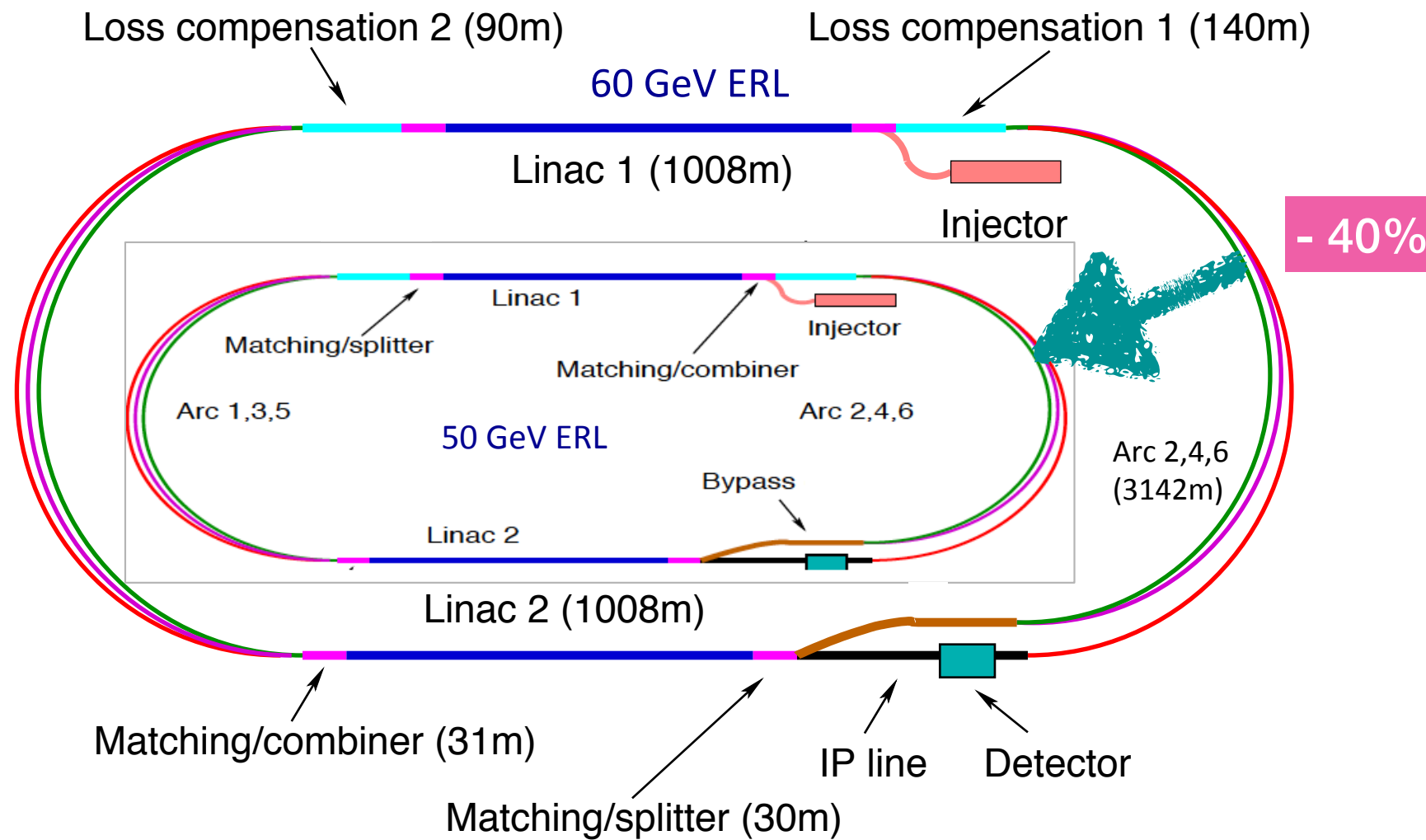


1. LHeC

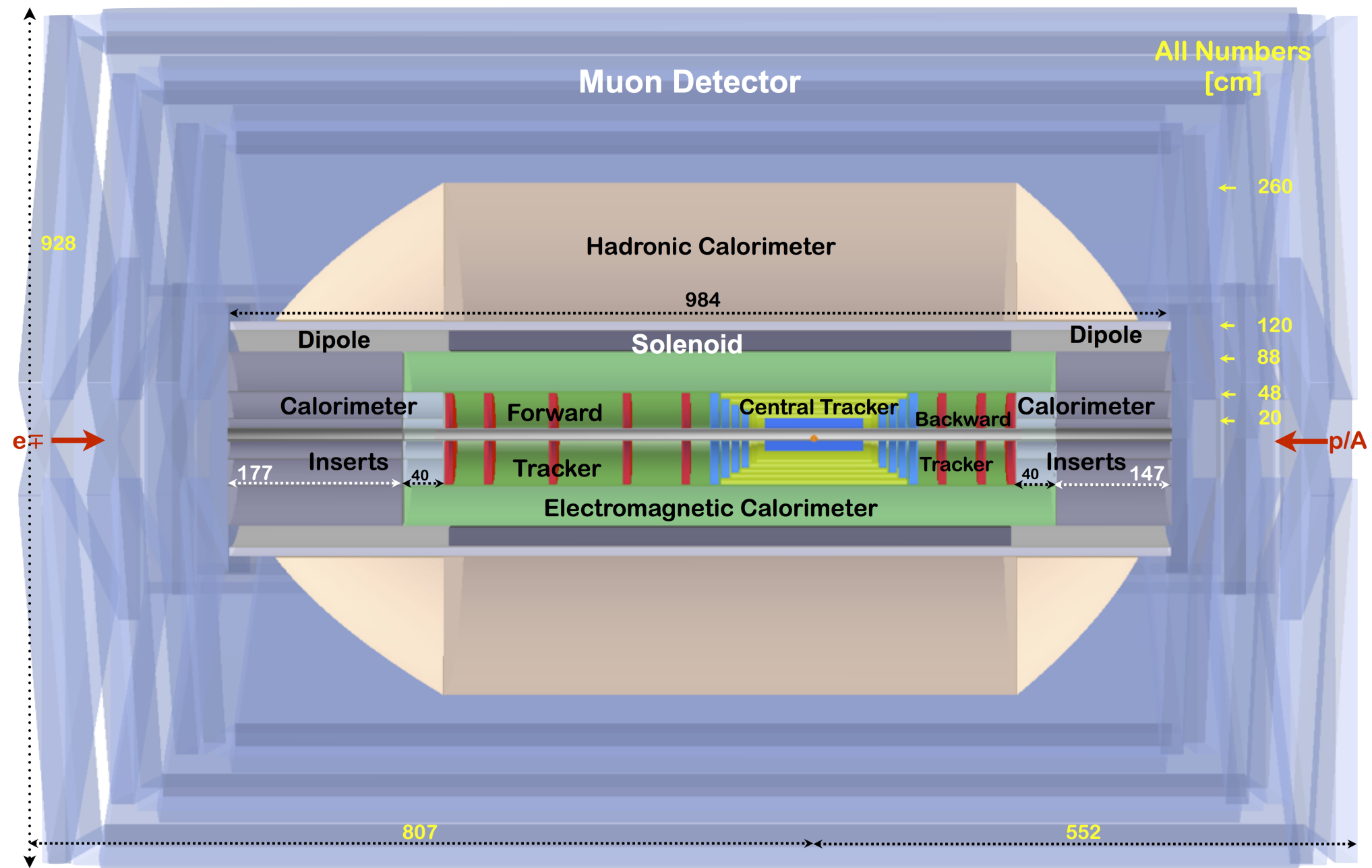


- Default LHeC racetrack configuration.
- After 3 passes, we have the target electron energy.
- Simultaneous run of LHC and LHeC

CDR in 2020: cost reduction



1. LHeC



We can distinguish forward from backward

CDR in 2020: cost reduction

Parameter	Unit	LHeC				FCC-eh	
		CDR	Run 5	Run 6	Dedicated	$E_p=20$ TeV	$E_p=50$ TeV
E_e	GeV	60	30	50	50	60	60
N_p	10^{11}	1.7	2.2	2.2	2.2	1	1
ϵ_p	μm	3.7	2.5	2.5	2.5	2.2	2.2
I_e	mA	6.4	15	20	50	20	20
N_e	10^9	1	2.3	3.1	7.8	3.1	3.1
β^*	cm	10	10	7	7	12	15
Luminosity	$10^{33} \text{ cm}^{-2} \text{ s}^{-1}$	1	5	9	23	8	15

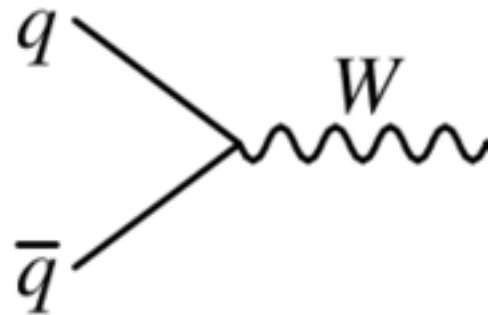

with LHC



a final, dedicated, stand-alone ep phase

Merit 1: small backgrounds

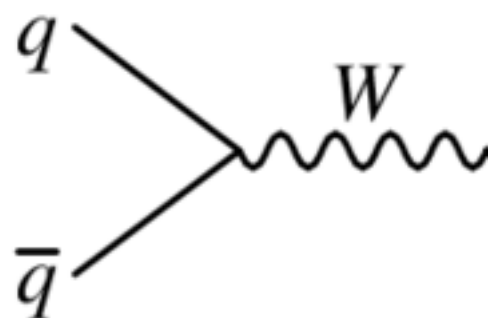
LHC: single W production



$$\sigma(pp \rightarrow W^{\pm}) \simeq 10^5 \text{ pb}$$

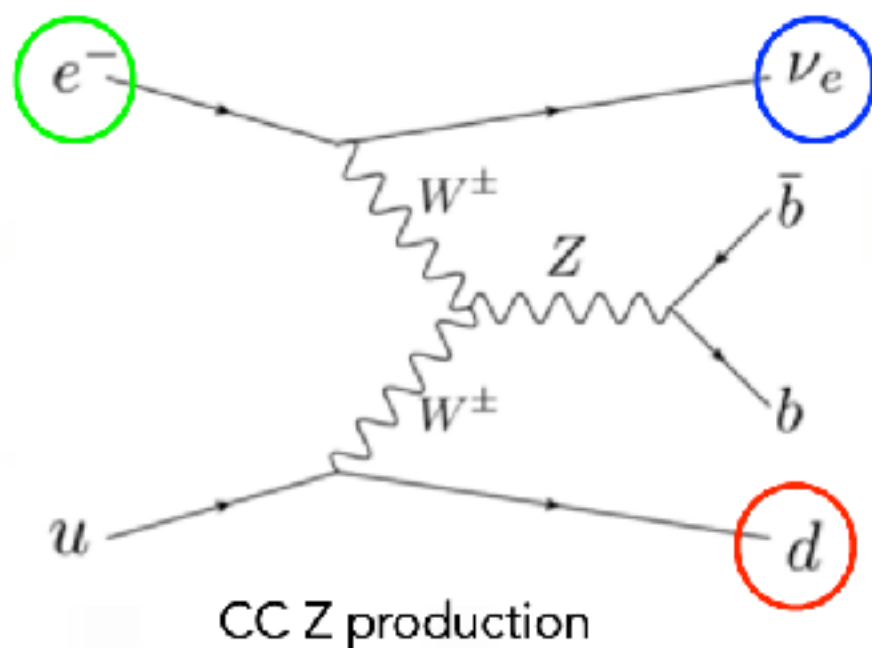
Merit 1: small backgrounds

LHC: single W production



$$\sigma(pp \rightarrow W^\pm) \simeq 10^5 \text{ pb}$$

LHeC: only through VBF



Process $E_e = 50 \text{ GeV}, E_p = 7 \text{ TeV}$

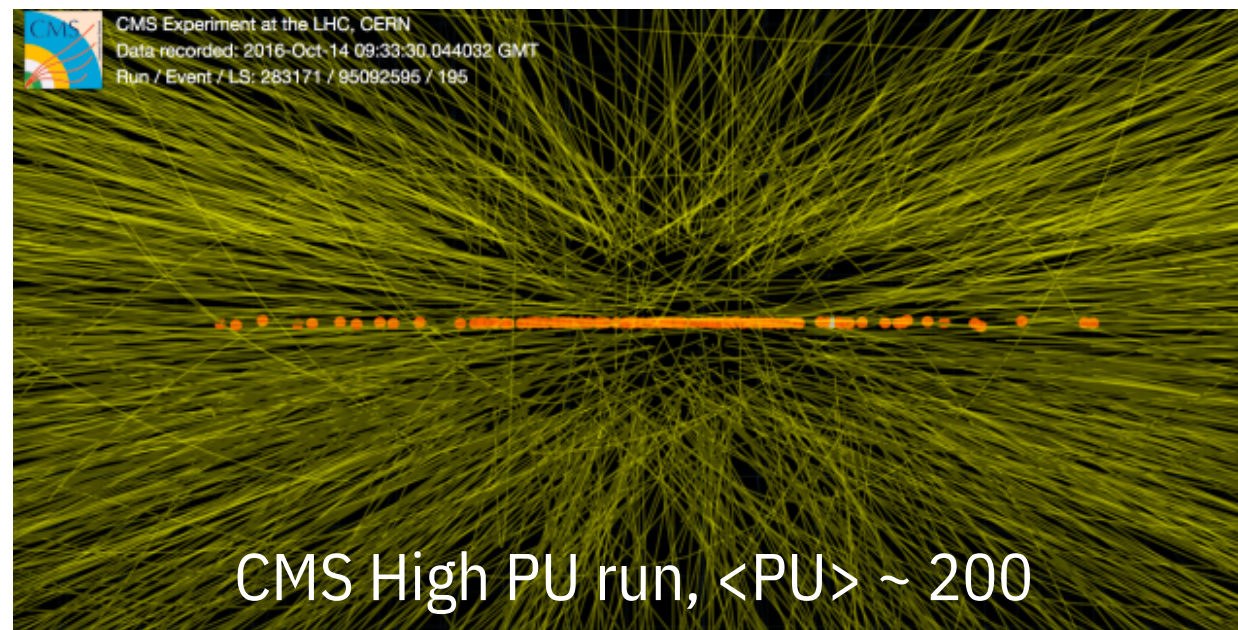
$p_T^e > 10 \text{ GeV}$

$e^- W^+ j$	1.00 pb
$e^- W^- j$	0.930 pb
$\nu_e^- W^- j$	0.796 pb
$\nu_e^- Z j$	0.412 pb
$e^- Z j$	0.177 pb

Merit 2: No gluon fusion at LO

Merit 2: No gluon fusion at LO

Merit 3: Practically no Pile-up



At LHeC, PU is only 0.1

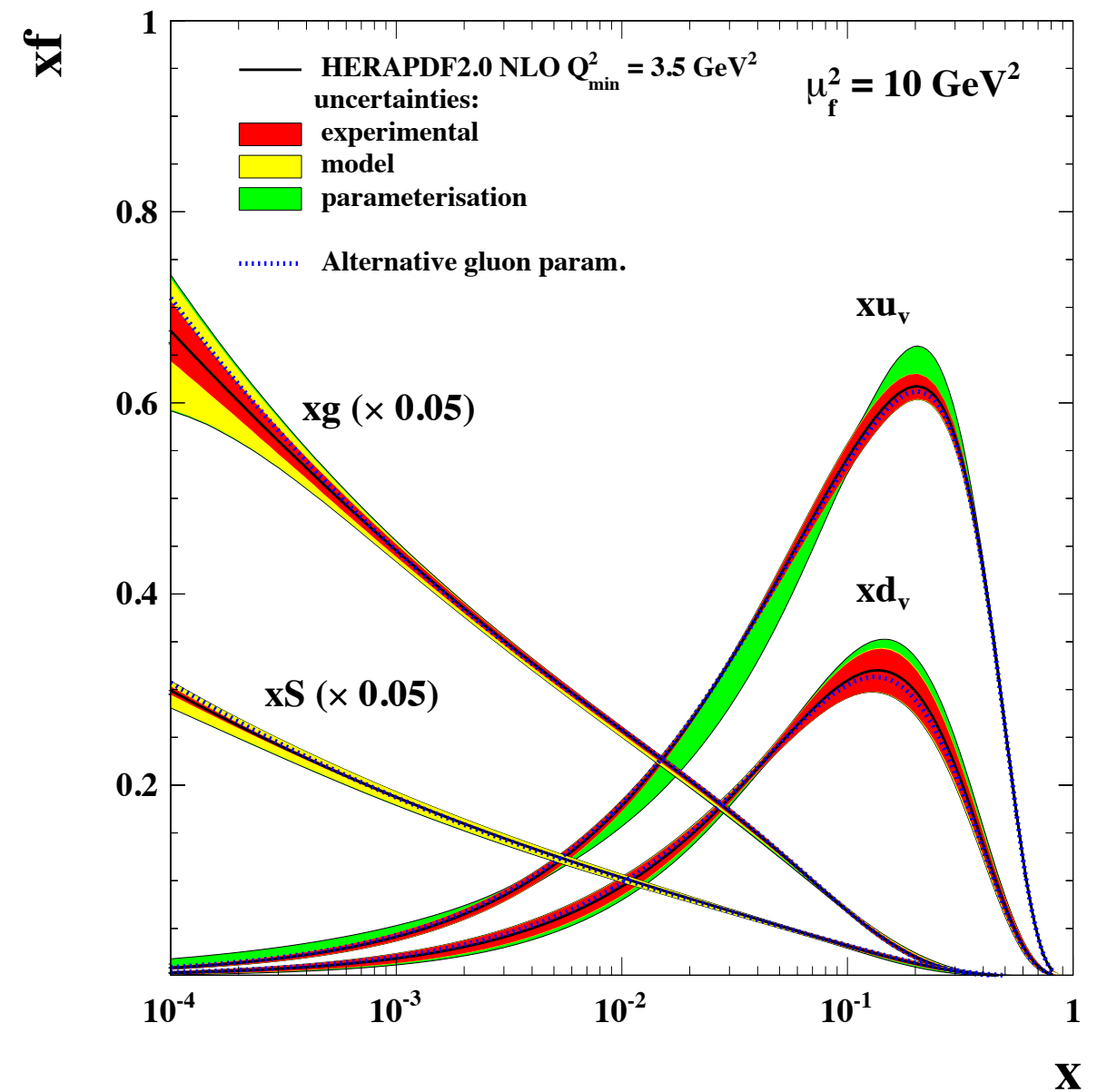
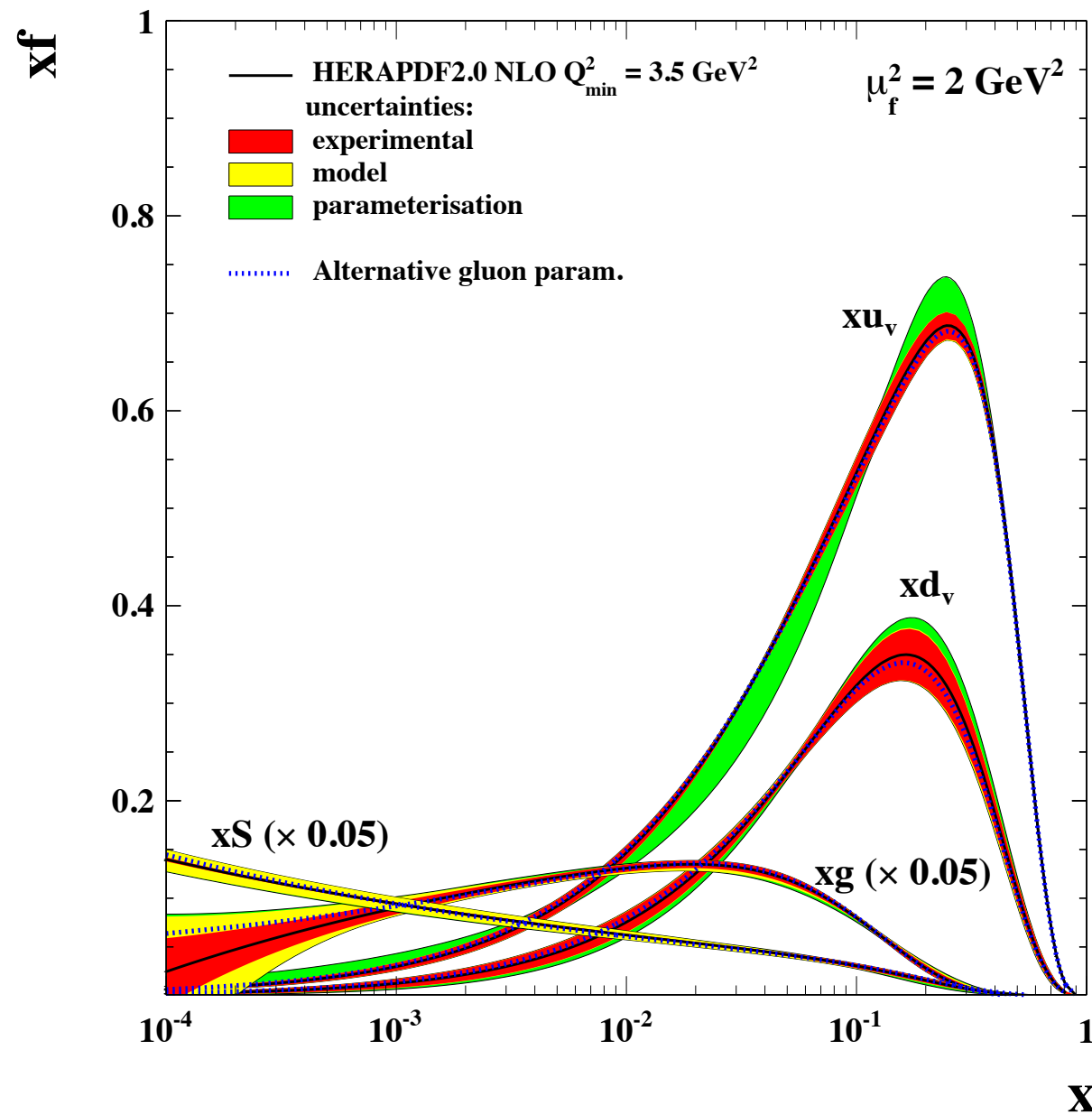
Merit 4: electron beam polarization

$P_e=80\%$ can enhance the CC mode.

Doubling the luminosity!

2. Parton Distribution Functions

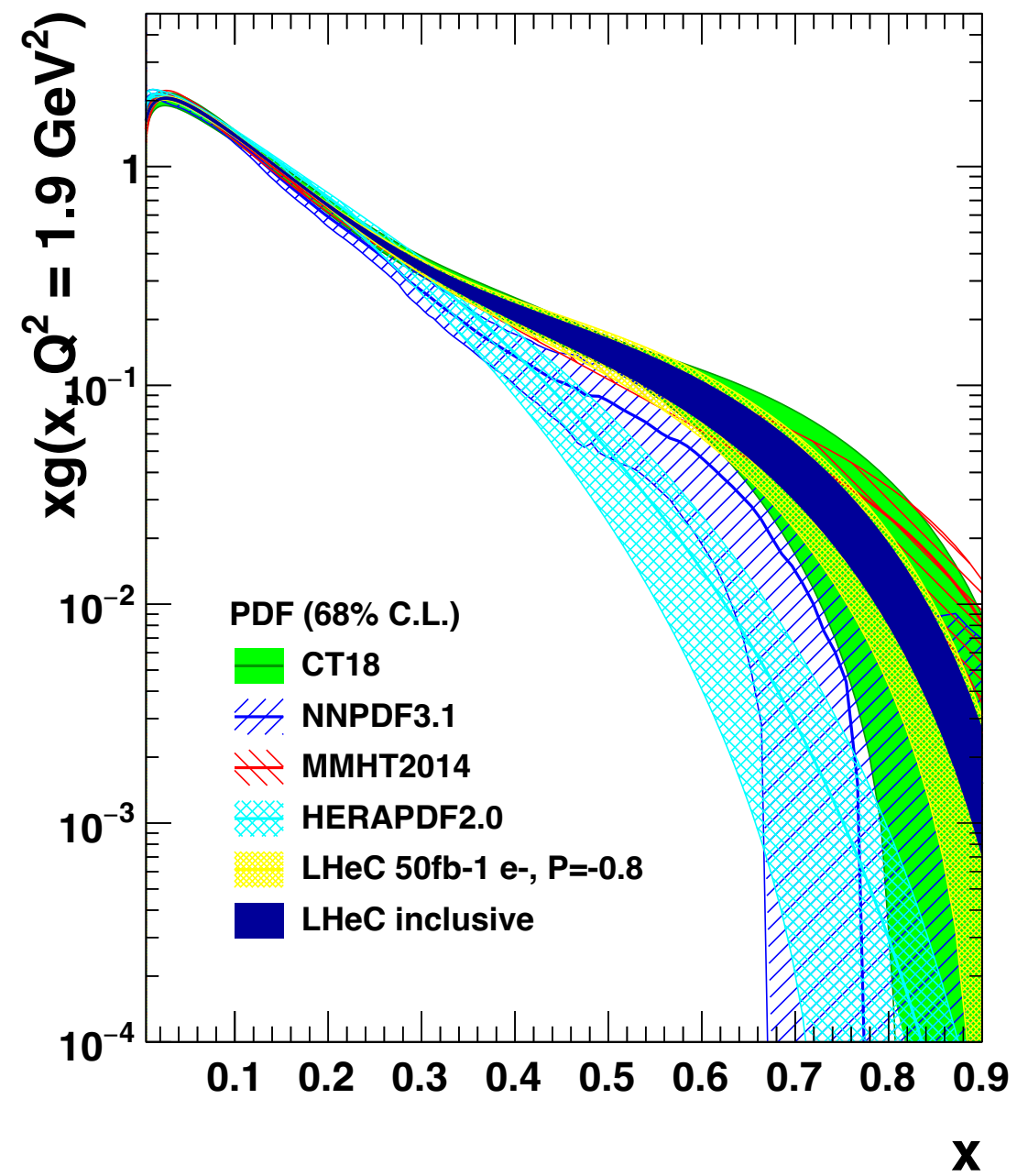
From the QCD fit to the combined H1 and ZEUS data



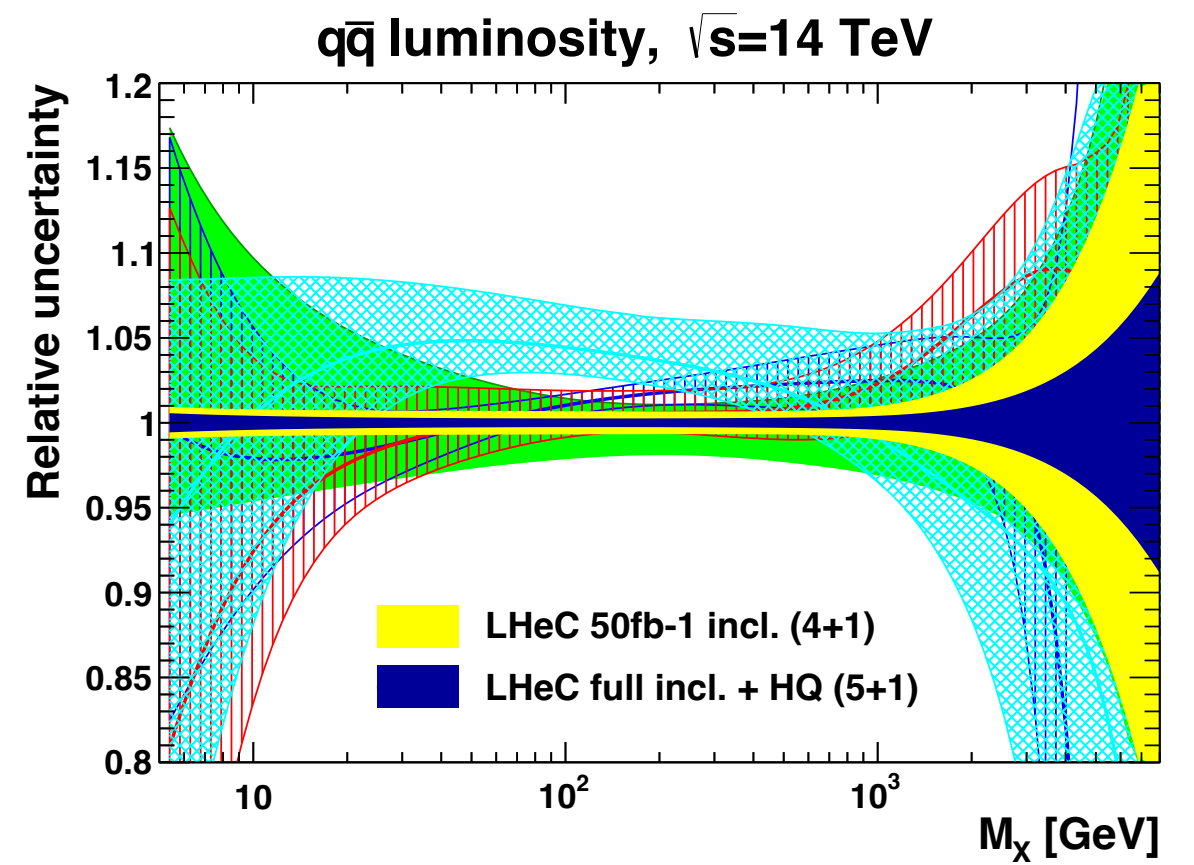
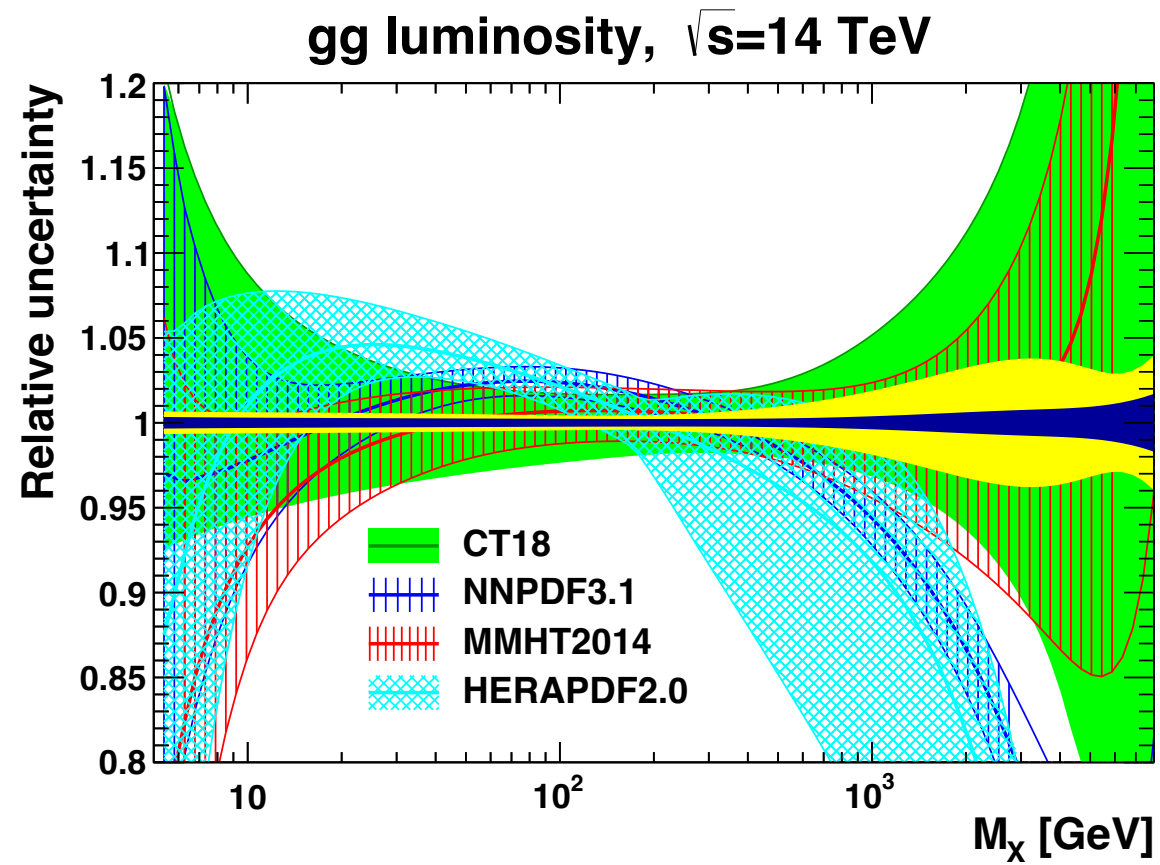
Large uncertainty, especially small x for gluon PDF

Significant improvement

gluon distribution at $Q^2 = 1.9 \text{ GeV}^2$



Uncertainty bands for parton luminosities as a function of the mass



3. Electroweak and Top Quark Physics

W-boson mass

LEP2

Tevatron

ATLAS

LHeC ($E_e=60\text{GeV}$, $\delta_{\text{unc.}}=0.5\%$)

LHeC ($E_e=60\text{GeV}$, $\delta_{\text{unc.}}=0.25\%$)

LHeC ($E_e=50\text{GeV}$, $\delta_{\text{unc.}}=0.5\%$)

LHeC ($E_e=50\text{GeV}$, $\delta_{\text{unc.}}=0.25\%$)

PDG [2019]

80.35

80.4

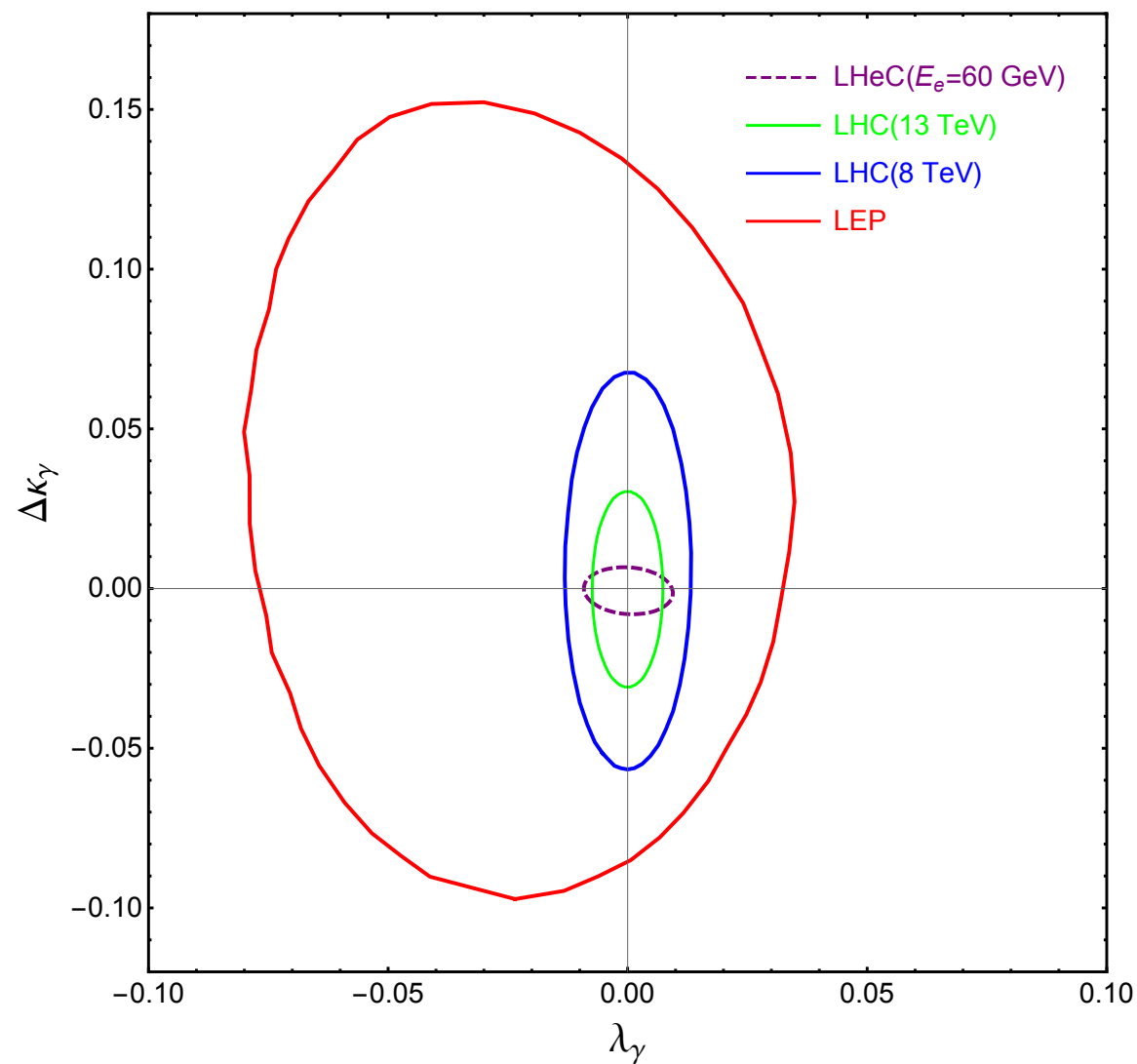
m_W [GeV]

Weak Neutral Current Couplings

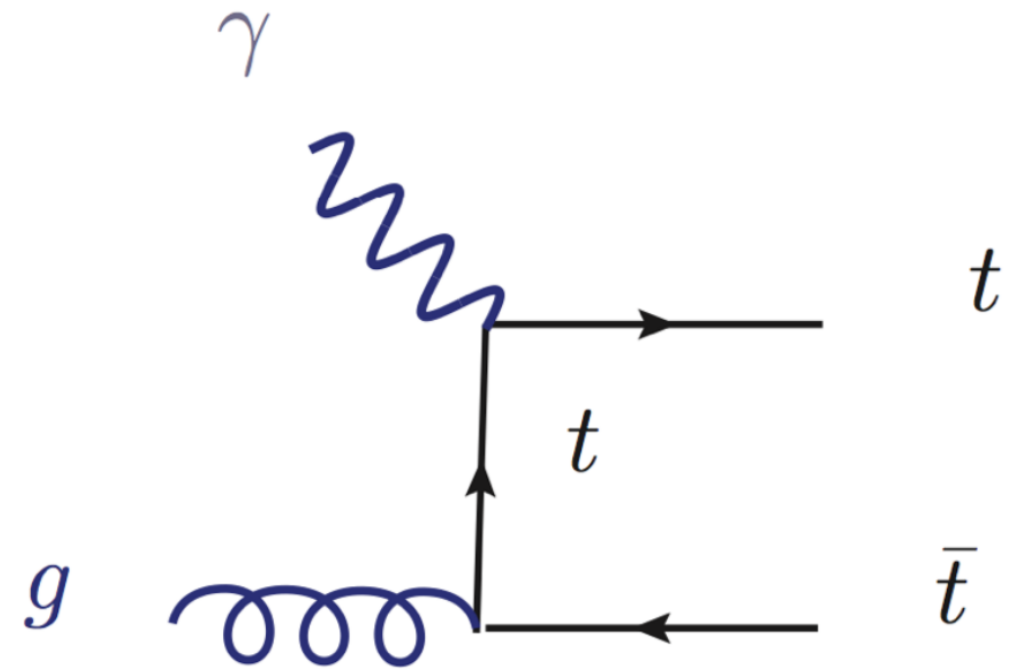
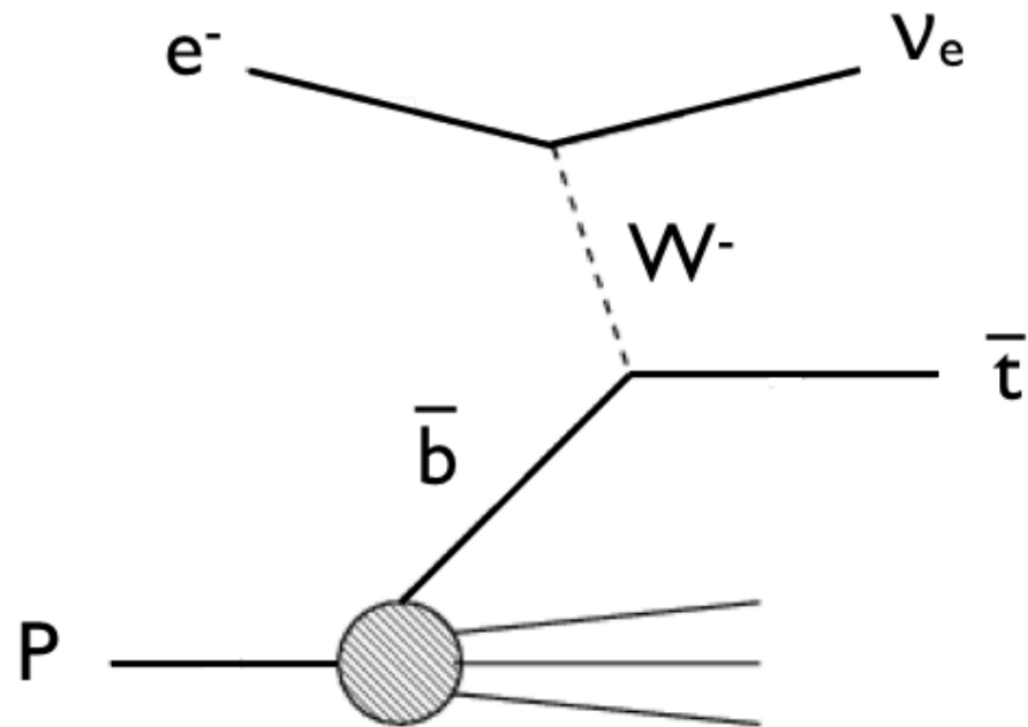
Coupling parameter	PDG		Expected uncertainties		
	value		LHeC-60	LHeC-60 ($\delta_{\text{uncor.}}=0.25\%$)	LHeC-50
g_A^u	0.50	$+0.04$ -0.05	0.0022	0.0015	0.0035
g_A^d	-0.514	$+0.050$ -0.029	0.0055	0.0034	0.0083
g_V^u	0.18	± 0.05	0.0015	0.0010	0.0028
g_V^d	-0.35	$+0.05$ -0.06	0.0046	0.0027	0.0067

Anomalous Triple Gauge Couplings

$$\begin{aligned}
 \mathcal{L}_{TGC}/g_{WWV} = & ig_{1,V}(W_{\mu\nu}^+ W_\mu^- V_\nu - W_{\mu\nu}^- W_\mu^+ V_\nu) + i\kappa_V W_\mu^+ W_\nu^- V_{\mu\nu} + \frac{i\lambda_V}{M_W^2} W_{\mu\nu}^+ W_{\nu\rho}^- V_{\rho\mu} \\
 & + g_5^V \epsilon_{\mu\nu\rho\sigma} (W_\mu^+ \overleftrightarrow{\partial}_\rho W_\nu^-) V_\sigma - g_4^V W_\mu^+ W_\nu^- (\partial_\mu V_\nu + \partial_\nu V_\mu) \\
 & + i\tilde{\kappa}_V W_\mu^+ W_\nu^- \tilde{V}_{\mu\nu} + \frac{i\tilde{\lambda}_V}{M_W^2} W_{\lambda\mu}^+ W_{\mu\nu}^- \tilde{V}_{\nu\lambda},
 \end{aligned} \tag{5.1}$$

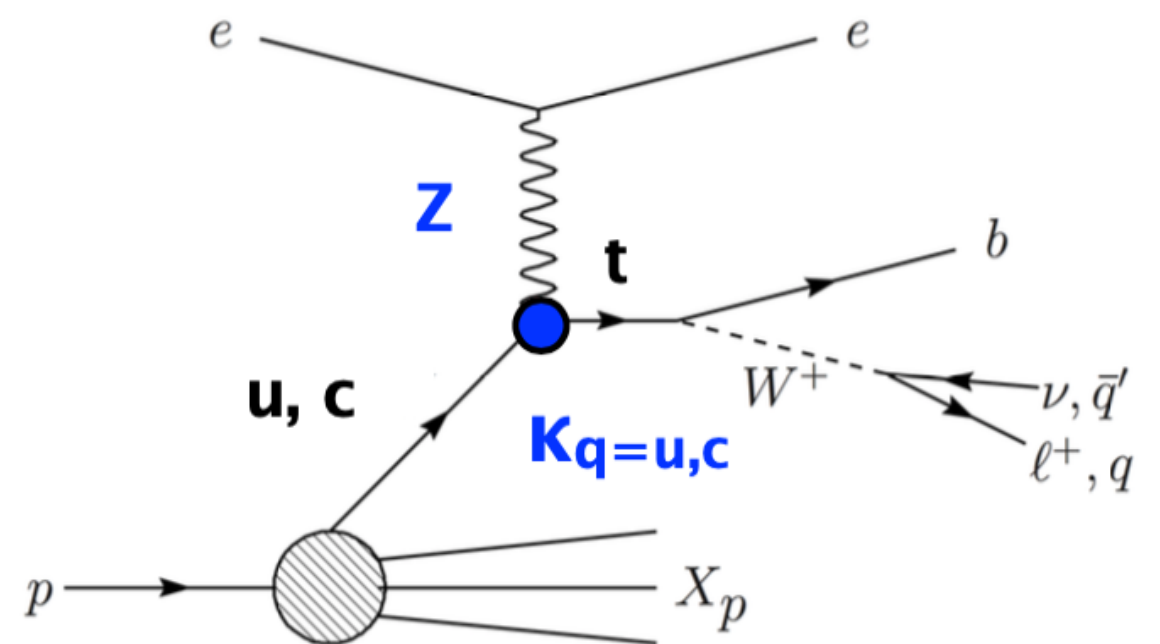
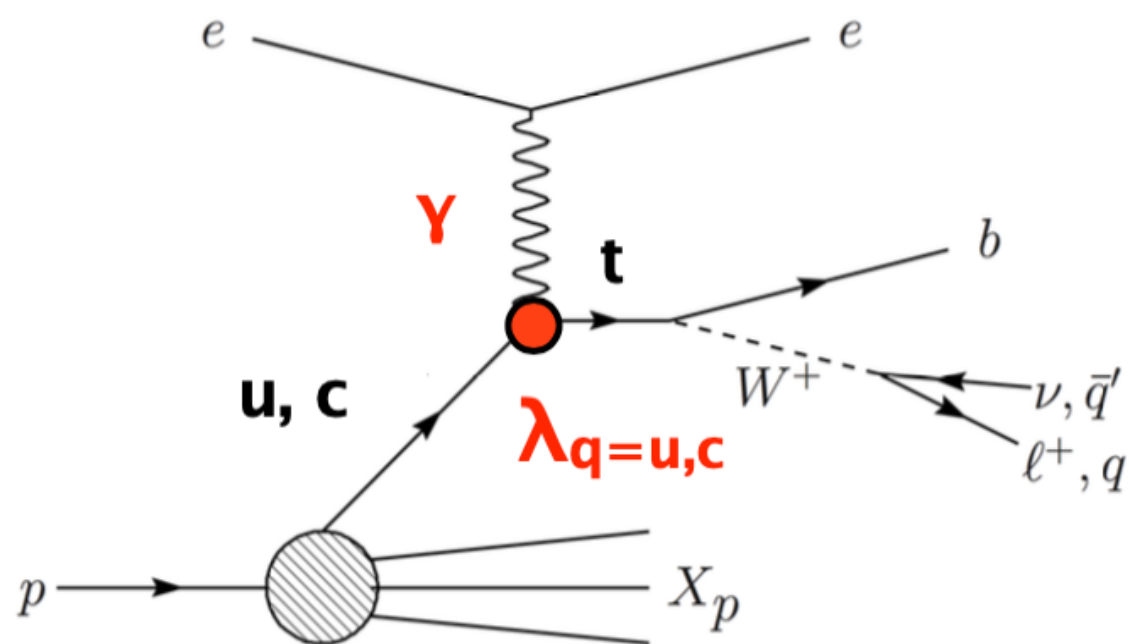


Top quark production @ ep

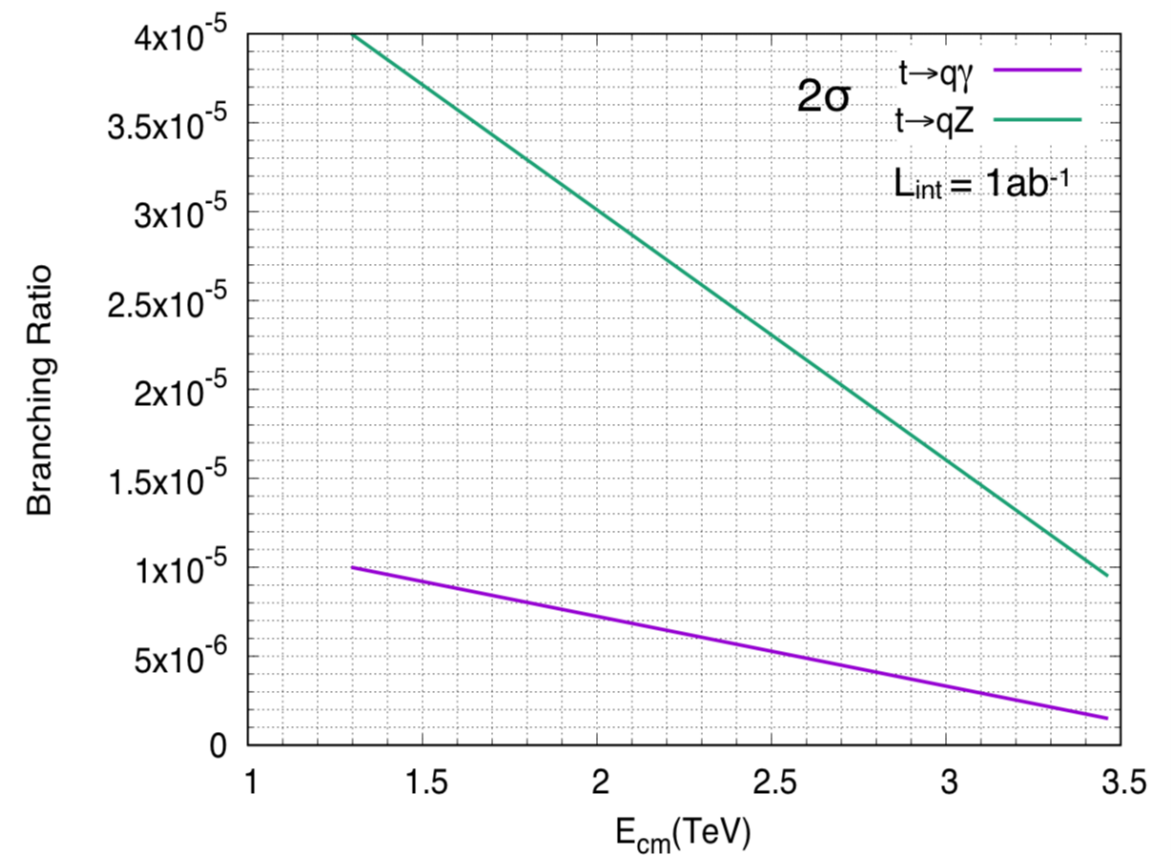
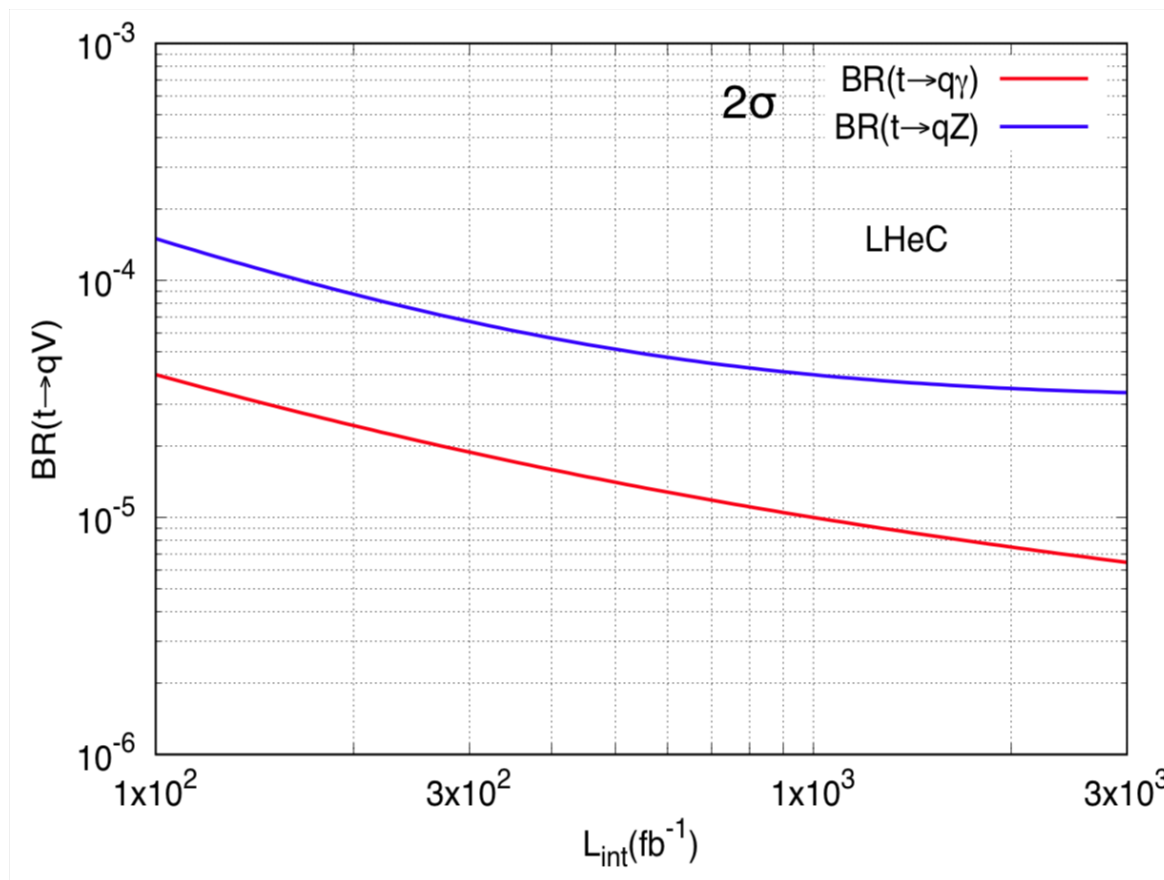


FCNC Top Quark Couplings @ ep

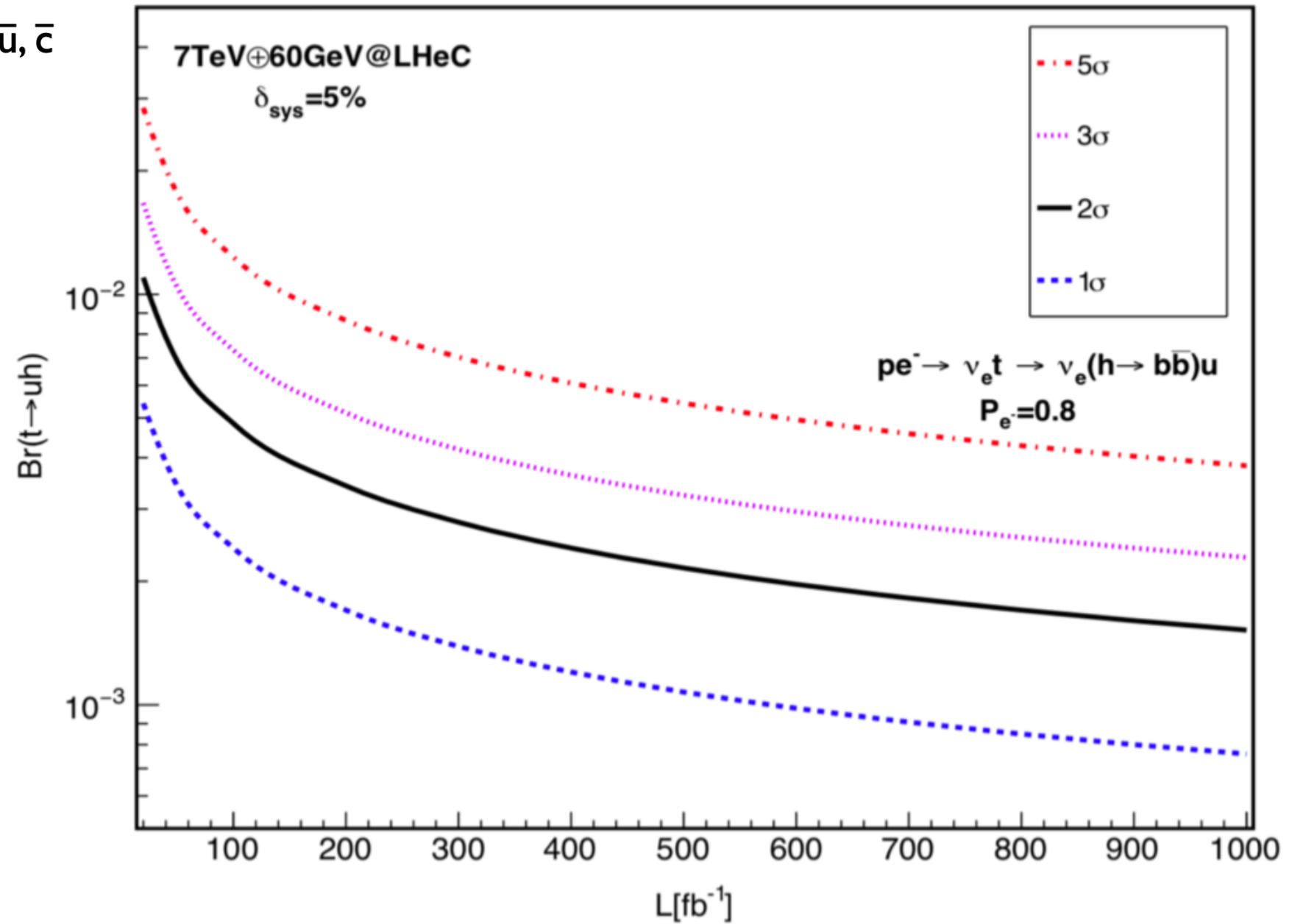
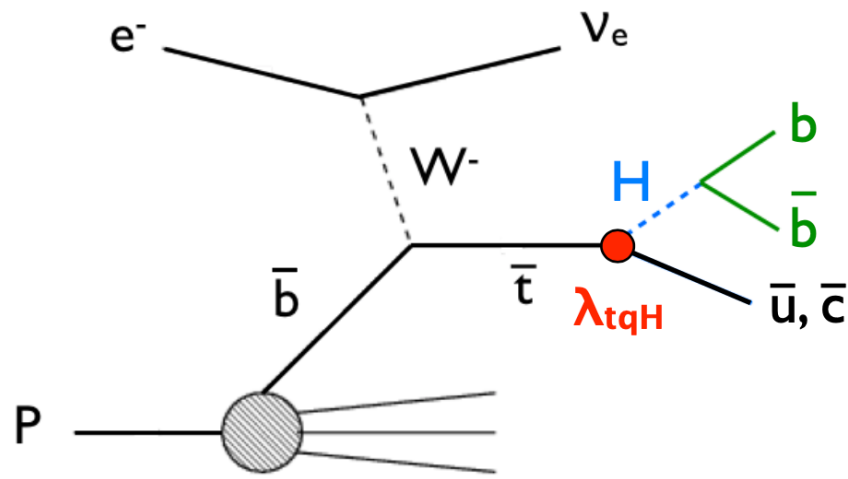
$t u \gamma$, $t c \gamma$, $t u Z$, $t c Z$

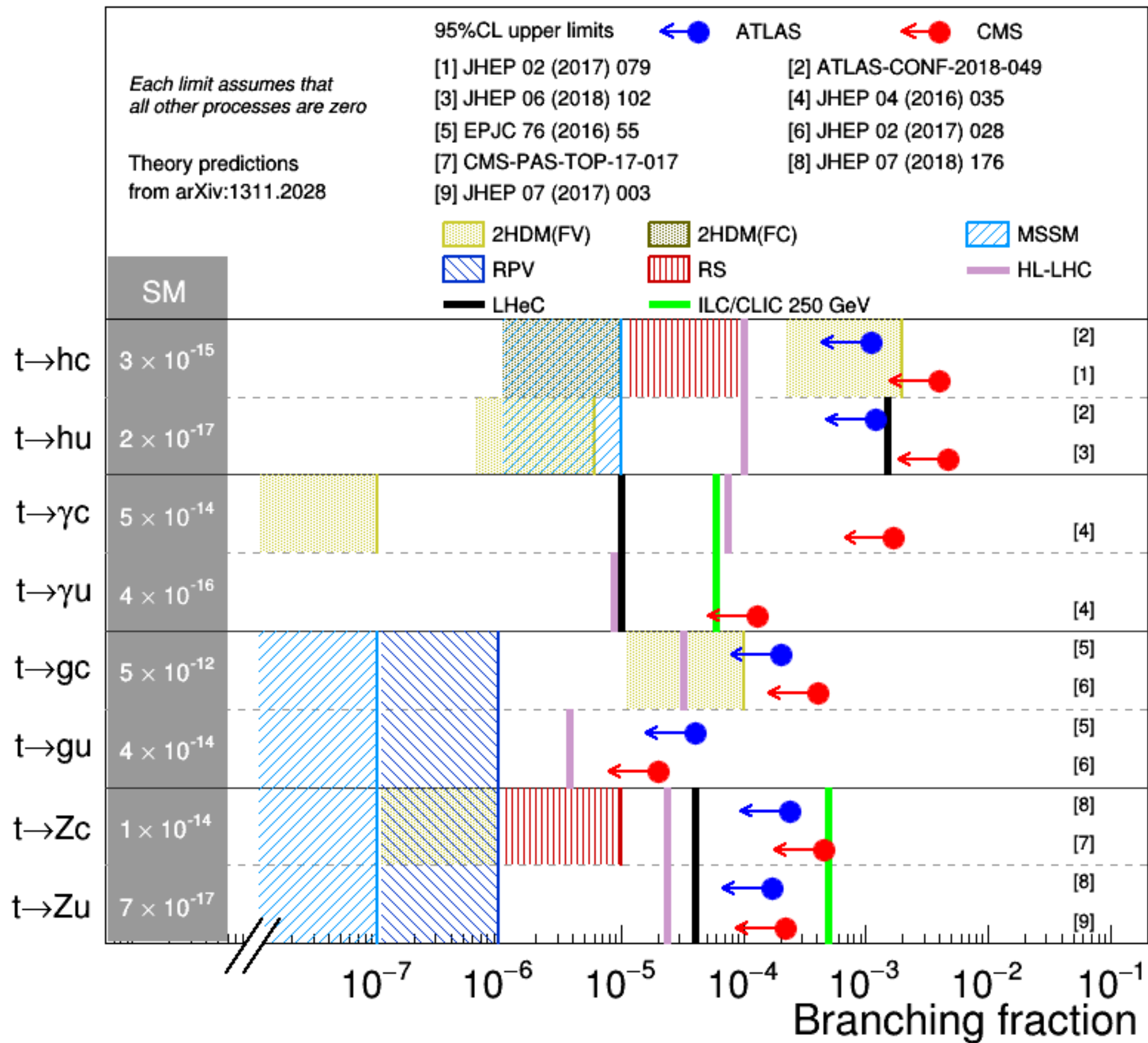


Expected sensitivities on FCNC

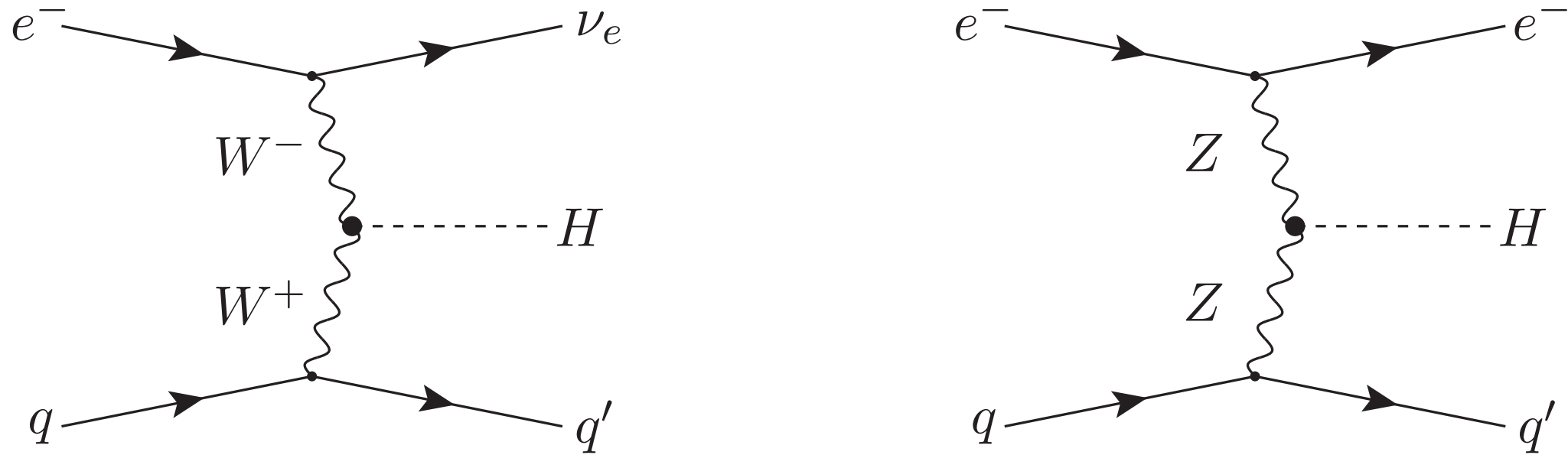


FCNC tqH couplings





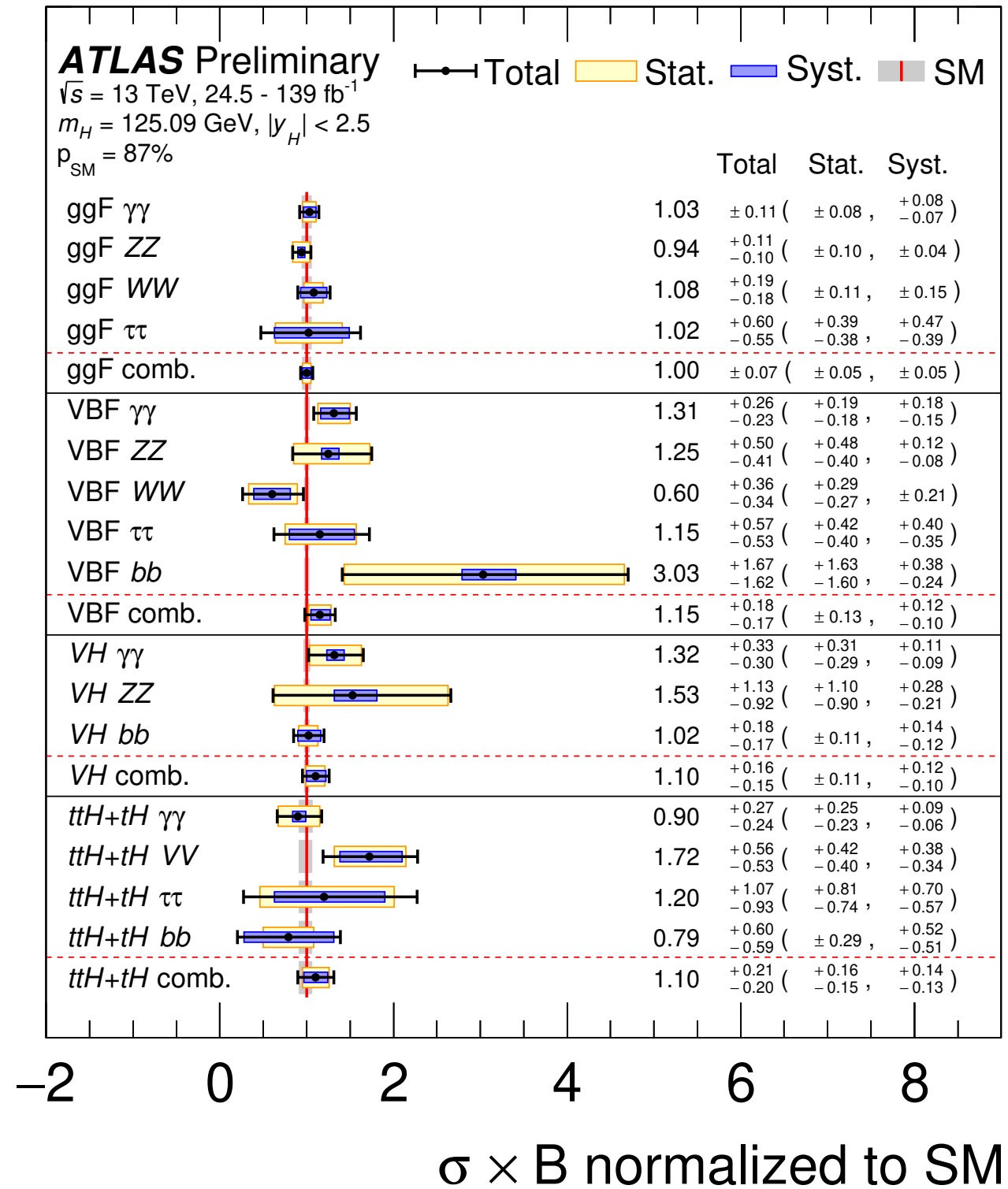
3. Higgs Physics: bb and cc modes



Higgs production cross section in fb

Parameter	Unit	LHeC	HE-LHeC	FCC-eh	FCC-eh
E_p	TeV	7	13.5	20	50
\sqrt{s}	TeV	1.30	1.77	2.2	3.46
$\sigma_{CC} (P = -0.8)$	fb	197	372	516	1038
$\sigma_{NC} (P = -0.8)$	fb	24	48	70	149
$\sigma_{CC} (P = 0)$	fb	110	206	289	577
$\sigma_{NC} (P = 0)$	fb	20	41	64	127
HH in CC	fb	0.02	0.07	0.13	0.46

Higgs precision at the LHC



Higgs precision test at the other future colliders

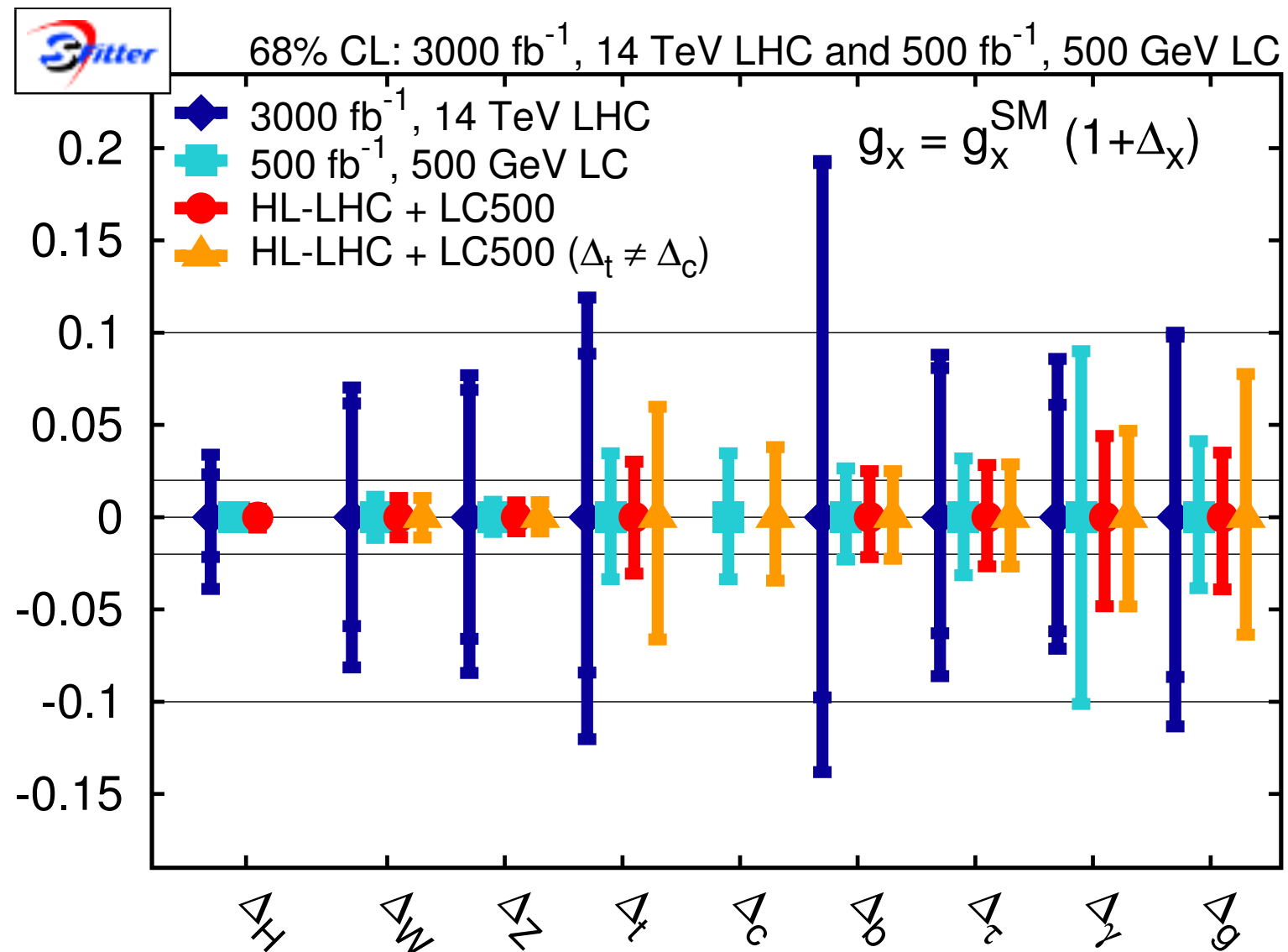
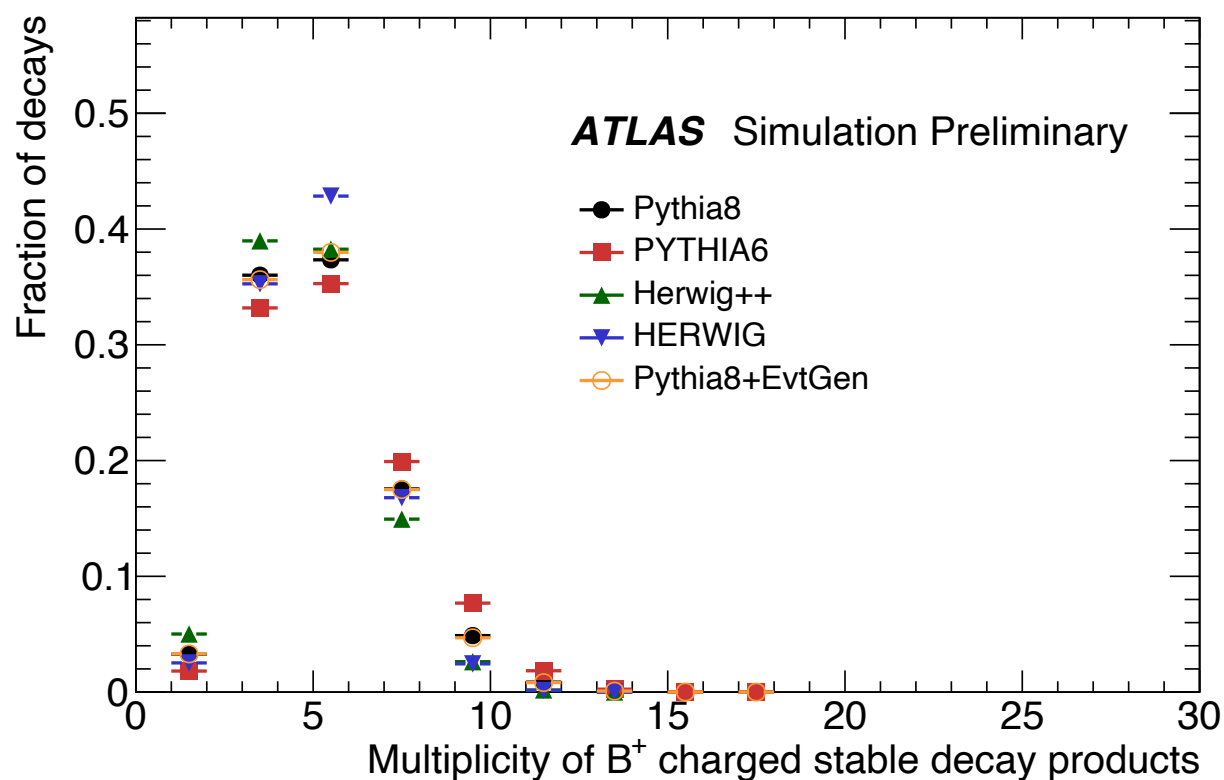


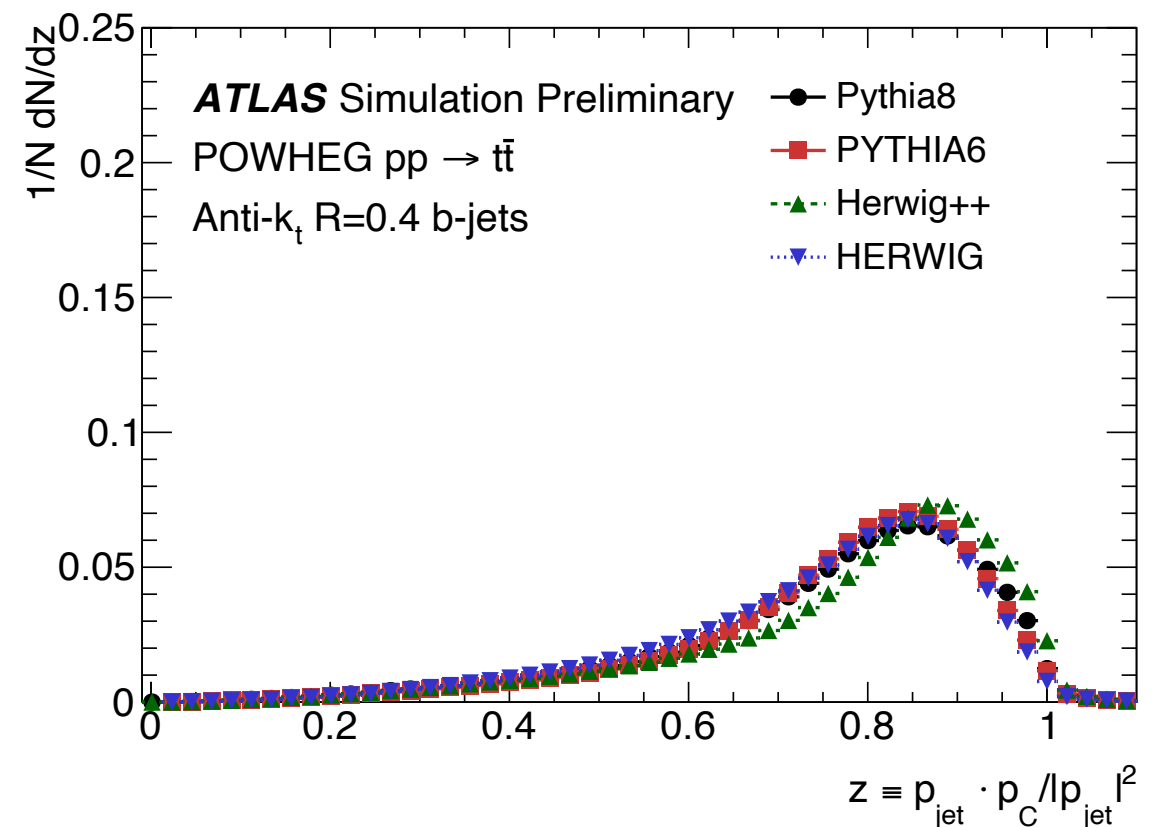
Figure 3. Expected precision for Higgs couplings from a high-luminosity LHC, a 500 GeV ILC, and their combination. For the LHC we also show a scenario with improved systematic uncertainties. Figure from Ref. [31].

Properties of B hadrons

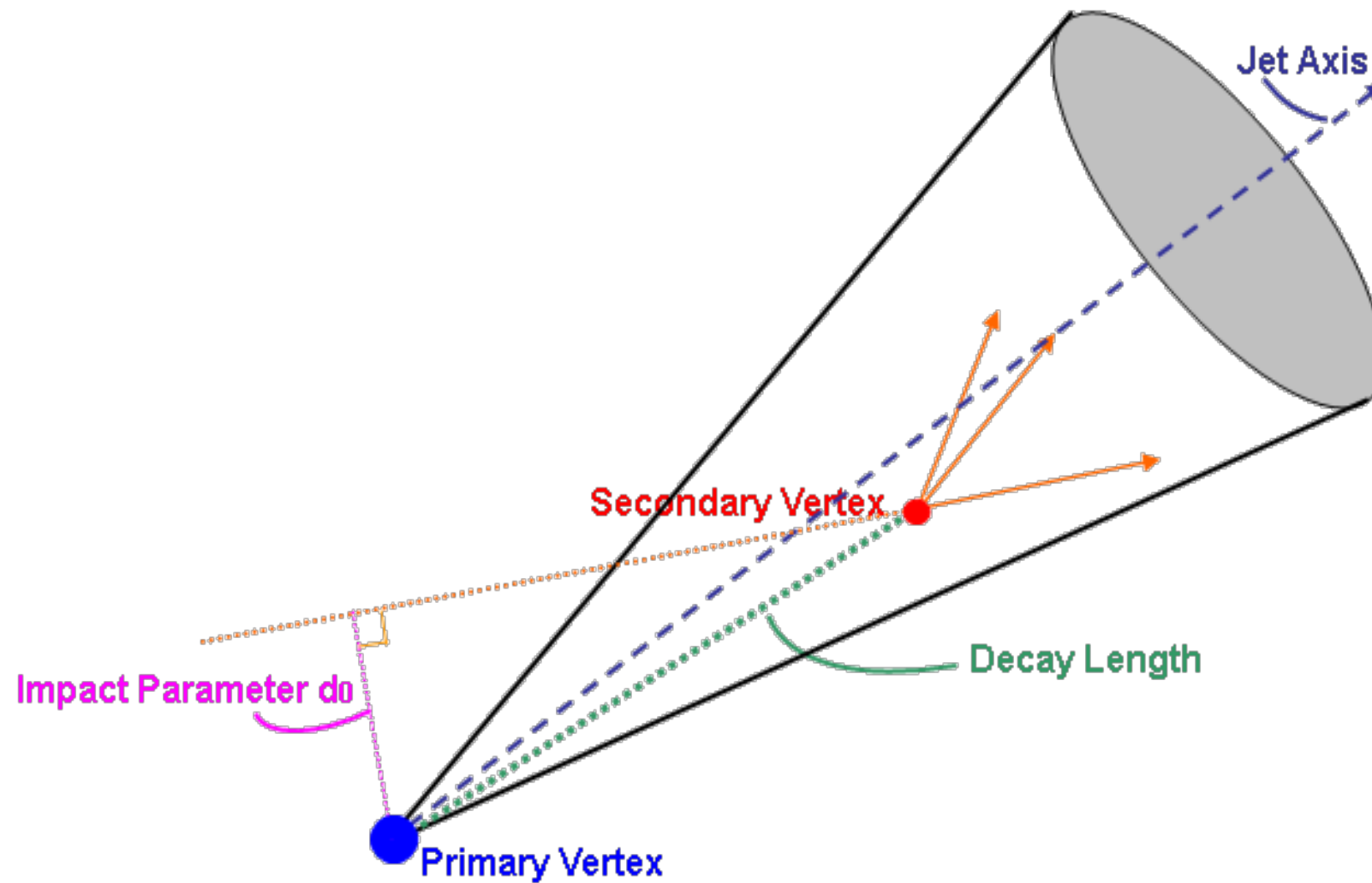
- **Lifetime:** Long enough to lead to a measurable decay length (around 5mm for a 50 GeV boost)
- **Mass:** Weakly decaying b -hadrons have masses around 5 GeV, leading to high decay product multiplicities (average of 5 charged particles per decay)
- **Fragmentation:** Much harder than jets initiated by other species (b -hadrons carry around 75% of jet energy, on average)



Left: Mean charged multiplicity in B^+ mesons decays

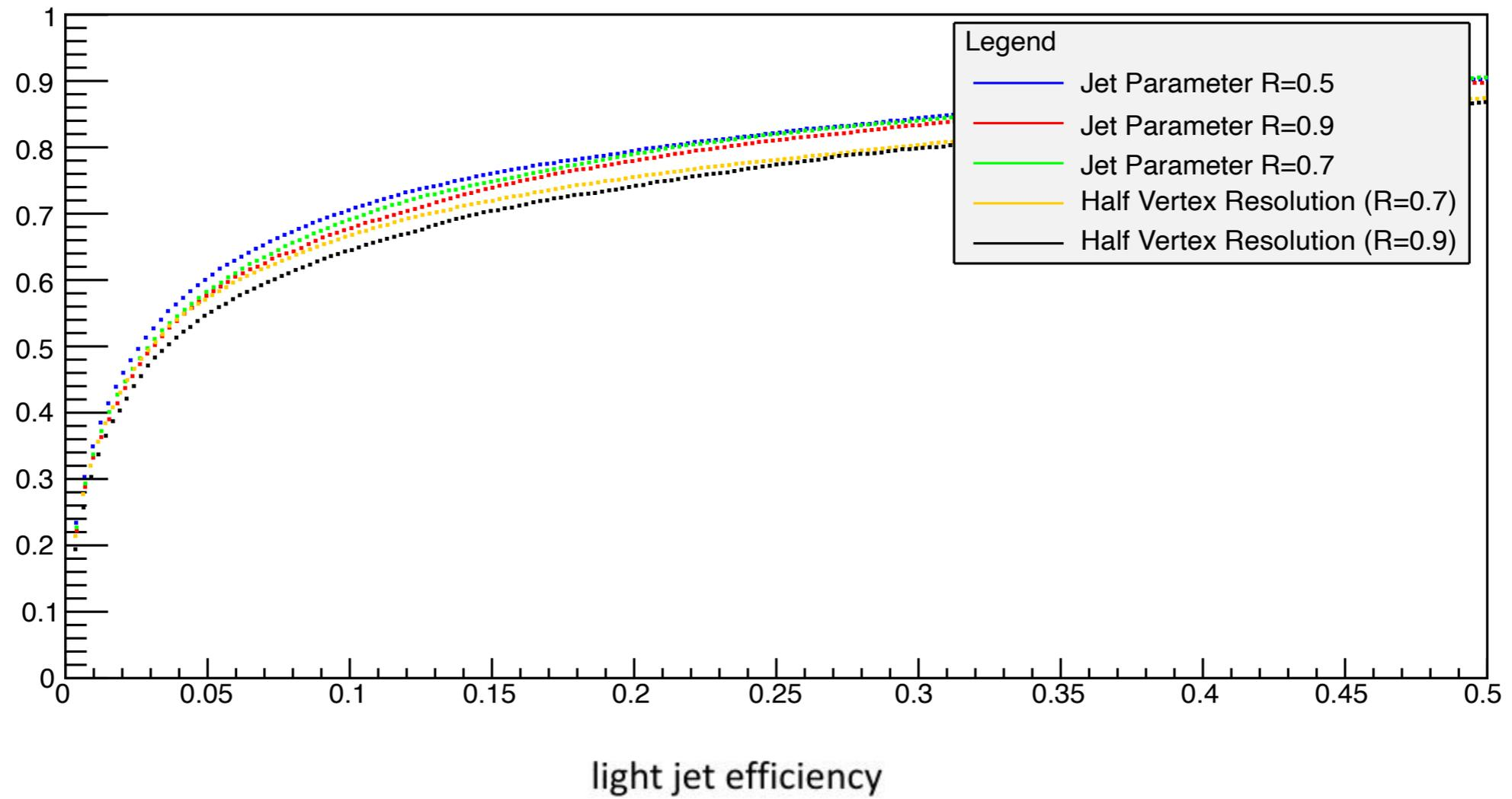


Right: b -quark fragmentation function



- B-tagging algorithms are used to tag the b-jets originating from b quarks. In first data, three algorithms are going to be used:
 - TrackCounting: use tracks with large impact parameter.
 - JetProb: calculate the probability of a track to be from light jet.
 - Secondary Vertex Reconstruction (SV0): use the **signed decay length significance** of the secondary vertex .

B-jet efficiency vs light-jet efficiency

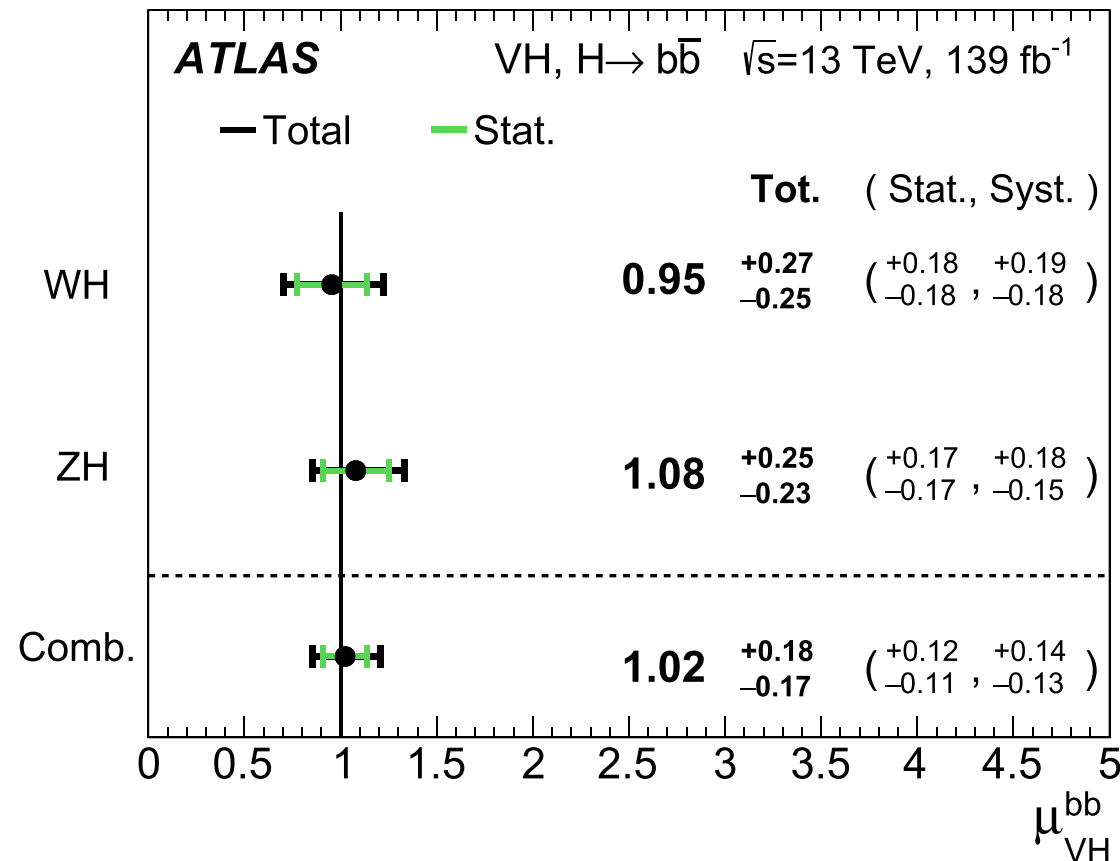




Measurements of WH and ZH production in the $H \rightarrow b\bar{b}$ decay channel in pp collisions at 13 TeV with the ATLAS detector

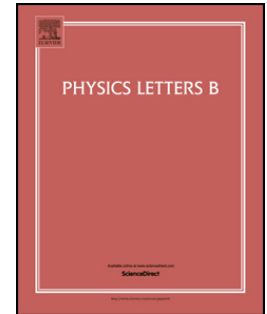
ATLAS Collaboration*

$$\mu_{VH}^{bb} = 1.02^{+0.18}_{-0.17} = 1.02^{+0.12}_{-0.11}(\text{stat.})^{+0.14}_{-0.13}(\text{syst.}).$$



Contents lists available at [ScienceDirect](#)

Physics Letters B

www.elsevier.com/locate/physletb

Measurement of the associated production of a Higgs boson decaying into b -quarks with a vector boson at high transverse momentum in pp collisions at $\sqrt{s} = 13$ TeV with the ATLAS detector



The ATLAS Collaboration*

VH with $p_{TW} > 250$ GeV and 139/fb

$$\mu_{VH}^{bb} = 0.72_{-0.36}^{+0.39} = 0.72_{-0.28}^{+0.29}(\text{stat.})_{-0.22}^{+0.26}(\text{syst.}).$$

2008.02508

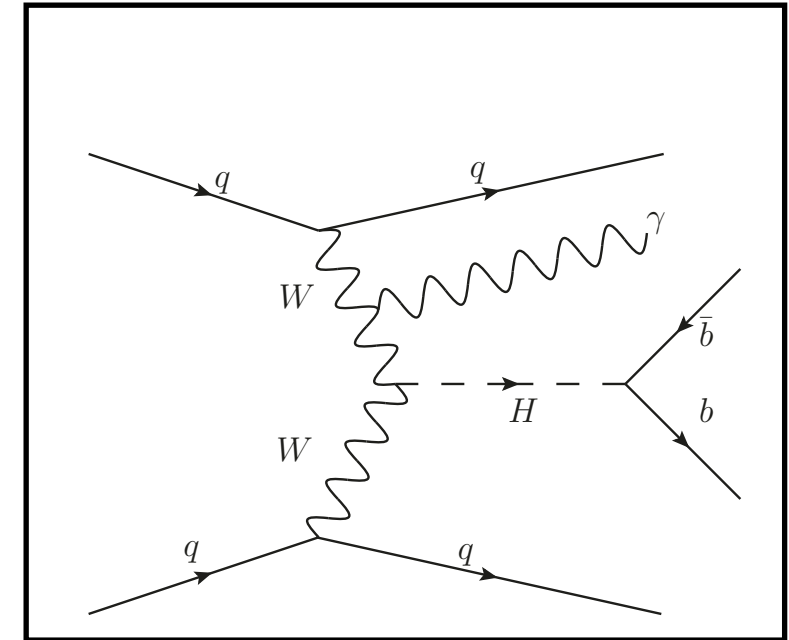
RECEIVED: October 27, 2020

REVISED: January 27, 2021

ACCEPTED: February 21, 2021

PUBLISHED: March 29, 2021

Search for Higgs boson production in association with a high-energy photon via vector-boson fusion with decay into bottom quark pairs at $\sqrt{s} = 13$ TeV with the ATLAS detector

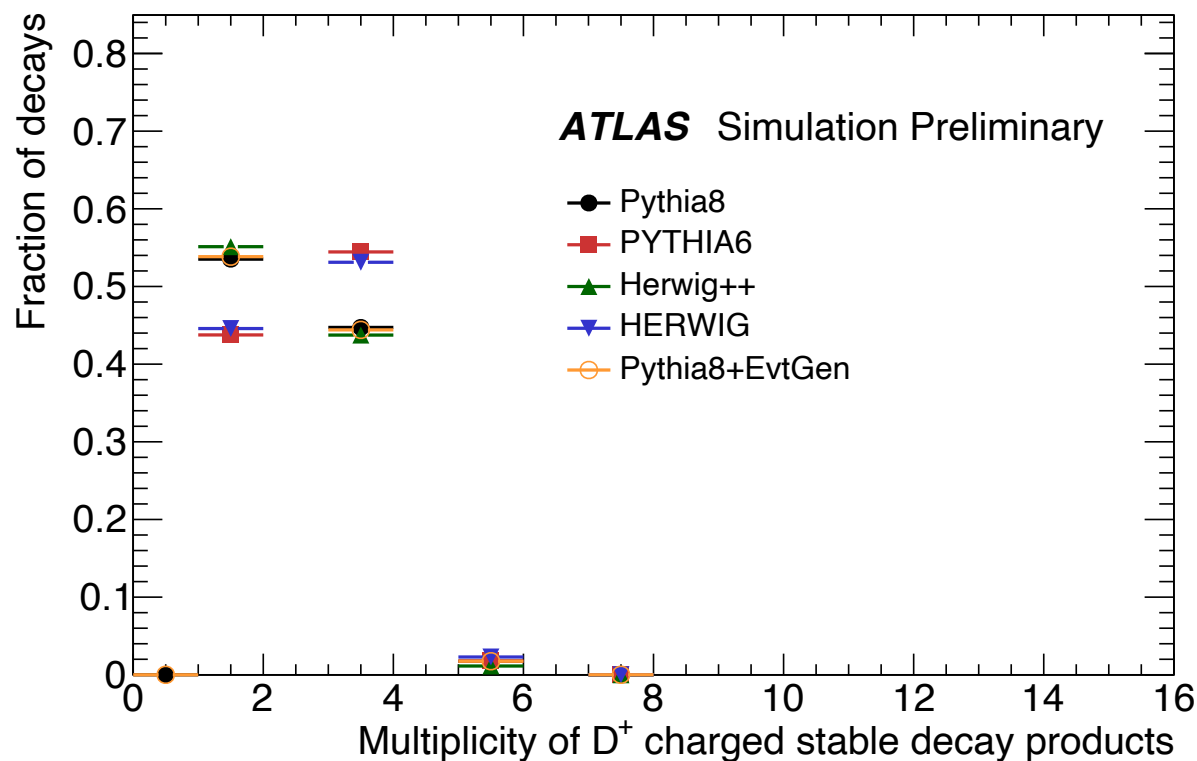


$$\mu_H = 1.3 \pm 1.0.$$

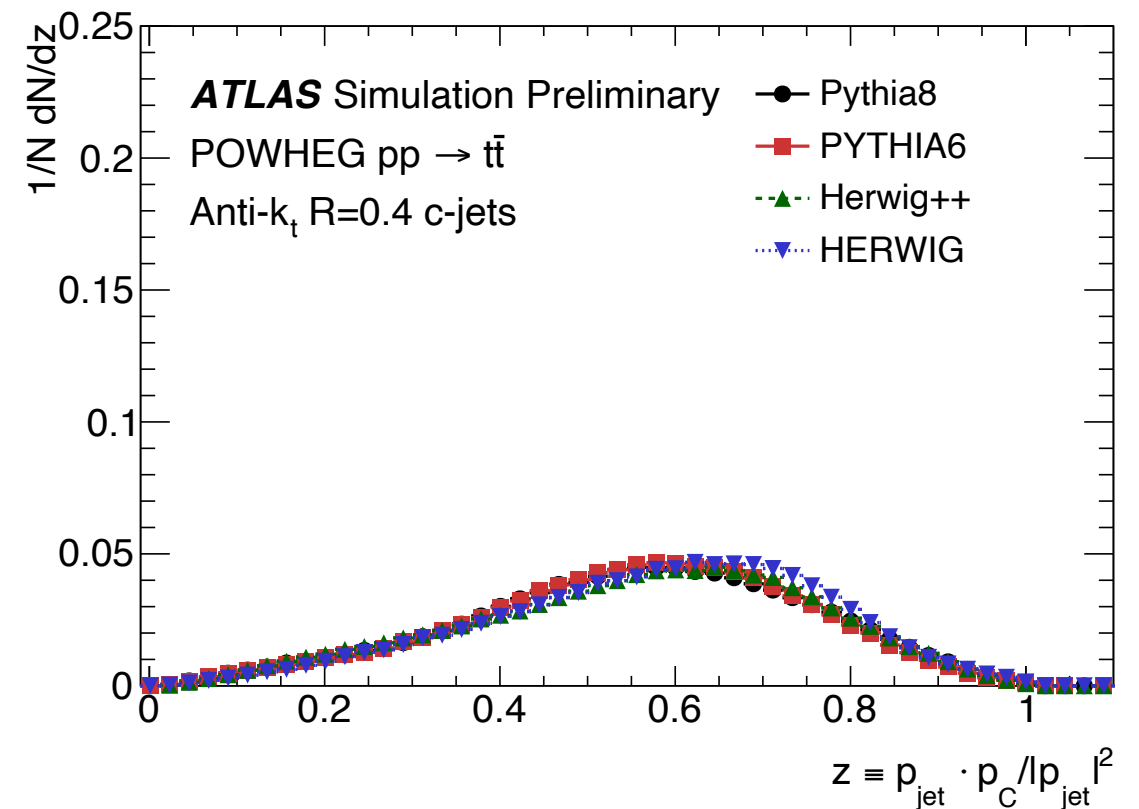
2010.13651

Properties of C hadrons

- **Lifetime:** Shorter than the b -hadrons by around a factor of 2-3, still enough for measureable decay length (around 1-3mm for a 50 GeV boost)
- **Mass:** Weakly decaying c -hadrons have masses around 2 GeV, around $2-3\times$ lower than b -hadrons (mean of ≈ 2 charged particles per decay)
- **Fragmentation:** Softer than b -jets, but still harder than jets initiated by light species (c -hadrons carry around 55% of jet energy, on average)

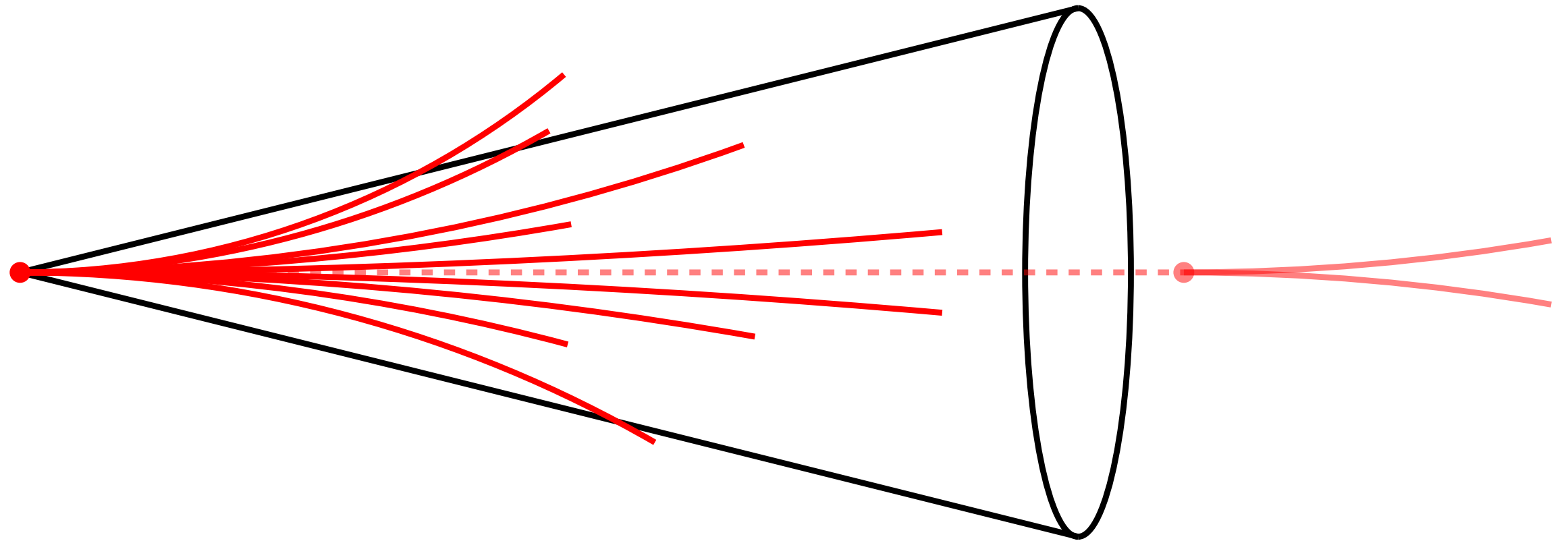


Left: Mean charged multiplicity in D^+ mesons decays



Right: c -quark fragmentation function

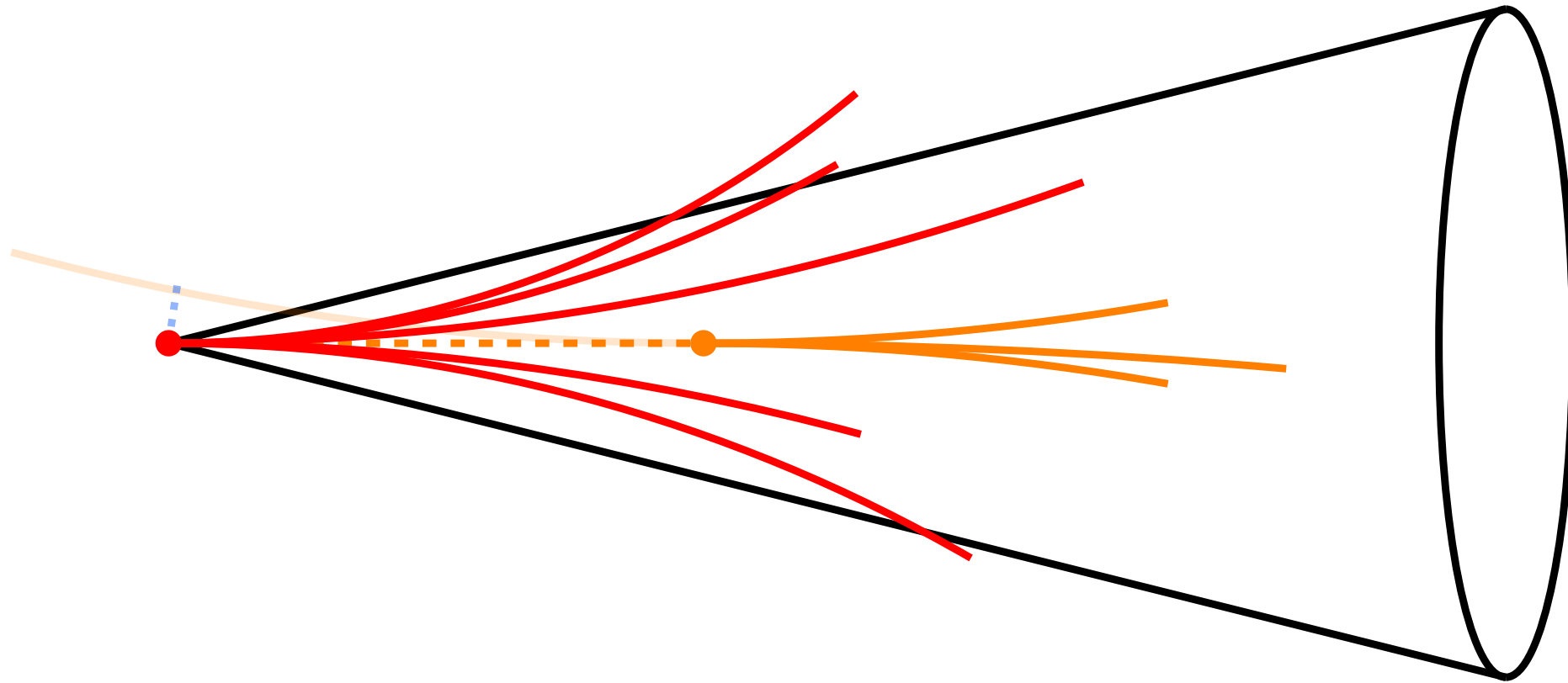
Anatomy of a light flavour (u, d, s) jet



Typical Experimental Signature

- Light-quarks hadronise into many **light hadrons** which share the jet energy
- Tracks from this vertex often have impact parameters consistent with zero
- **Long-lived light hadrons** (e.g. K_S^0 , Λ^0) can be produced, though they are more likely to decay very far (many cm) from the primary pp vertex

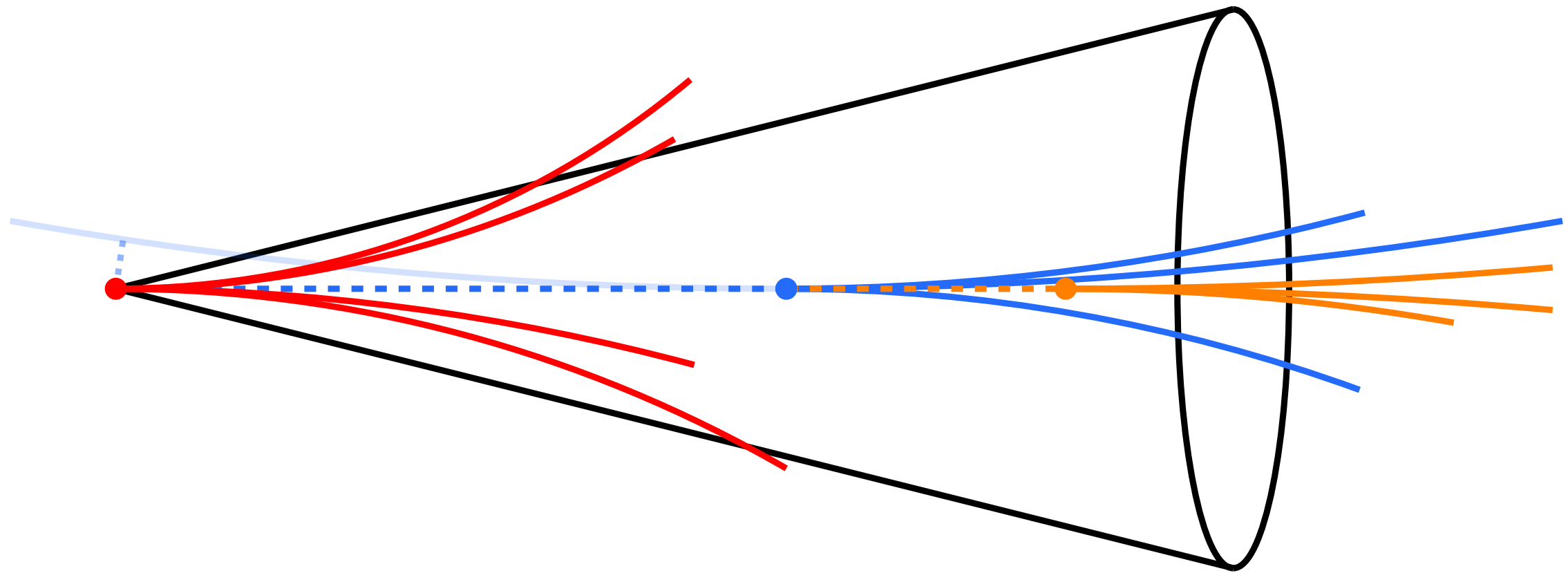
Anatomy of a c-jet



Typical Experimental Signature

- **c-quark fragments** into a **c-hadron** which carries around half of the jet energy
- **c-hadron decay vertex** often displaced from the **primary pp vertex** by a few mm
- Tracks from this vertex can often have **large impact parameters**

Anatomy of a b-jet



Typical Experimental Signature

- ***b*-quark fragments** into a ***b*-hadron** which carries most of the jet energy
- Most ***b*-hadrons** ($\approx 90\%$) decay into ***c*-hadrons**
- ***b*-hadron decay vertex** often displaced from the **primary *pp* vertex** by a few mm
- Subsequent ***c*-hadron decay vertex** often displaced by a further few mm
- Tracks from both of these vertices often have **large impact parameters**

- If a b hadron is found the jet is labeled as a b jet.
- If no b hadron is found, but a c hadron is present, then the jet is labeled as a c jet.
- Otherwise the jet is labeled as a light-flavor jet.

Introduction to charm jet tagging

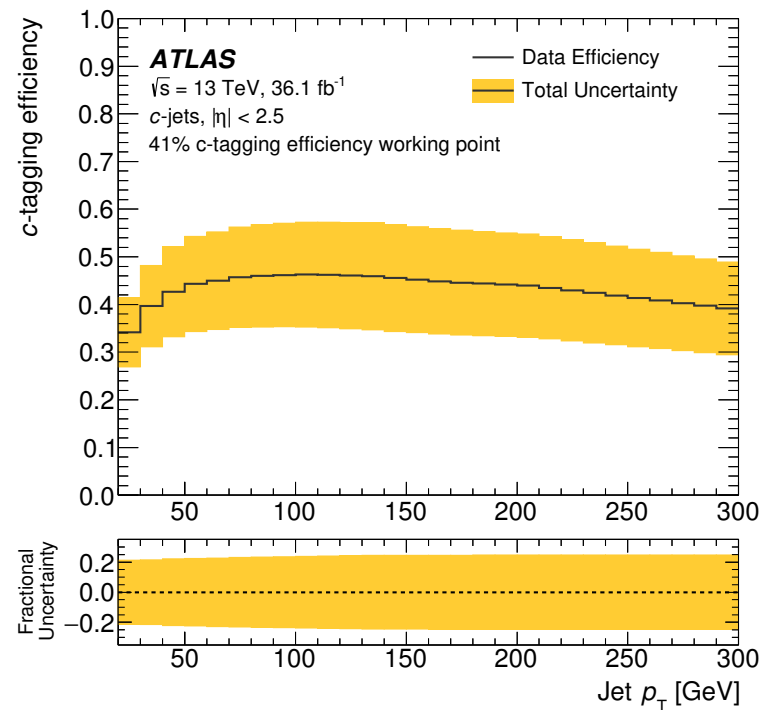
“Exclusive” charm jet tagging

- Focus on the full reconstruction of exclusive c -hadron decay chains (e.g. $D^{*\pm} \rightarrow D^0(K^-\pi^+)\pi^\pm$) or leptons from semi-leptonic c -hadron decays
- ✓ Can often provide a very pure sample of jets containing c -hadrons
- ✗ The efficiency is typically low $\mathcal{O}(1\%)$, limited by the c -hadron branching fractions of interest

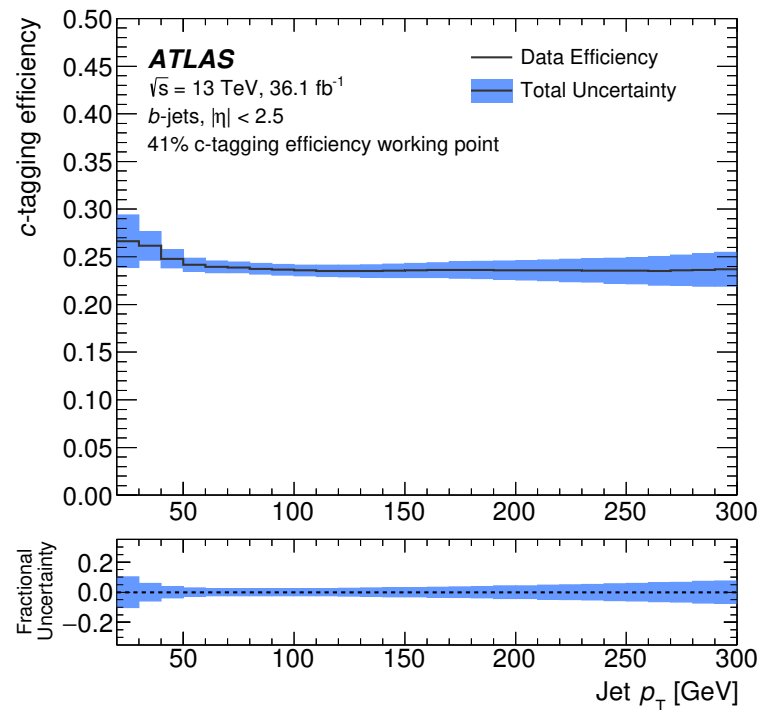
“Inclusive” charm jet tagging

- An alternative approach is to exploit more “inclusive” observables, such as track impact parameters or secondary vertices
- ✓ The efficiency of this approach is typically very high $\mathcal{O}(10\%)$
- ✗ The c -jet purity is often lower than these “traditional” approaches
- More suited for use with machine learning (ML) techniques

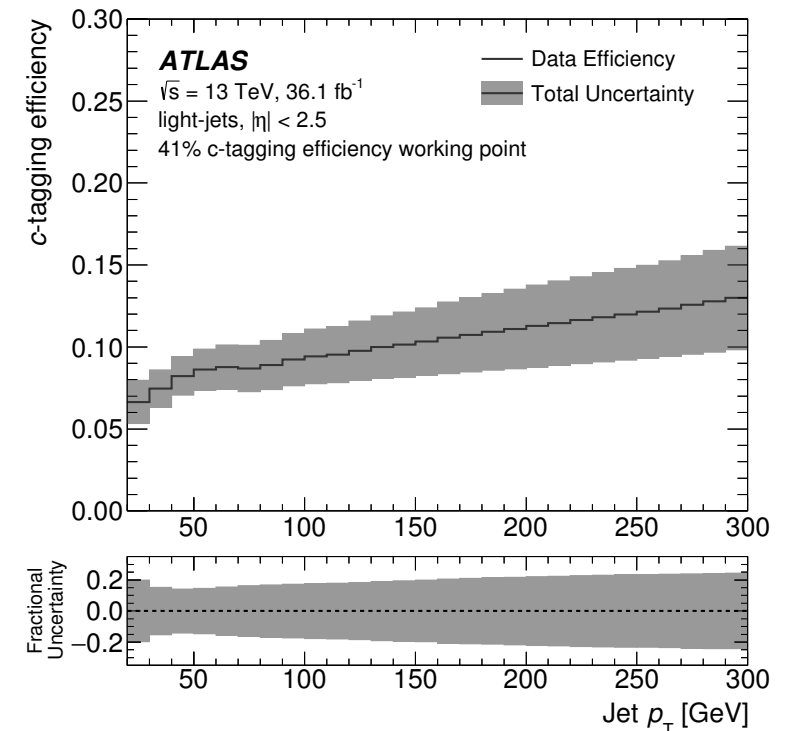
Performance of the ATLAS c-tagger



c-jets



b-jets

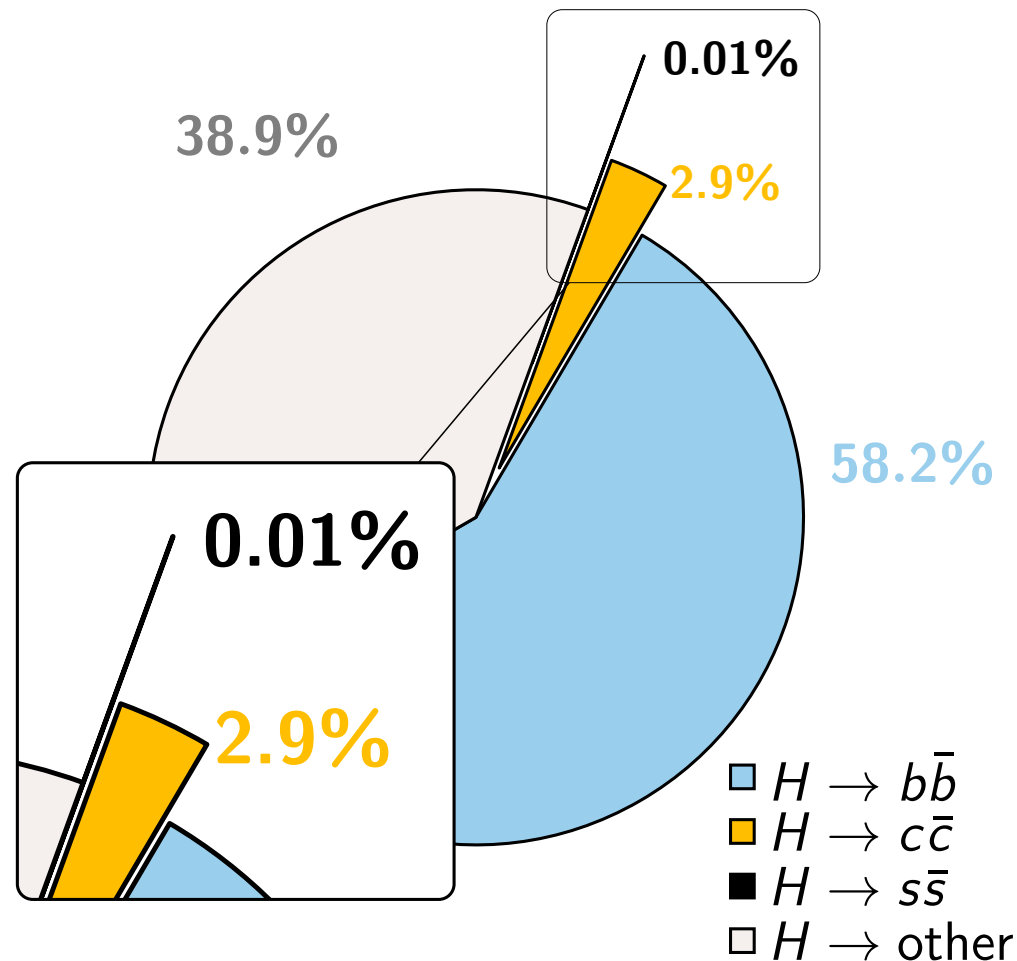


light flavour (*u, d, s, g*) jets

c-tagging efficiency for *b*-, *c*- and light flavour jets measured in data ↑

- Working point for $H \rightarrow c\bar{c}$ exhibits a *c*-jet tagging efficiency of around 40%
- Rejects *b*-jets by around a factor $4\times$ and light jets by around a factor $10\times$
- Efficiency calibrated in data with samples of *b*-jets from $t \rightarrow Wb$ decays and *c*-jets from $W \rightarrow cs, cd$ decays (in $t\bar{t}$ events)
- Typical total relative uncertainties of around **25%**, **5%** and **20%** for ***c*-**, ***b*-** and **light jets**, respectively

$$H > CC$$



What are the existing indirect constraints?

- Constraints on unobserved Higgs decays impose $\mathcal{B}(H \rightarrow c\bar{c}) < 20\%$, while global fits indirectly bound Γ_H leading to $y_c/y_c^{SM} < 6$, **assuming SM production and no BSM decays** (arXiv:1310.7029, arXiv:1503.00290)
- Direct bound of around $\Gamma_H < 1$ GeV from $H \rightarrow \gamma\gamma$ and $H \rightarrow 4\ell$ lineshapes impose around $y_c/y_c^{SM} < 120$, **but this is model independent** (arXiv:1503.00290)

H > cc at the LHC

Idea 1 - Exclusive $H \rightarrow J/\psi \gamma$ decays

- Rare exclusive radiative Higgs boson decays to vector mesons are sensitive to the $Hq\bar{q}$ couplings (arXiv:1503.00290)
- The $H \rightarrow J/\psi \gamma$ decay has been proposed as a clean probe of the $Hc\bar{c}$ coupling, though decay width “only” evolves as $(\text{const.} + y_c)^2$ ($\text{const.} \gg y_c$)
- ATLAS pioneered searches in this channel during Run 1 (arXiv:1501.03276)

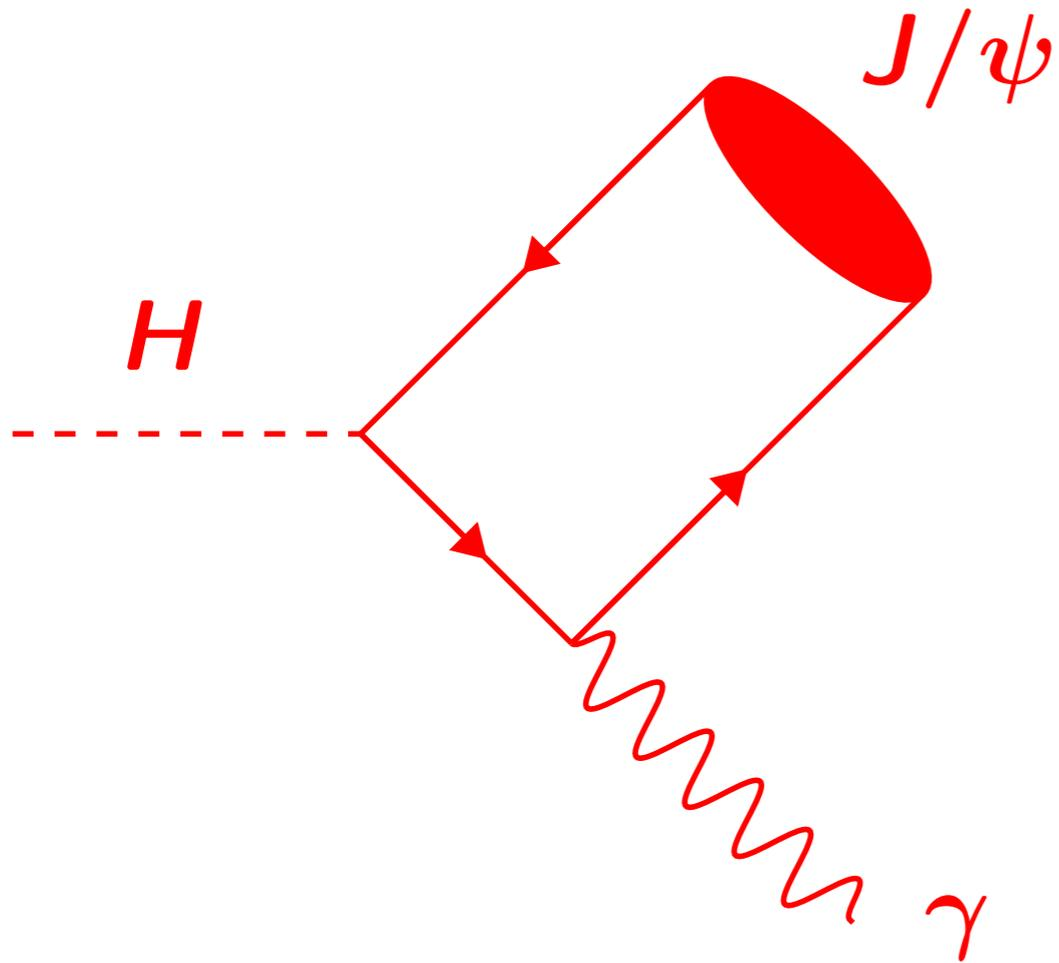
Idea 2 - Associated production of a Higgs boson and charm quark

- Tree level sensitivity to $Hc\bar{c}$ coupling (arXiv:1507.02916, arXiv:1606.09253)
- Use jet c -tagging to identify charm quark signature and a suitably “clean” Higgs decay (e.g. $H \rightarrow \gamma\gamma$)
- Alternatively, study p_T^H distribution to look for potential shape modifications...

Idea 3 - Inclusive $H \rightarrow c\bar{c}$ decays (The focus of this seminar...)

- Inclusive $H \rightarrow c\bar{c}$ decays are directly sensitive to the $Hc\bar{c}$ coupling, with the decay width evolving as $\Gamma_{H \rightarrow c\bar{c}} \propto y_c^2$
- Use double jet c -tagging and focus on VH ($V = W, Z$) production with leptonic V decays to mitigate the large multi-jet backgrounds

$$H > J/\psi + \gamma$$



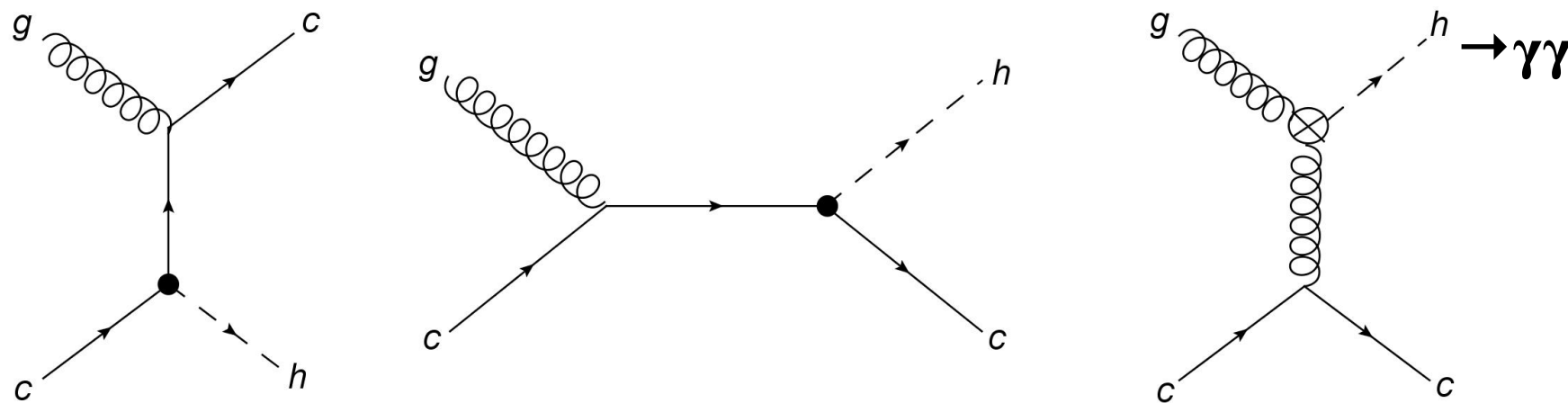
$$\mathcal{B}(H \rightarrow J/\psi \gamma) = (2.99 \pm 0.16) \times 10^{-6}$$

Expt.	95% CL upper limit on $\mathcal{B}(H \rightarrow J/\psi \gamma)$		
	Expected	Observed	Obs./ \mathcal{B}_{SM}
ATLAS [†]	$(3.0^{+1.4}_{-0.8}) \times 10^{-4}$	3.5×10^{-4}	117 ×
CMS [‡]	$(5.2^{+2.4}_{-1.6}) \times 10^{-4}$	7.6×10^{-4}	253 ×

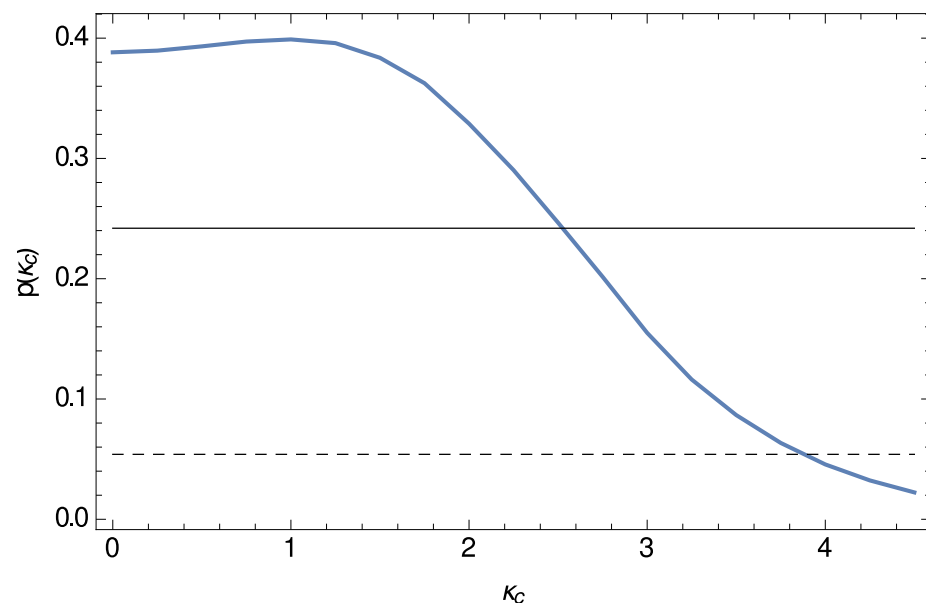
Phys. Lett. B 786 (2018) 134 (arXiv:1807.00802)

Associated Higgs boson + charm quark production

The production of Higgs boson in association with a charm quark is directly sensitive to the charm quark Yukawa coupling

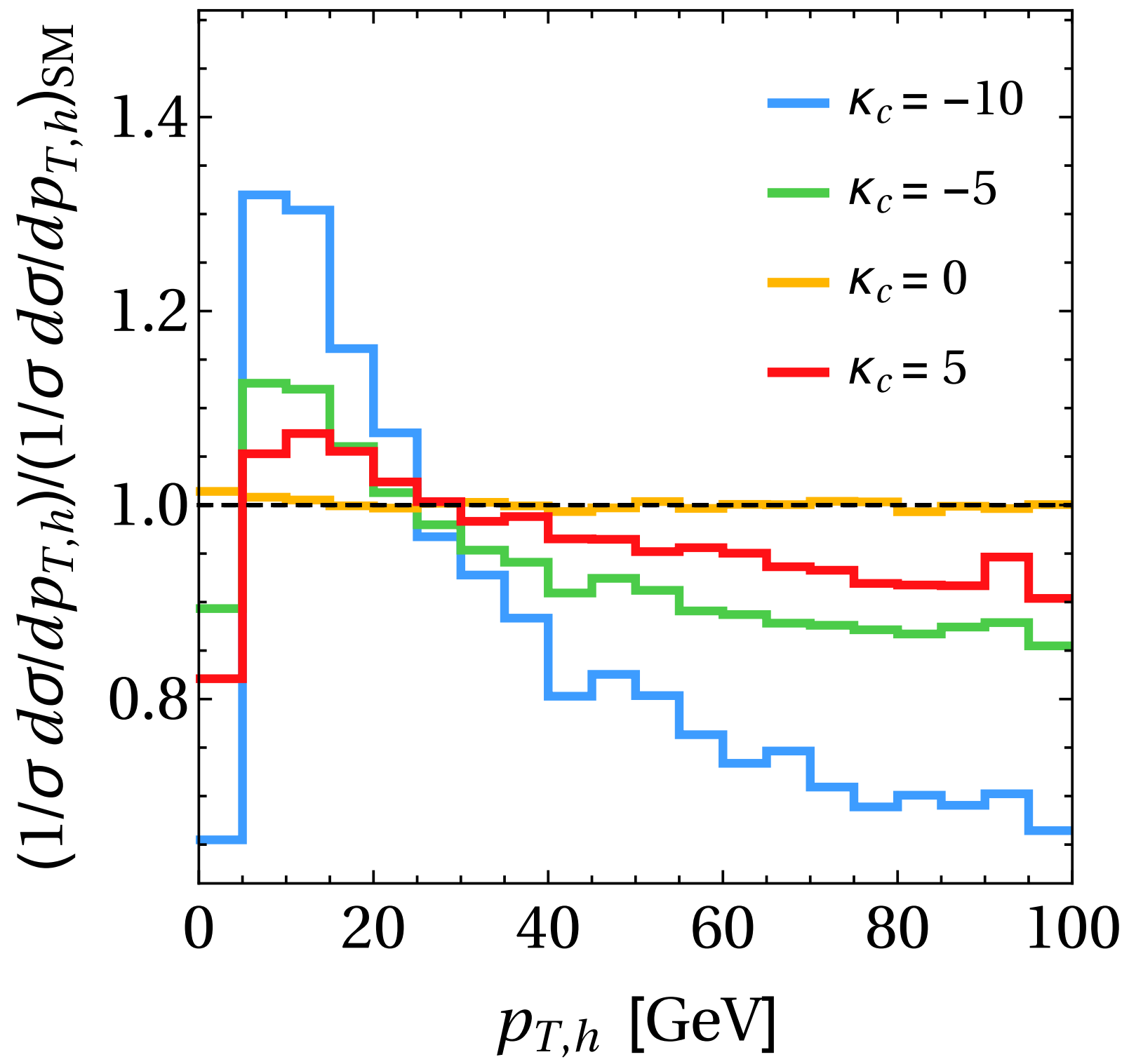


↑ Examples of “direct” (left and centre) and “indirect” (right) $cg \rightarrow Hc$ diagrams (from arXiv:1507.02916)

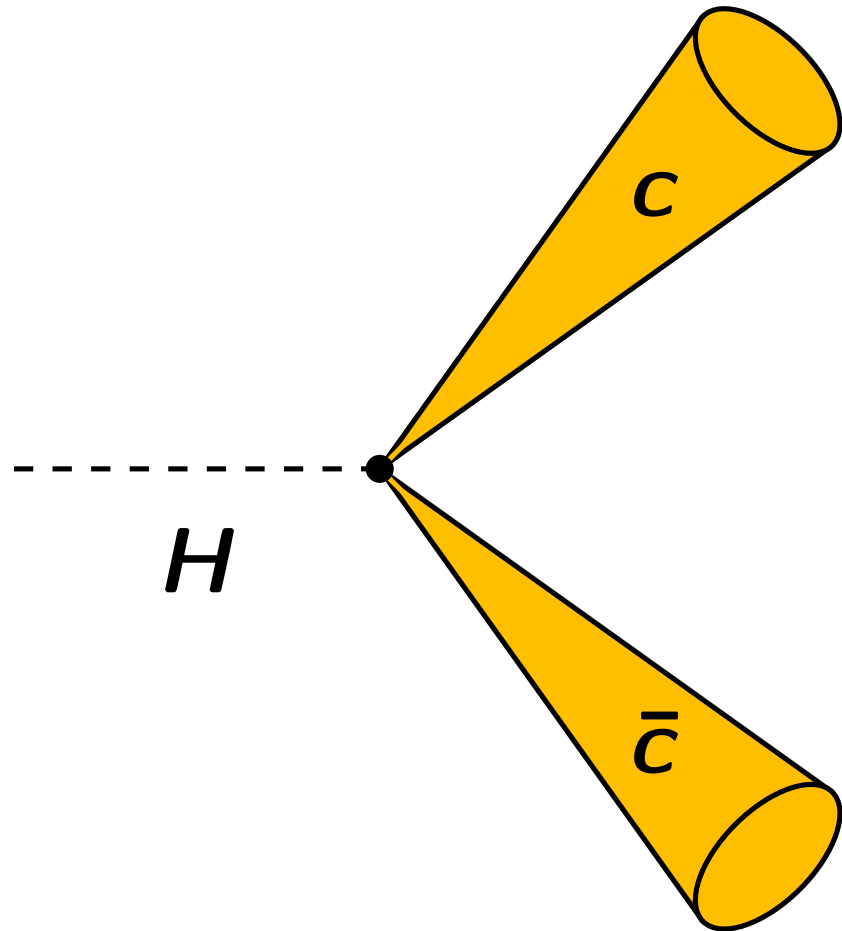


↑ Expected p -value as a function of $\kappa_c = y_c / y_c^{SM}$ (from arXiv:1507.02916)

- t -channel diagram (left) is expected to dominate the cross-section and is sensitive to the $Hc\bar{c}$ coupling, highly sensitive channel!
- No experimental measurements yet, though the sensitivity at the HL-LHC has been surveyed in the literature (arXiv:1507.02916)
- Assuming a data sample of 3 ab^{-1} at $\sqrt{s} = 14 \text{ TeV}$, $\mathcal{O}(1)$ constraints on y_c / y_c^{SM} are expected to be obtained...



Inclusive $H \rightarrow c\bar{c}$ decays

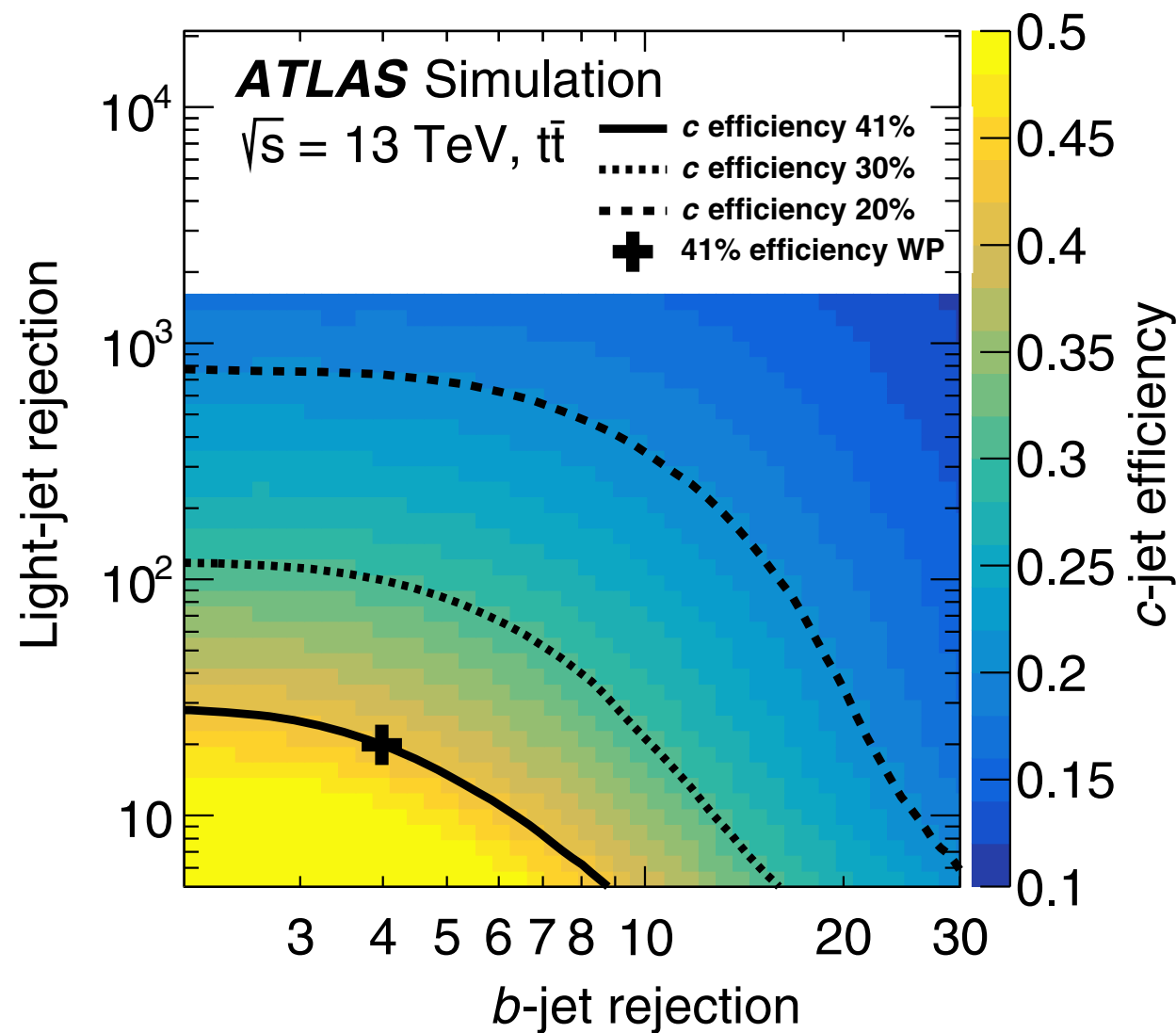


- In $\sqrt{s} = 13$ TeV pp collisions, one expects around 1600 $H \rightarrow c\bar{c}$ decays in every 1 fb^{-1} of data!
- **But**, how can we hope to separate $H \rightarrow c\bar{c}$ from the **HUGE** jet background at the LHC?

Search for the Decay of the Higgs Boson to Charm Quarks with the ATLAS Experiment

M. Aaboud *et al.**
(ATLAS Collaboration)

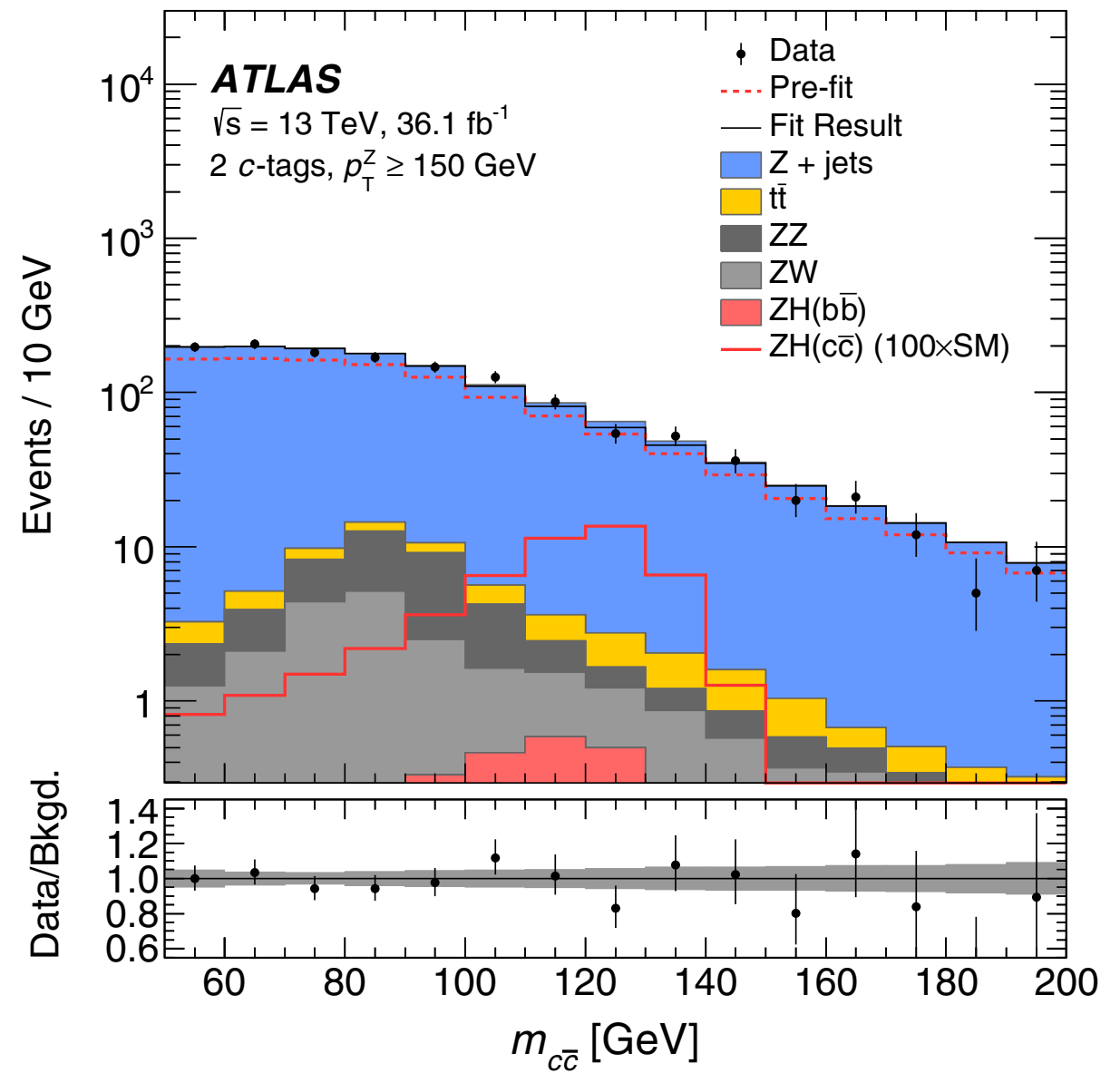
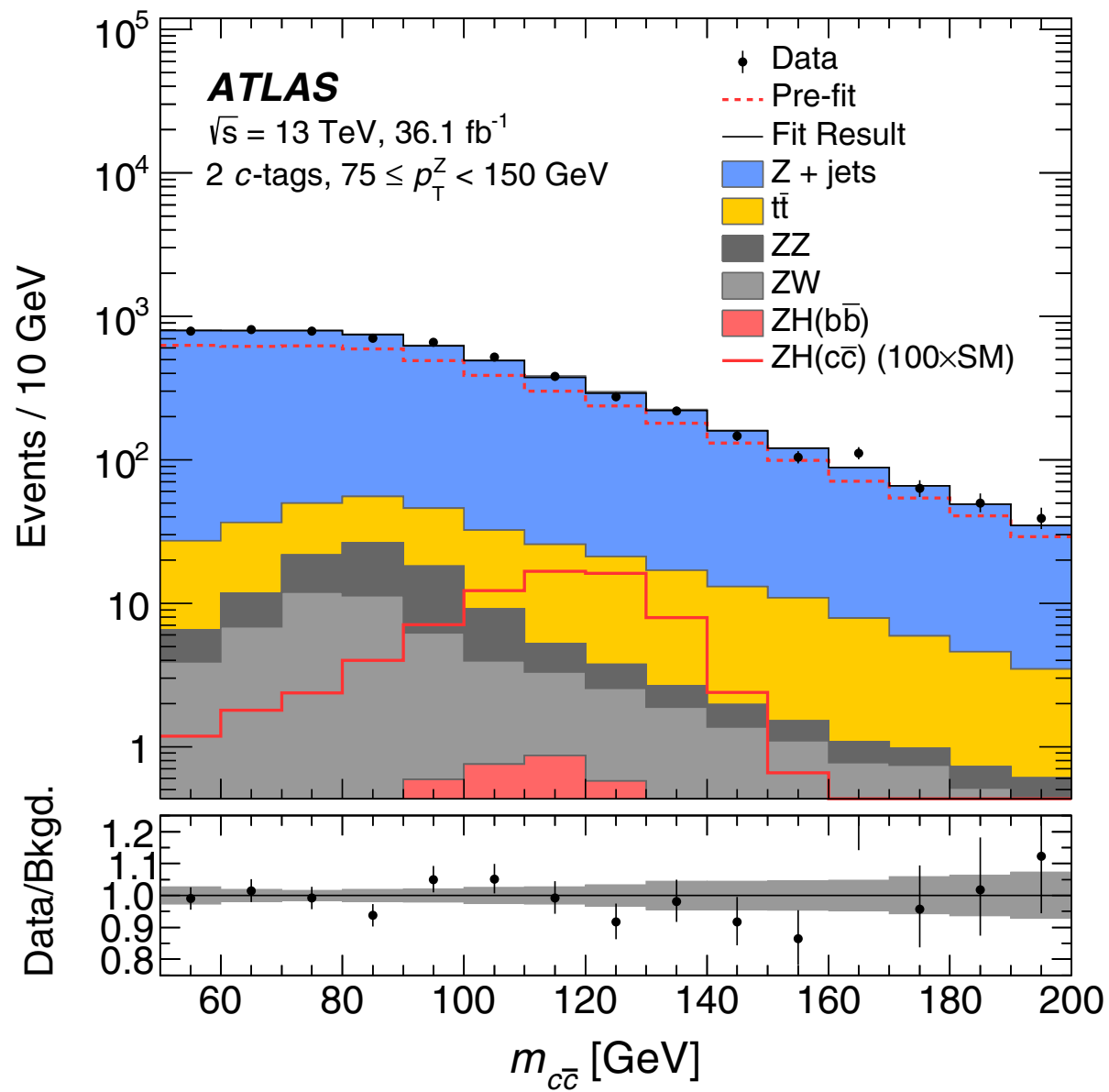
$$ZH \rightarrow \ell^+ \ell^- c \bar{c}$$



The c -jet-tagging efficiency (colored scale) as a function of the b jet and l jet rejection

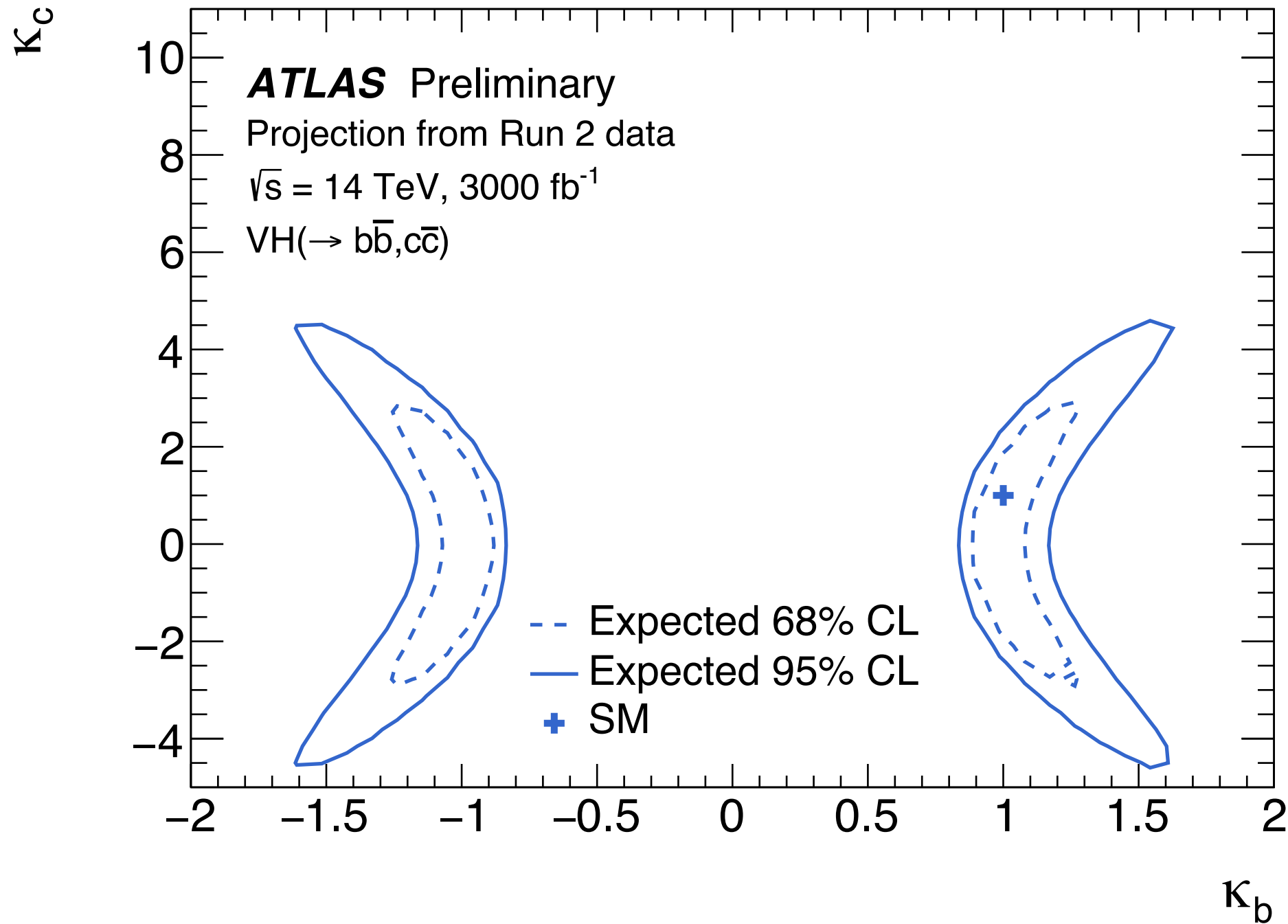
TABLE III. Postfit yields for the signal and background processes in each category from the profile likelihood fit. Uncertainties include statistical and systematic contributions. The prefit SM expected $ZH(c\bar{c})$ signal yields are indicated in parenthesis.

Sample	Yield, $50 \text{ GeV} < m_{c\bar{c}} < 200 \text{ GeV}$			
	1 c tag		2 c tags	
	$75 \leq p_{\text{T}}^Z < 150 \text{ GeV}$	$p_{\text{T}}^Z \geq 150 \text{ GeV}$	$75 \leq p_{\text{T}}^Z < 150 \text{ GeV}$	$p_{\text{T}}^Z \geq 150 \text{ GeV}$
$Z + \text{jets}$	69400 ± 500	15650 ± 180	5320 ± 100	1280 ± 40
ZW	750 ± 130	290 ± 50	53 ± 13	20 ± 5
ZZ	490 ± 70	180 ± 28	55 ± 18	26 ± 8
$t\bar{t}$	2020 ± 280	130 ± 50	240 ± 40	13 ± 6
$ZH(b\bar{b})$	32 ± 2	19.5 ± 1.5	4.1 ± 0.4	2.7 ± 0.2
$ZH(c\bar{c})$ (SM)	-143 ± 170 (2.4)	-84 ± 100 (1.4)	-30 ± 40 (0.7)	-20 ± 29 (0.5)
Total	72500 ± 320	16180 ± 140	5650 ± 80	1320 ± 40
Data	72504	16181	5648	1320



an observed upper limit on μ at the 95% C.L. of 110

22nd October 2021



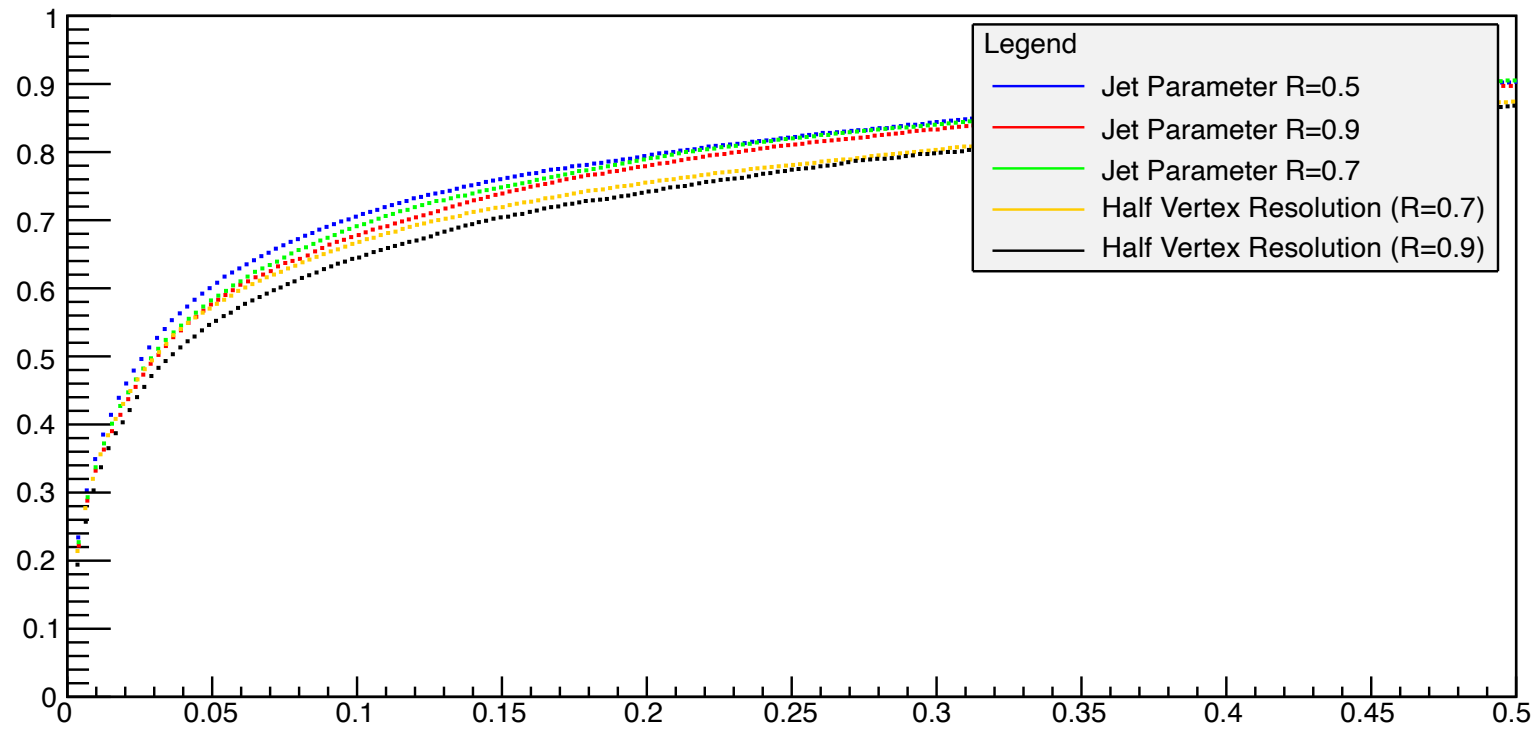
Can LHeC do better?

Higgs at LHeC vs Fcc-eh

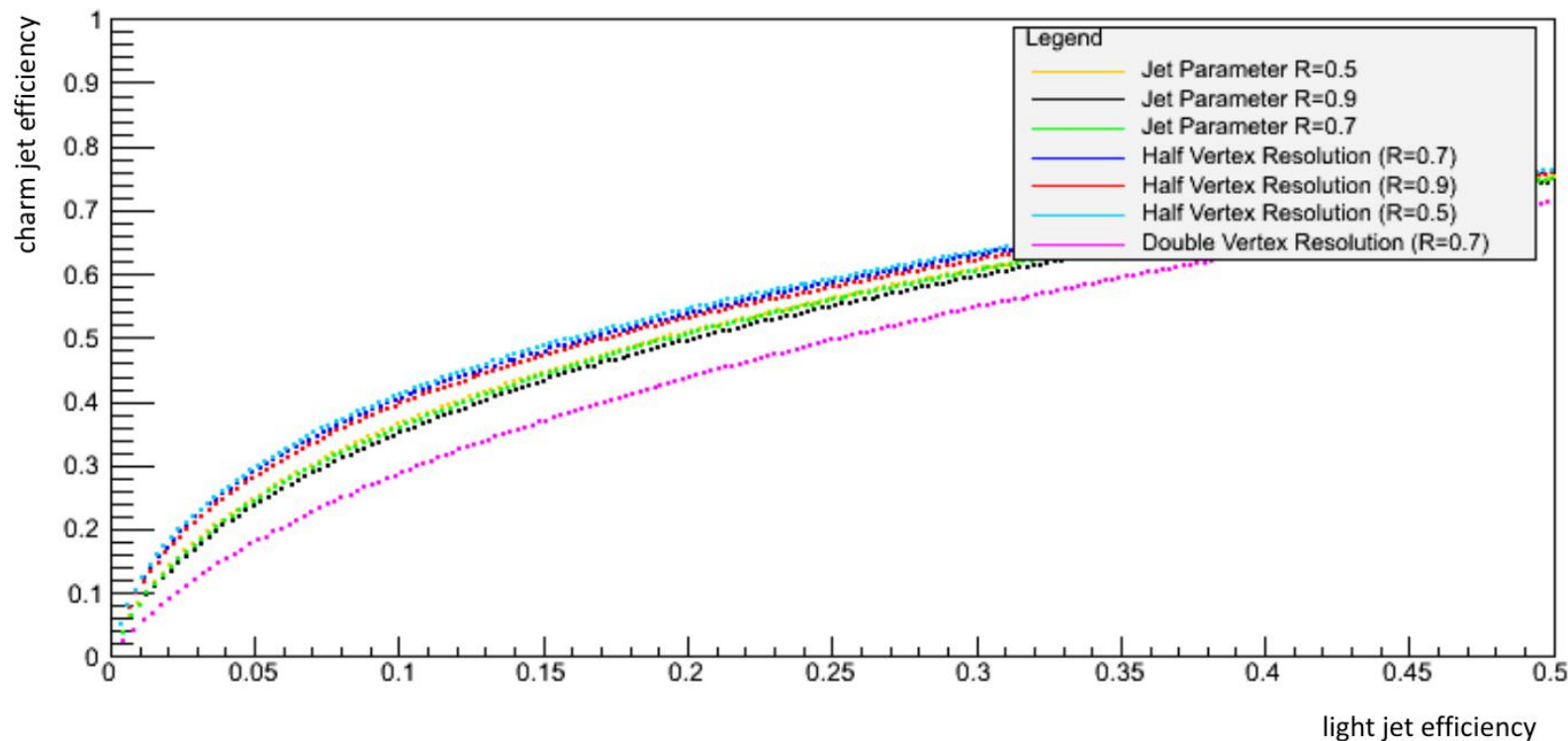
Channel	Fraction	Number of Events			
		Charged Current		Neutral Current	
		LHeC	FCC-eh	LHeC	FCC-eh
$b\bar{b}$	0.581	114 500	1 208 000	14 000	175 000
W^+W^-	0.215	42 300	447 000	5 160	64 000
gg	0.082	16 150	171 000	2000	25 000
$\tau^+\tau^-$	0.063	12 400	131 000	1 500	20 000
$c\bar{c}$	0.029	5700	60 000	700	9 000
ZZ	0.026	5 100	54 000	620	7 900
$\gamma\gamma$	0.0023	450	5 000	55	700
$Z\gamma$	0.0015	300	3 100	35	450
$\mu^+\mu^-$	0.0002	40	410	5	70
σ [pb]		0.197	1.04	0.024	0.15

H \rightarrow bb, cc

B-jet efficiency vs light-jet efficiency



C-jet efficiency vs light-jet efficiency



At DELPHES detector level using a CC multi-jet sample and for an integrated luminosity of 100 fb^{-1} . The coloured lines correspond to the choice of the anti-kt distance parameter R and different assumptions in the impact parameter resolution of 10 (5) μm (nominal, no text added in legend), 5 (2.5) μm (Half Vertex Resolution), 20 (10) μm (Double Vertex Resolution) for tracks with $0.5 < p_T < 5 (> 5) \text{ GeV}$ within $|\eta| < 3.5$.

Kinematics at ep

DIS Kinematics

$$s = (k+p)^2 = 4E_e E_p$$

$$Q^2 = -q^2 = (k-k')^2 = 2E_e E'_e (1 - \cos\theta'_e)$$

$$v = q \cdot p / M_p$$

$$v_{\max} = s / (2M_p)$$

$$y = (q \cdot p) / (k \cdot p) = v / v_{\max}$$

$$x = Q^2 / (2q \cdot p)$$

$$W^2 = (p+q)^2 = M_p^2 - Q^2 + 2M_p v$$

Centre-of-mass energy squared

Negative squared four momentum transfer

Energy transfer in proton rest frame

Maximum energy transfer

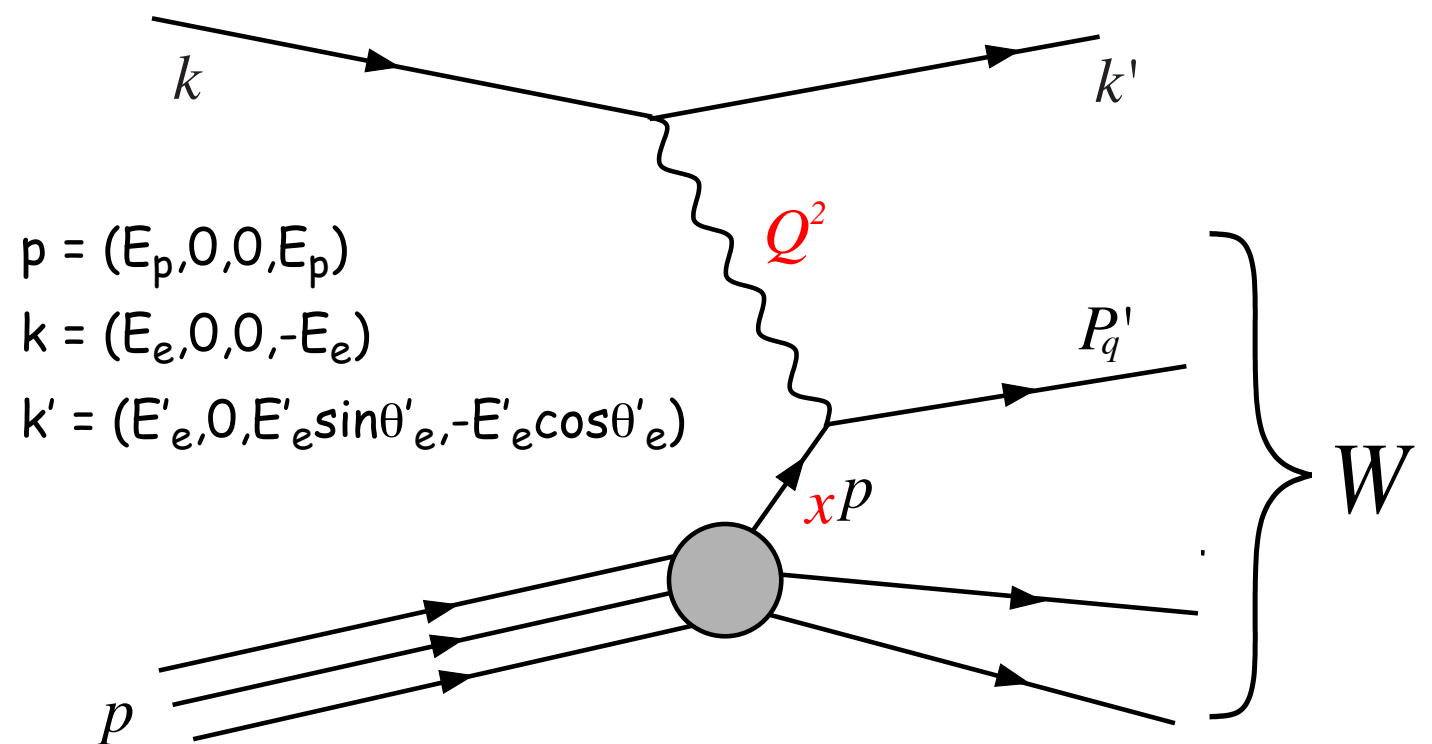
Fraction of energy transfer

Bjorken scaling variable

Invariant mass of total hadronic system

$$Q^2 = sxy$$

At fixed s only two independent variables



CDR-1: $h \rightarrow bb$ through CC

- **cut (1): Primary cuts**

- Exclude electron-tagged events

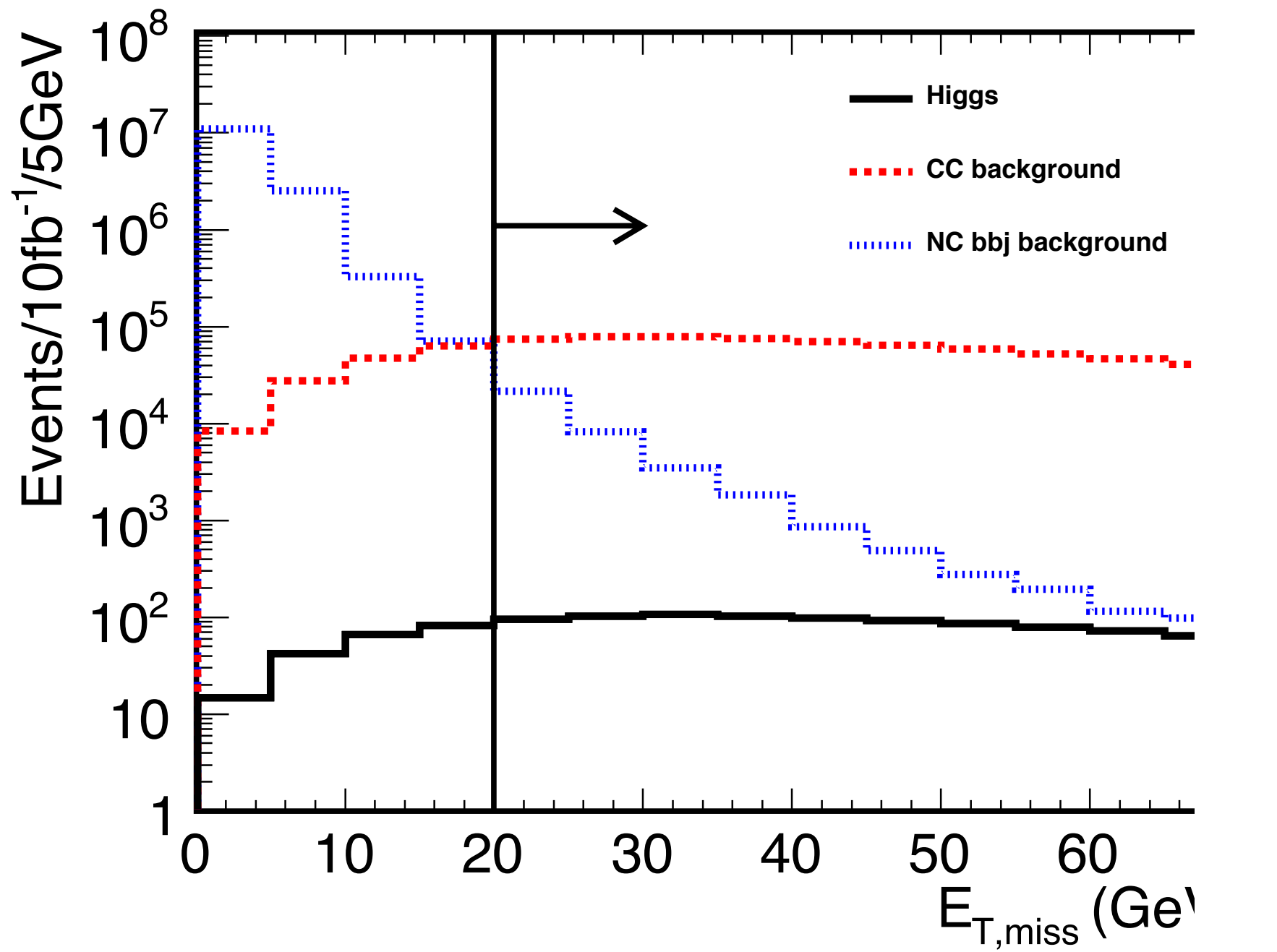
- $E_{T,miss} > 20 \text{ GeV}$

- $N_{jet}(P_{T,jet} > 20 \text{ GeV}) \geq 3$

- $E_{T,total} > 100 \text{ GeV}$

- $y_{JB} < 0.9$, where $y_{JB} = \Sigma(E - p_z)/2E_e$, as shown in Fig. 5.27 c)

- $Q_{JB}^2 > 400 \text{ GeV}$, where $Q_{JB}^2 = E_{T,miss}^2/(1 - y_{JB})$, as shown in Fig. 5.27 d)

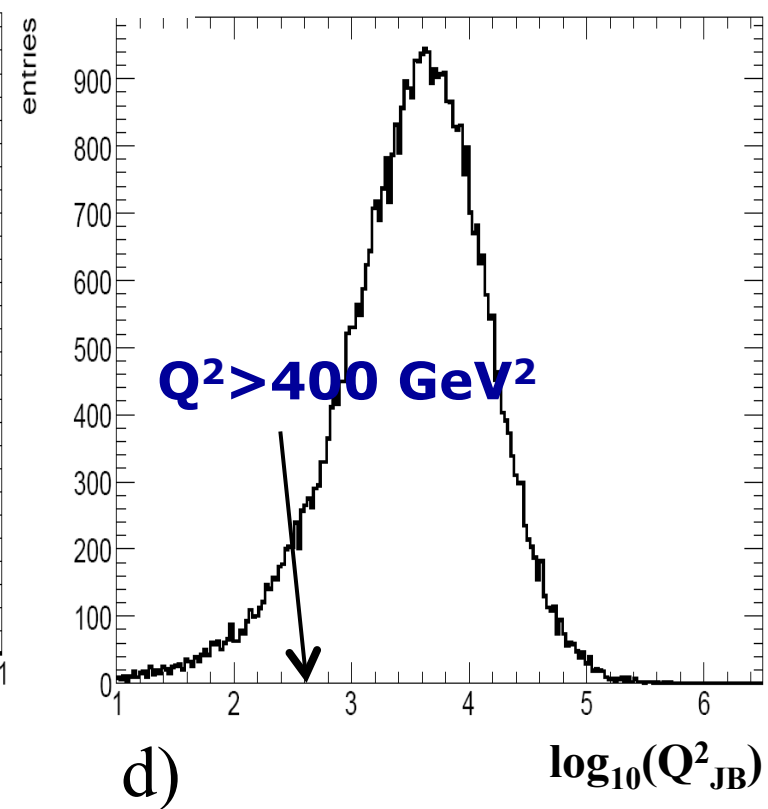
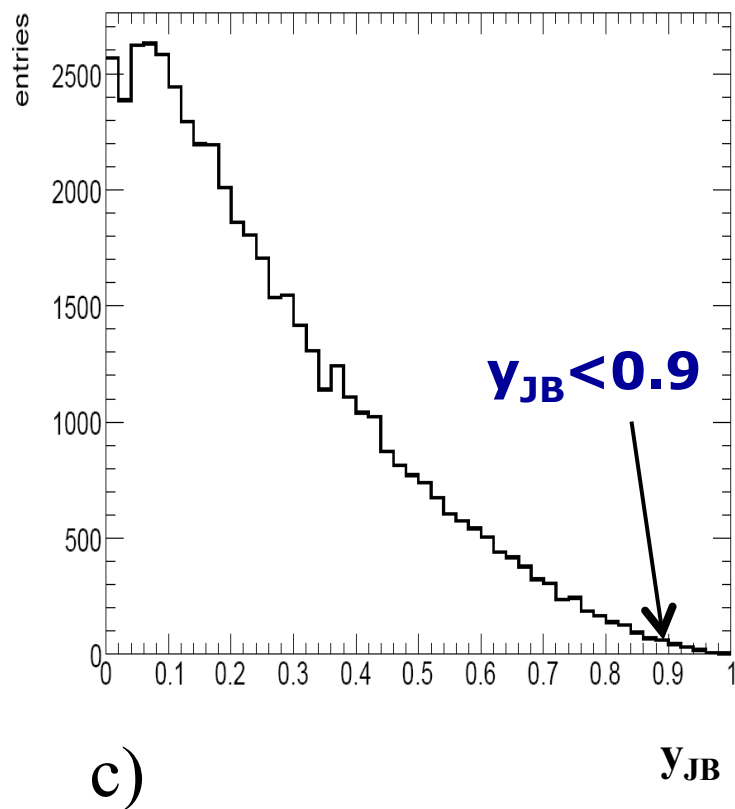
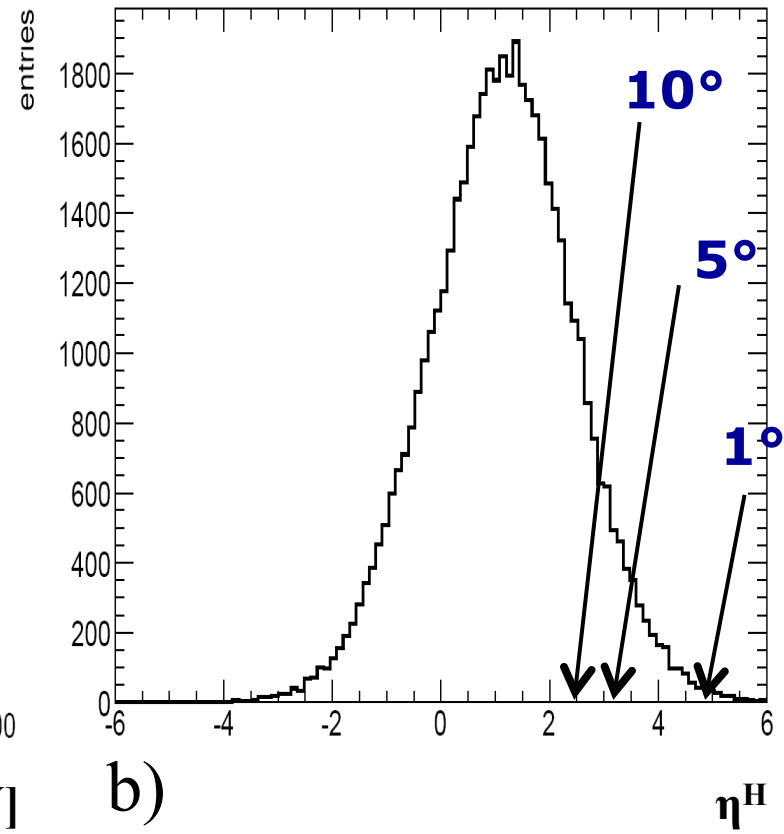
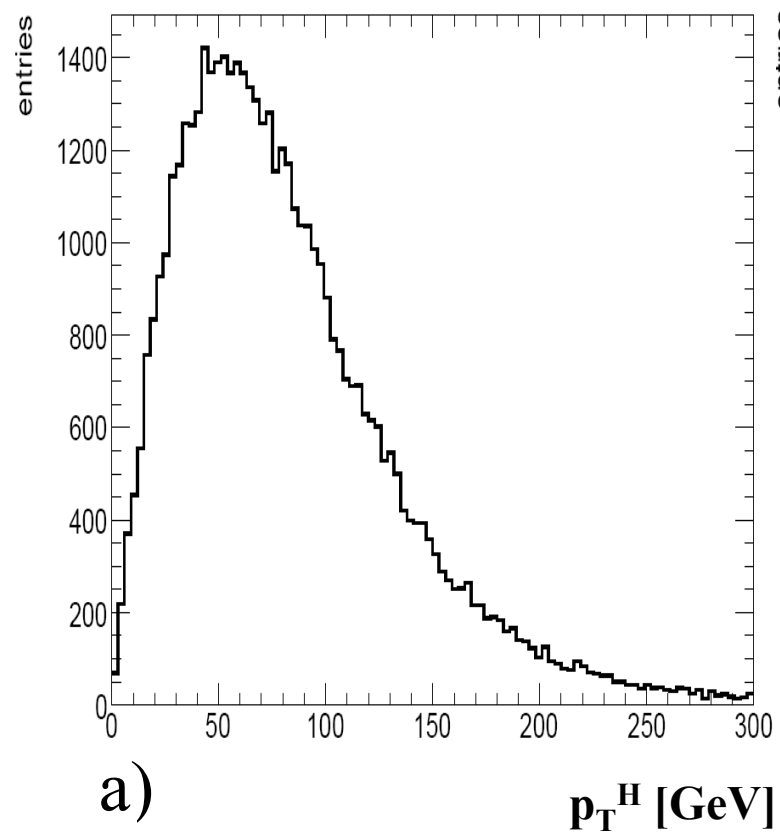


CDR-1: $h \rightarrow bb$ through CC

- **cut (1): Primary cuts**

- Exclude electron-tagged events
- $E_{T,miss} > 20 \text{ GeV}$
- $N_{jet}(P_{T,jet} > 20 \text{ GeV}) \geq 3$
- $E_{T,total} > 100 \text{ GeV}$
- $y_{JB} < 0.9$, where $y_{JB} = \Sigma(E - p_z)/2E_e$, as shown in Fig. 5.27 c)
- $Q_{JB}^2 > 400 \text{ GeV}$, where $Q_{JB}^2 = E_{T,miss}^2/(1 - y_{JB})$, as shown in Fig. 5.27 d)

Kinematics of the Higgs boson at LHeC



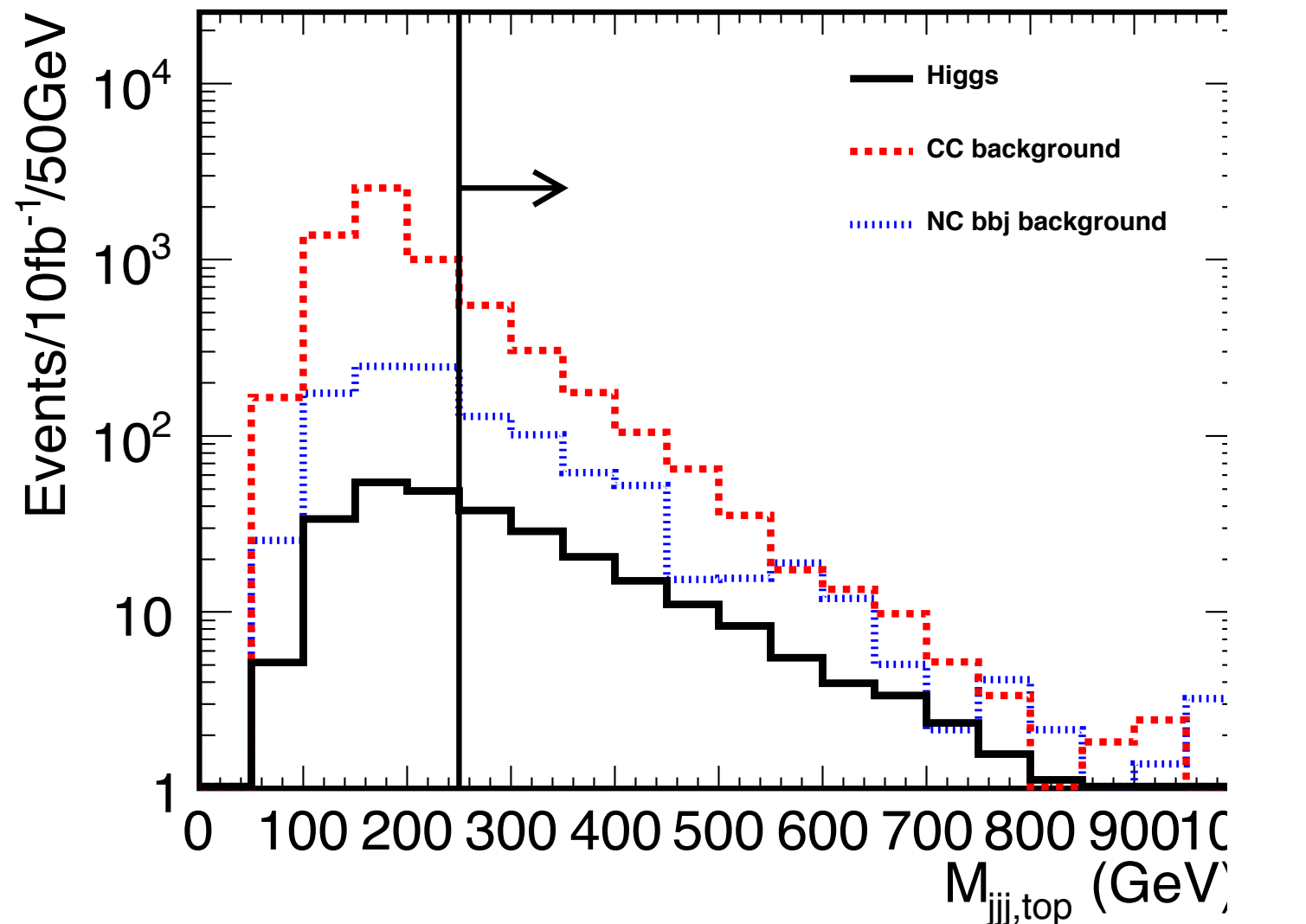
- **cut (2): b-tag requirement**

- $N_{b\text{-jet}}(P_{T,\text{jet}} > 20 \text{ GeV}) \geq 2$, where b-jet means a b-tagged jet

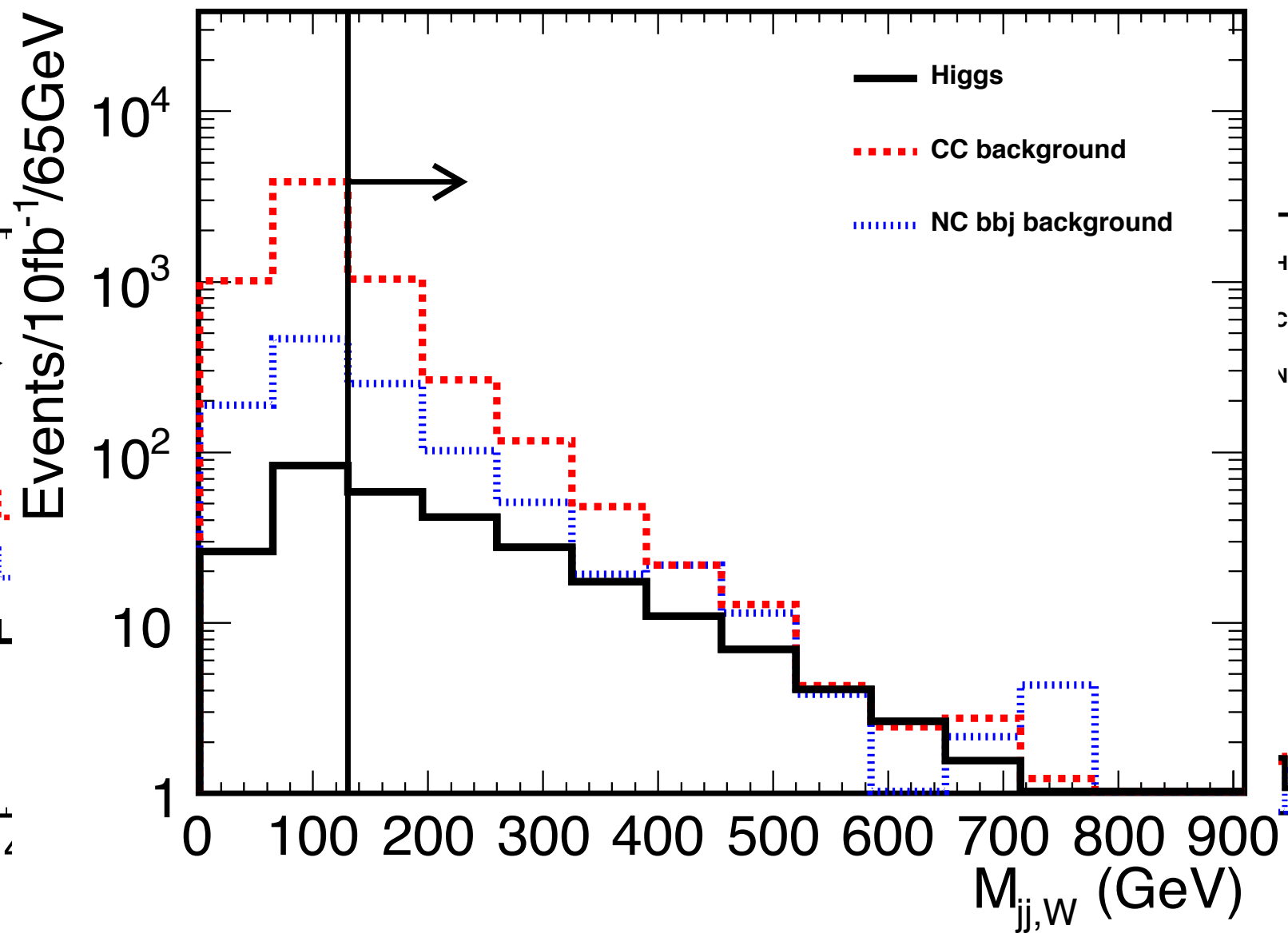
- **cut (3): Higgs invariant mass cut**

- $90 < M_H < 120 \text{ GeV}$; due to the energy carried by the neutrino from b decays, the mass peaks are slightly lower than the true Higgs mass

- **cut (4): Rejection of single top production** Single top events result in a final state with one b-jet and a W boson decaying into two light-quark jets. The following cuts are found to be efficient in suppressing this background.
 - $M_{jjj,top} > 250$ GeV, where the three-jet invariant mass ($M_{jjj,top}$) is reconstructed from three mainly centrally produced jets using two b-tagged jets with the lowest η and any third jet with the lowest η (b-tag not required for the third jet)

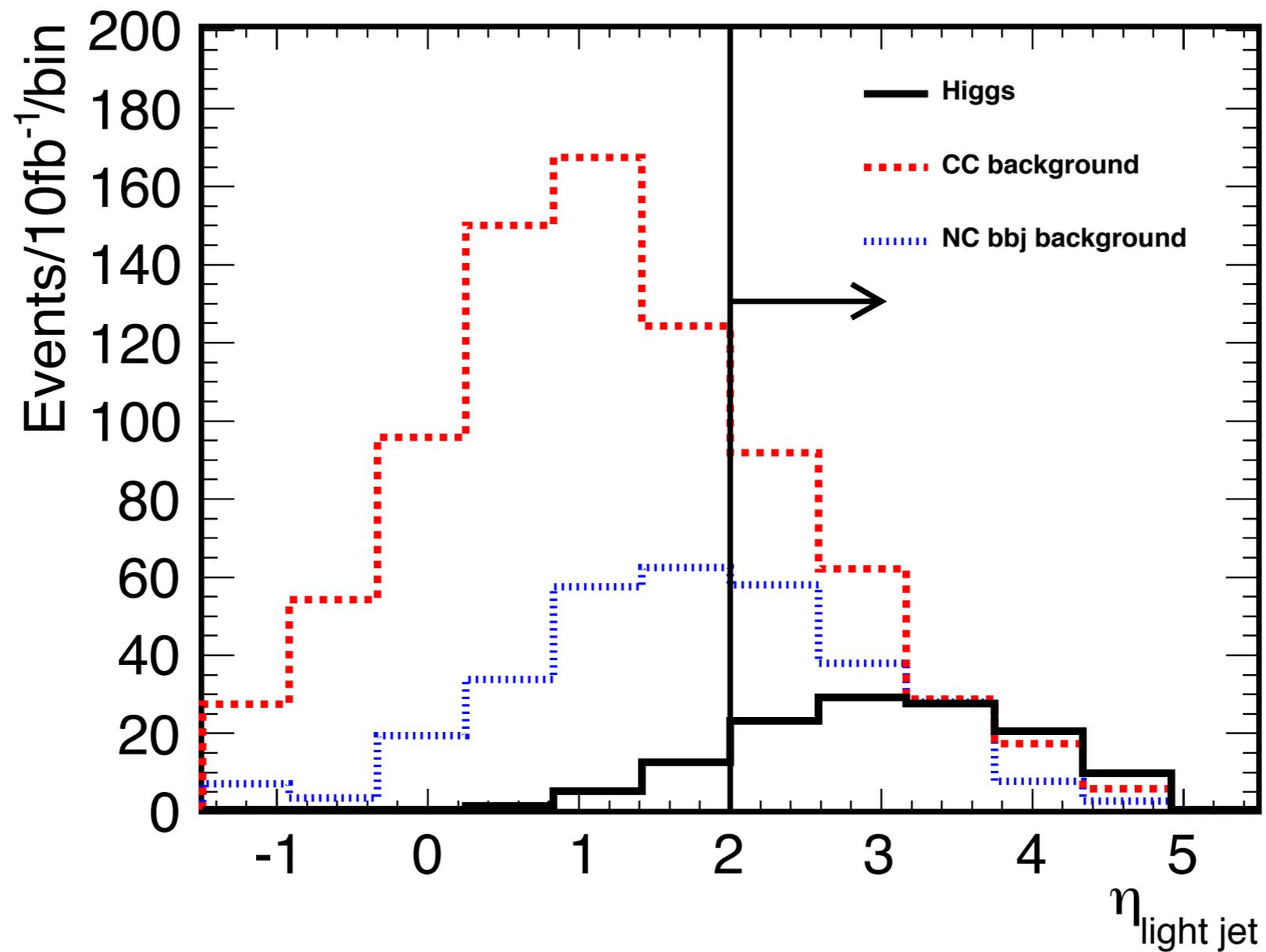


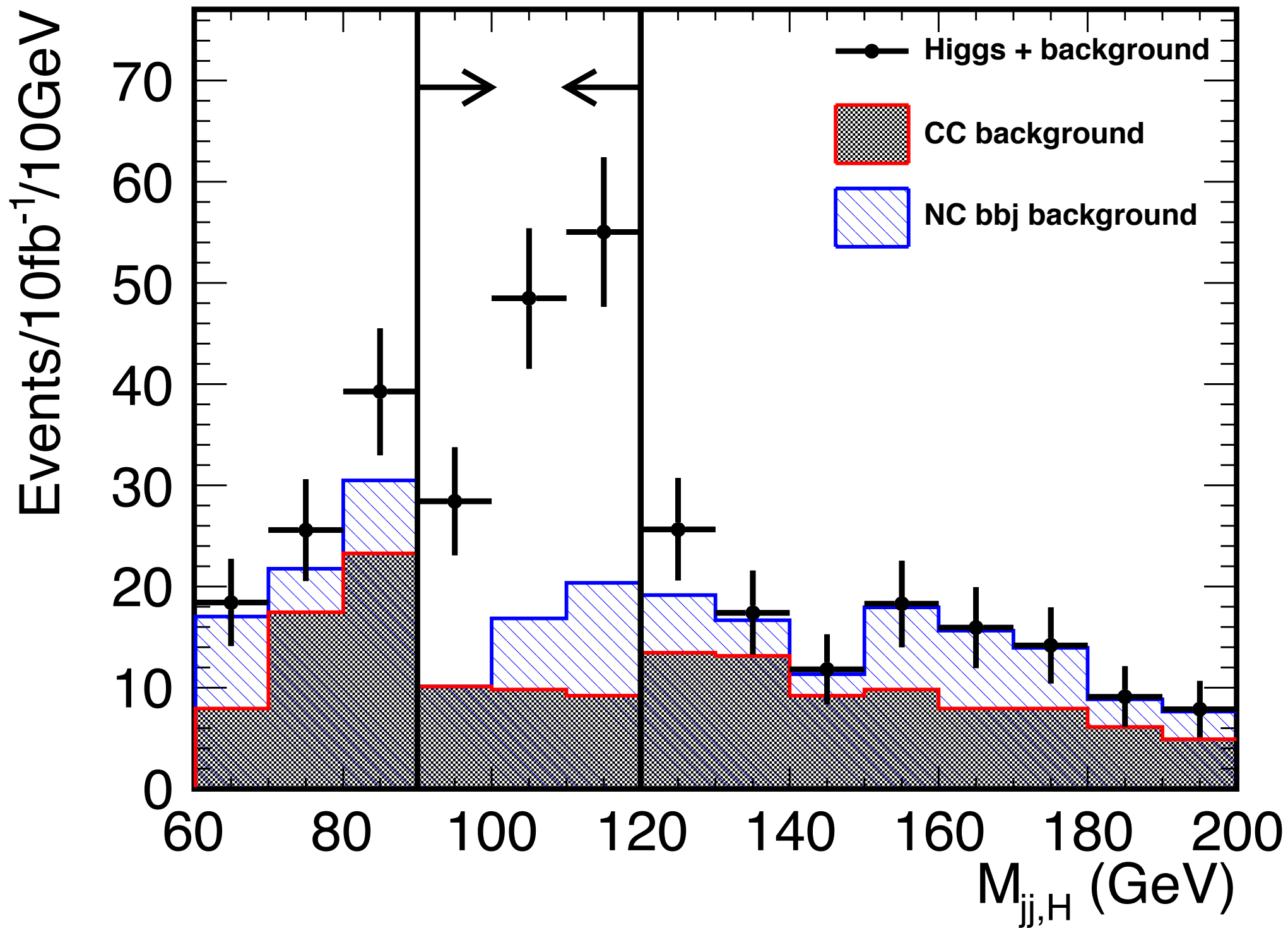
- $M_{jj,W} > 130 \text{ GeV}$, where the di-jet invariant mass ($M_{jj,W}$) is reconstructed from one b-tagged jet with the lowest η and any second jet with the lowest η regardless of b-tag but excluding the second lowest η b-jet



- cut (5): Forward jet tagging

- $\eta_{jet} > 2$ for the jet with the lowest pseudorapidity (lowest- η jet) but excluding the two b-tagged jets used to reconstruct the Higgs boson candidate



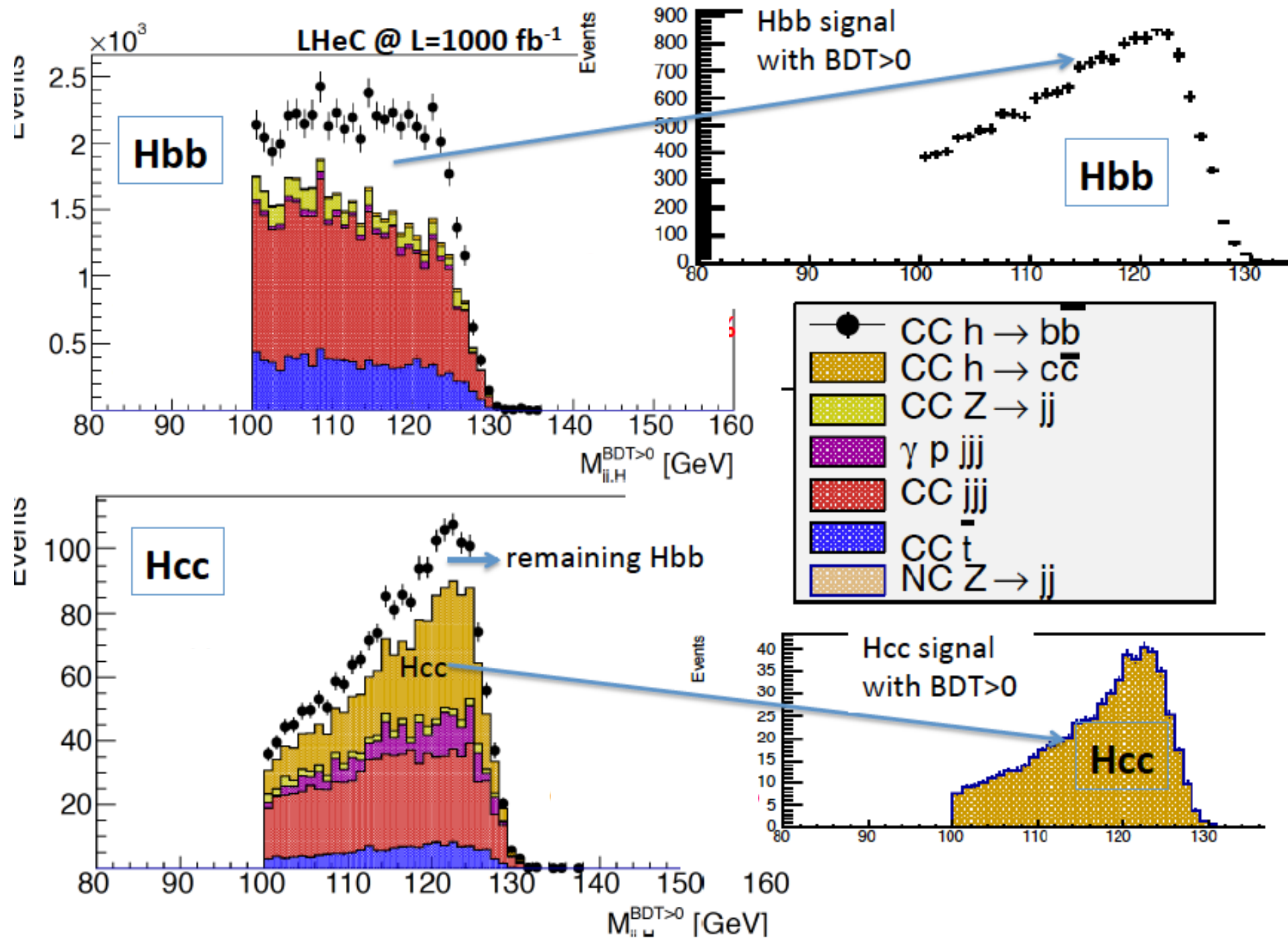


CDR 2020: $h \rightarrow b\bar{b}$

- CC DIS kinematic cuts of $Q_h^2 > 500 \text{ GeV}^2$, $y_h < 0.9$, missing energy $E_T^{\text{miss}} > 30 \text{ GeV}$, and no electrons in the final state to reject NC DIS;
- at least three anti-kt $R = 0.7$ jets with $p_T > 20 \text{ GeV}$ which are subject to further b-tagging requirements;
- a Higgs candidate from two b-tagged jets with b-tagging efficiencies of 60 to 75 %, charm (light quark) misidentification efficiencies of 10 to 5 % (1 %) ;
- rejection of single-top events via requiring a dijet W candidate mass of greater than 130 GeV and a three-jet top candidate mass of larger than 250 GeV using a combination with one of the b-jets of the Higgs mass candidate;
- a forward scattered jet with $\eta > 2$, and a large $\Delta\phi_{b, MET} > 0.2$ between the b-tagged jet and the missing energy.

The dominant backgrounds are CC DIS multijet and single top production.

The background due to multijets from photoproduction, where $Q^2 \sim 0$, can be reduced considerably due to the tagging of the small angle scattered electron with an electron tagger.

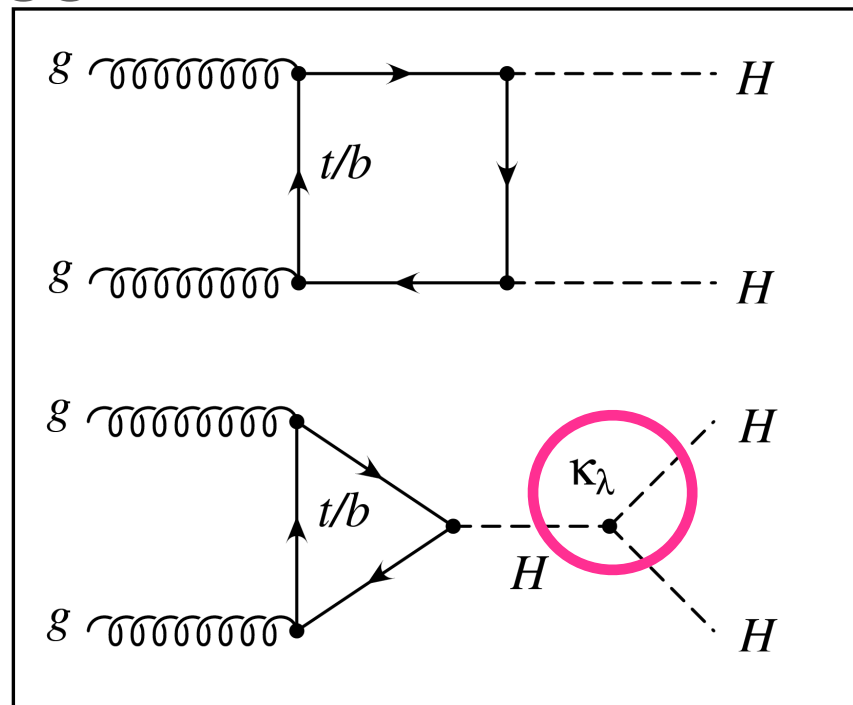


**5. Why is the ep collider
better for HHWW?**

HH: very challenging

Dominant!

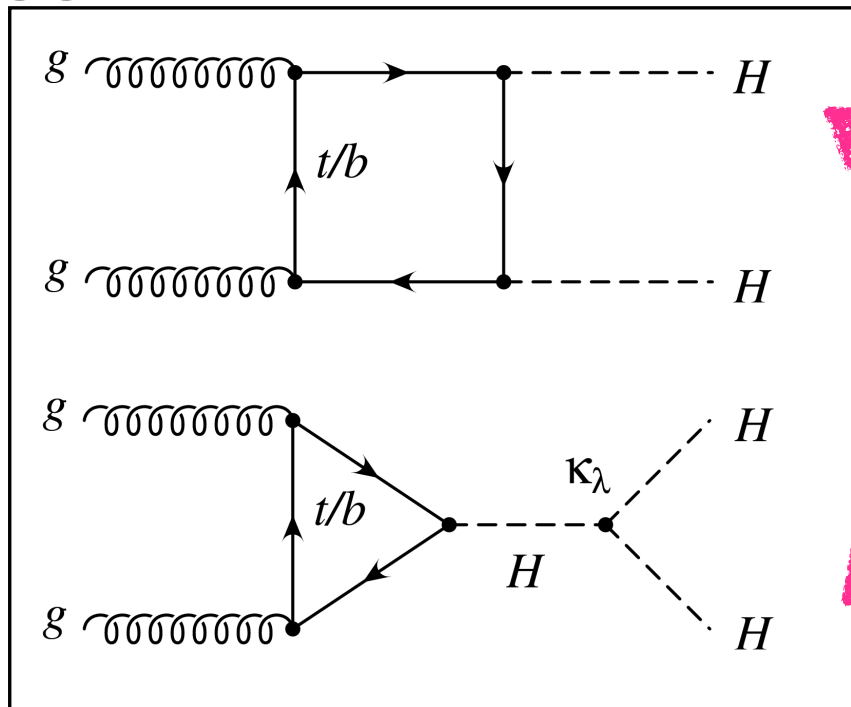
ggHH LO PRODUCTION



- ggHH sensitive to λ

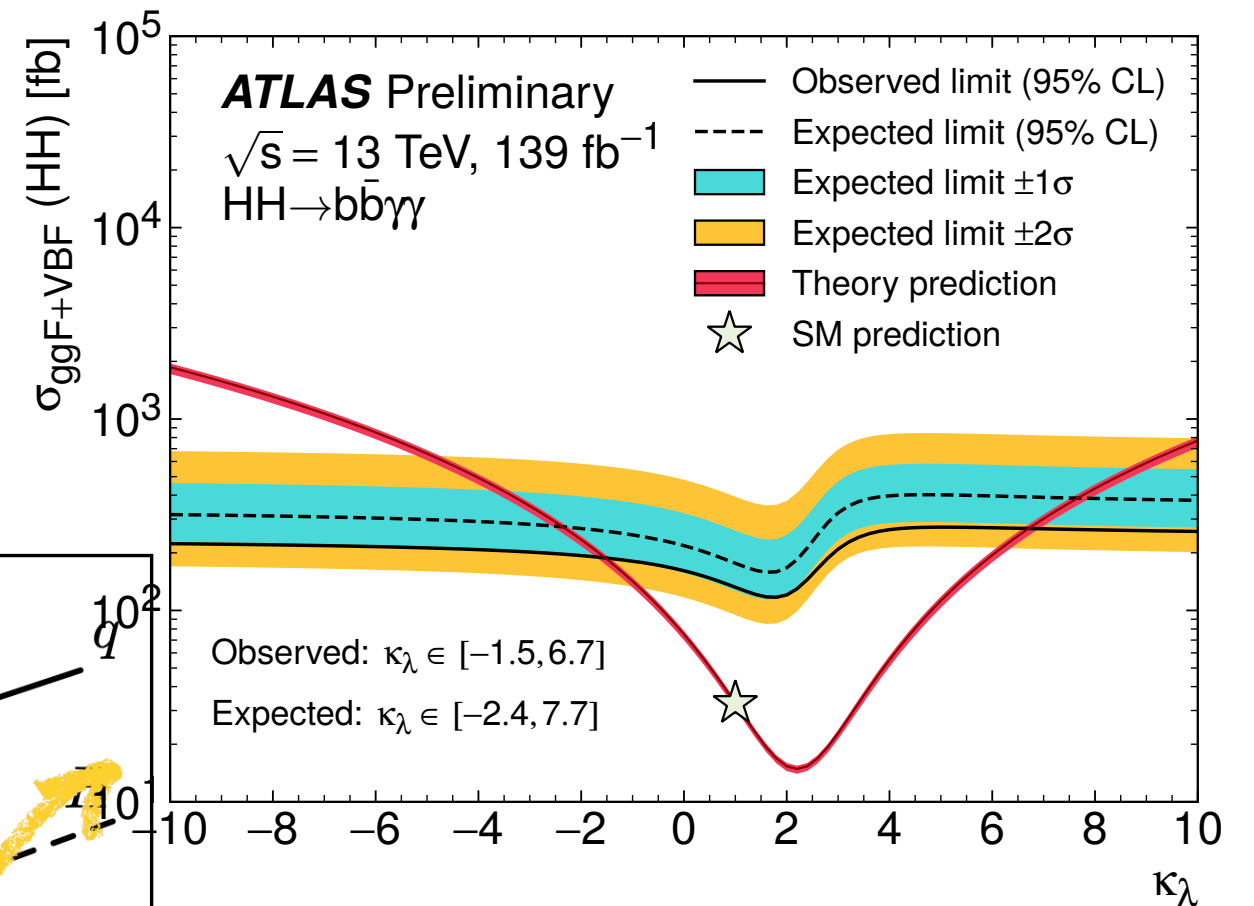
HH: very challenging

ggHH LO PRODUCTION



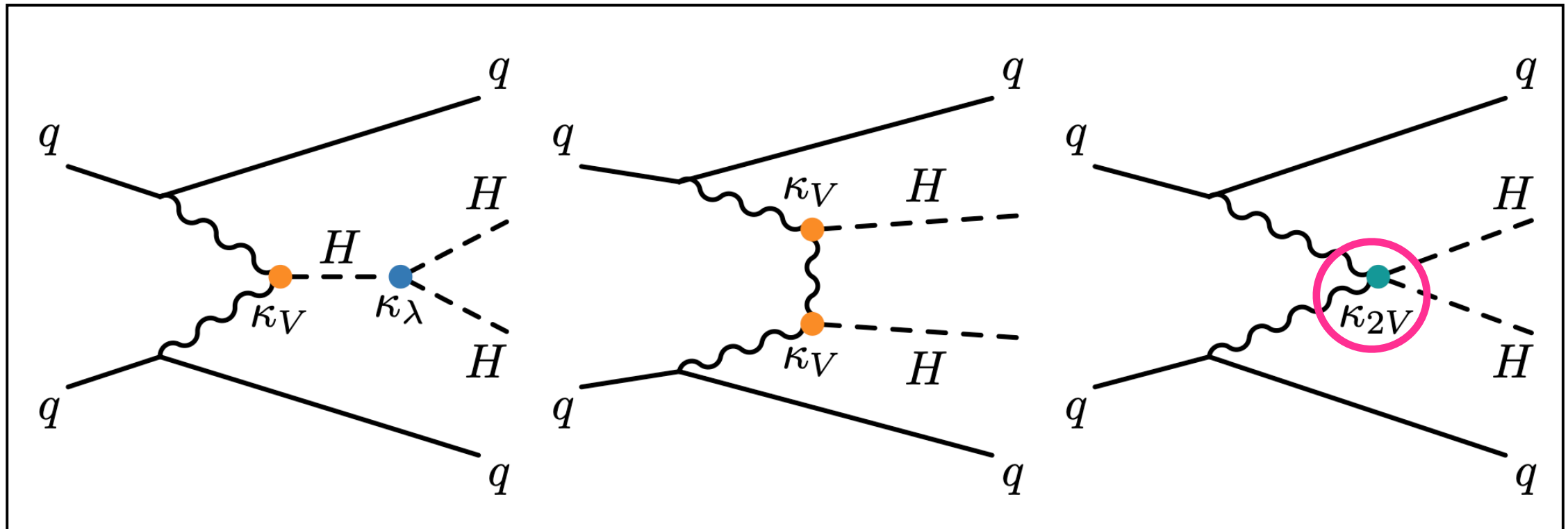
In the SM

Destructive interference b/w box and triangle

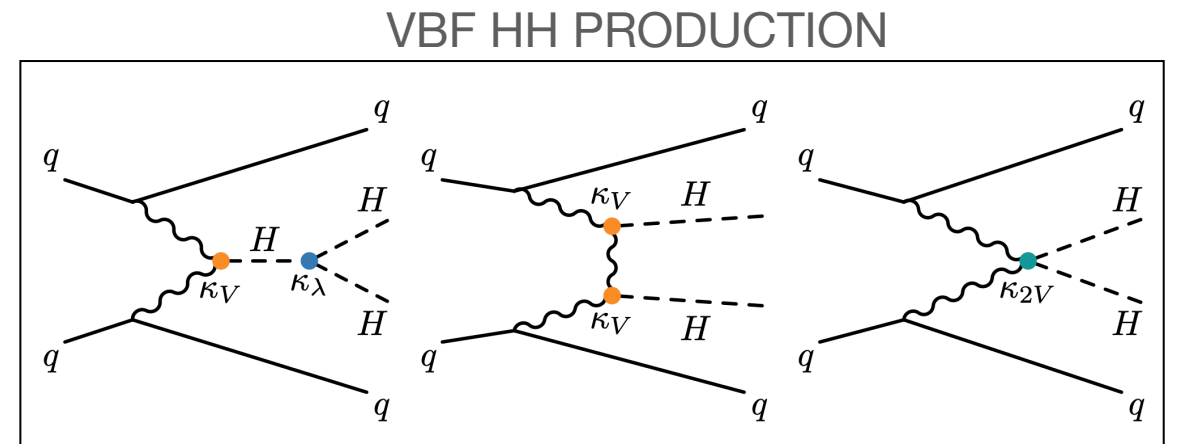
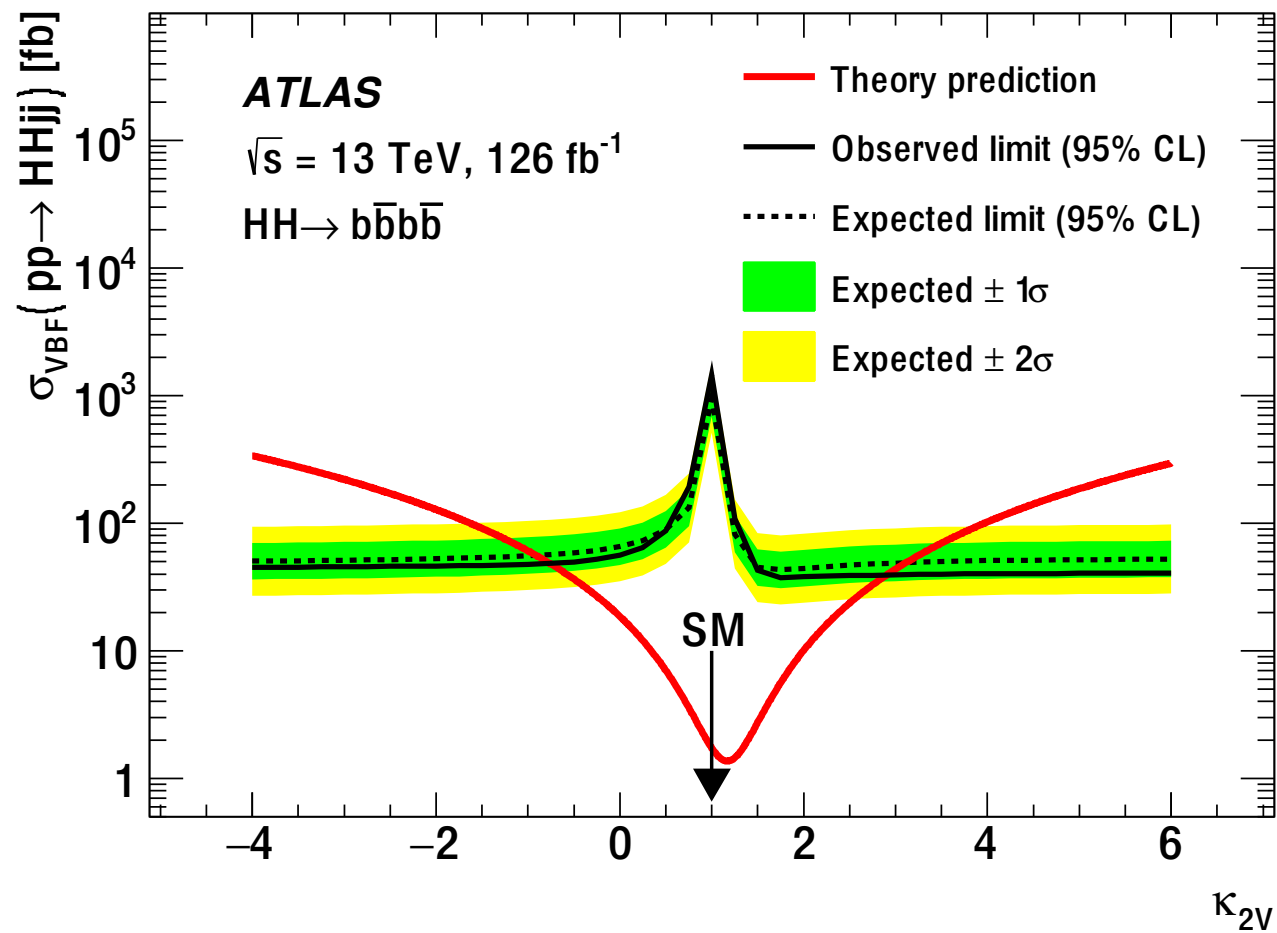


ATLAS measurement of κ_{2V} : limited

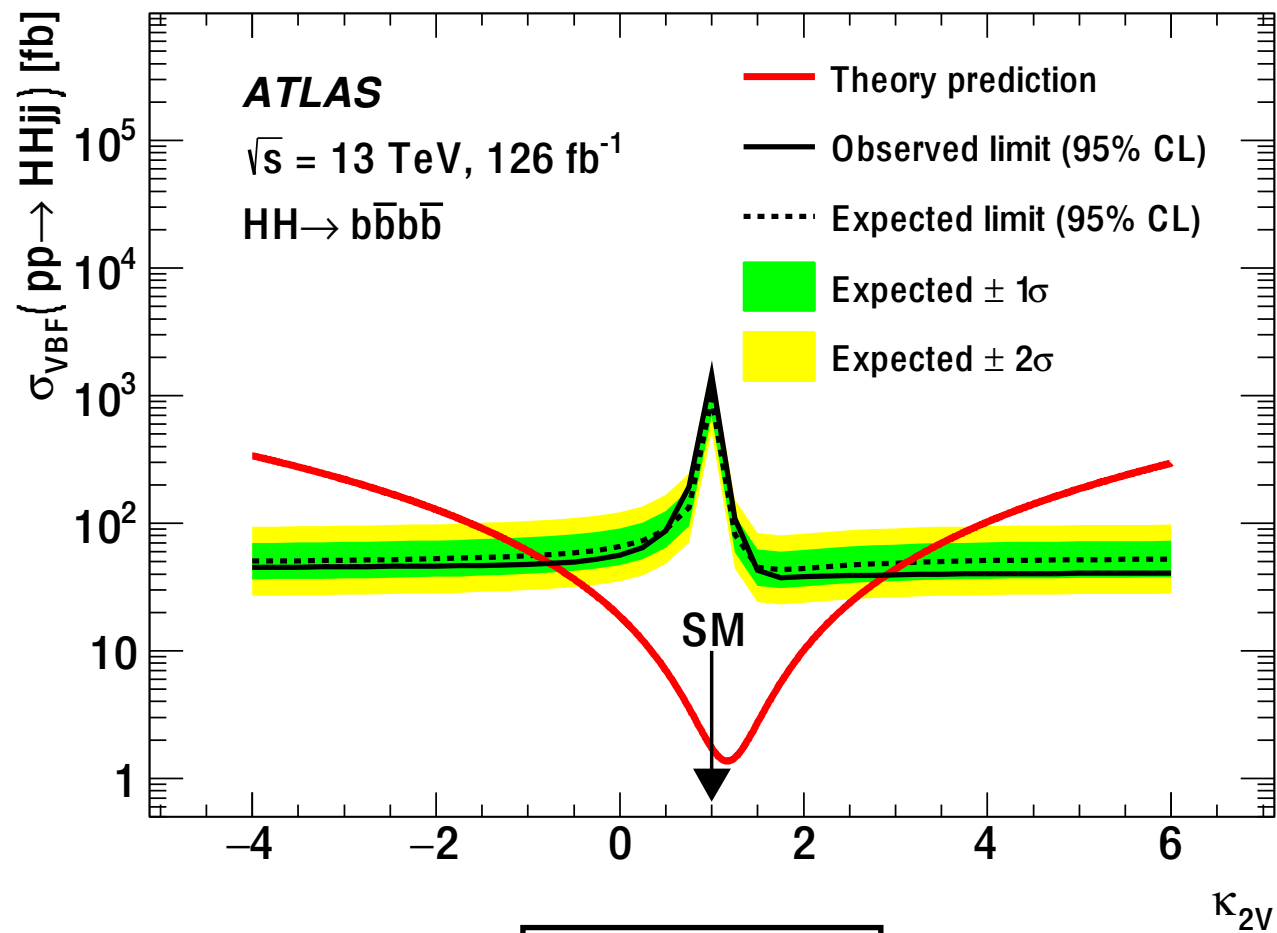
VBF HH PRODUCTION



ATLAS measurement of κ_{2V} : limited

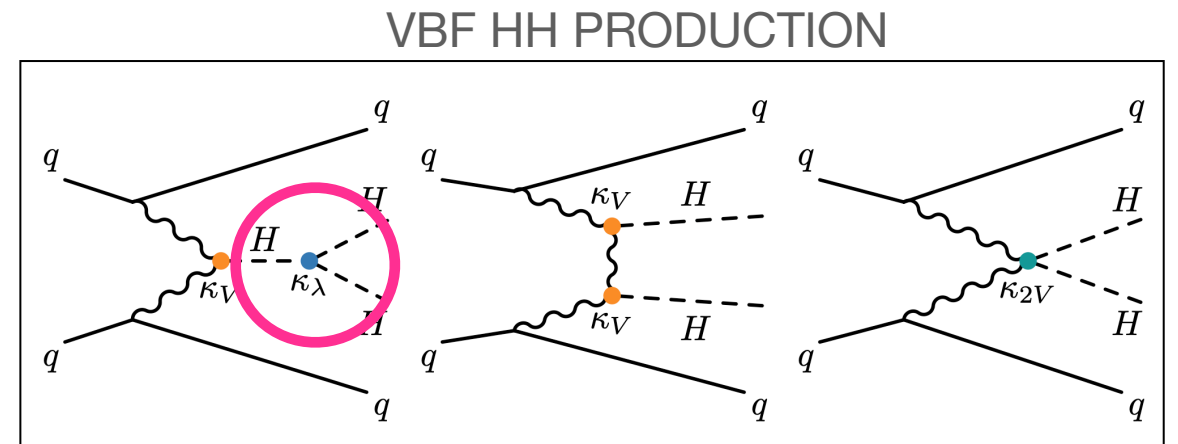


ATLAS measurement of κ_{2V} : limited

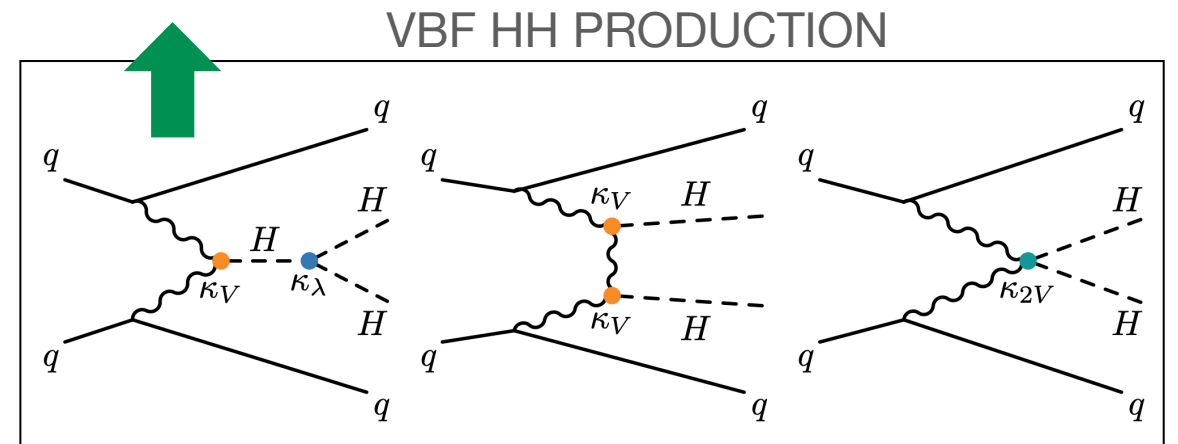
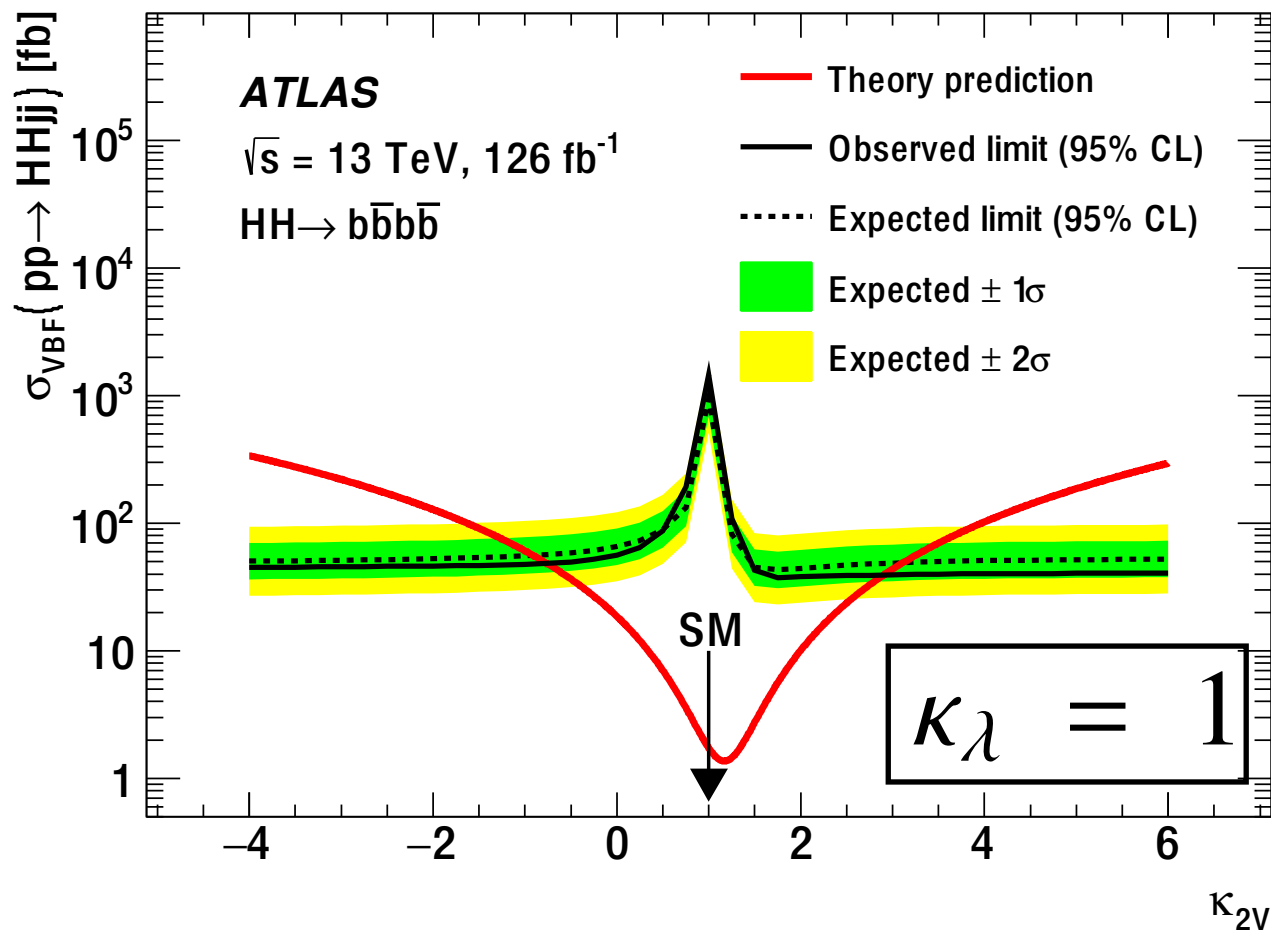


Assumption!

$$\kappa_{\lambda} = 1$$



ATLAS measurement of κ_{2V} : limited



IF $\kappa_\lambda \neq 1$

With large NLO

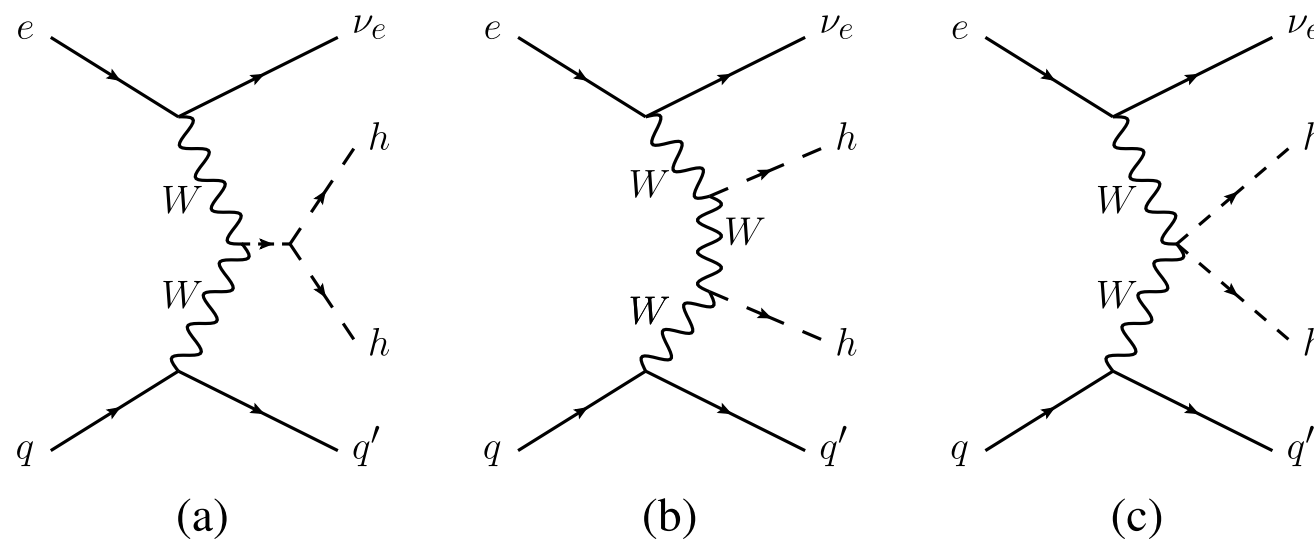
- Gluon fusion pollution becomes severe!

$gg \rightarrow HHjj$ ↑

electron-proton collider is better for κ_{2V}

- Gluon fusion pollution becomes severe!

$$gg \rightarrow HHjj$$



Consider

$$\begin{array}{l} \text{LHeC:} \quad E_e = 50 \text{ GeV}, \quad E_p = 7 \text{ TeV}, \\ \text{FCC-he:} \quad E_e = 60 \text{ GeV}, \quad E_p = 50 \text{ TeV}, \end{array}$$

Basic setup

Single Higgs couplings are SM-like.

$$\kappa_{Hij} = 1$$

Double and triple Higgs couplings are free.

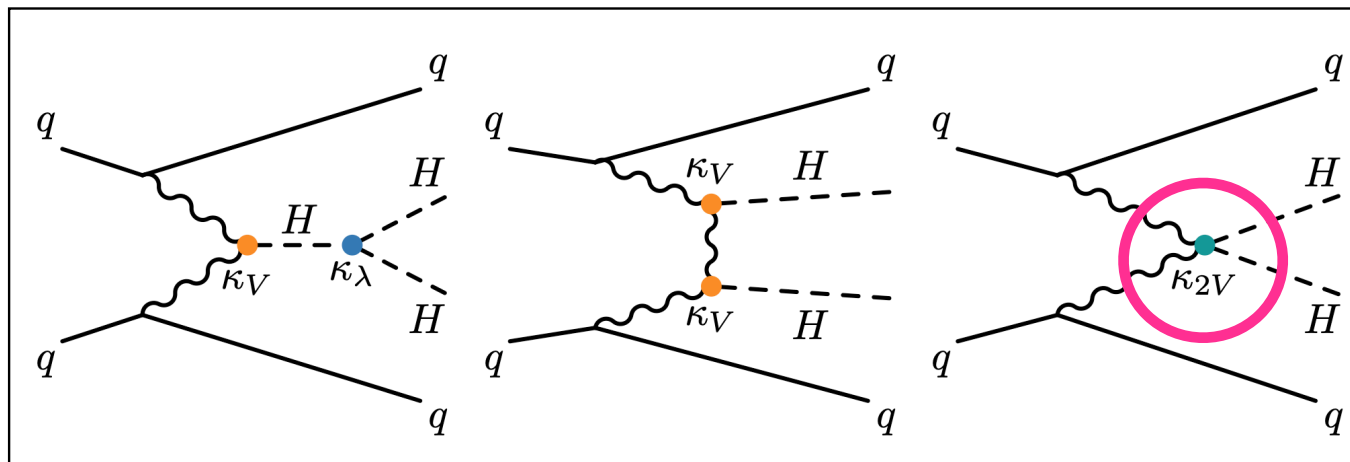
$$\mathcal{L} \supset \kappa_{2V} \frac{g^2}{4} W^{+\mu} W_{\mu}^{-} H^2 - \kappa_{\lambda} \frac{3m_H^2}{v} H^3$$

Conspiracy? Also suppressed in the SM

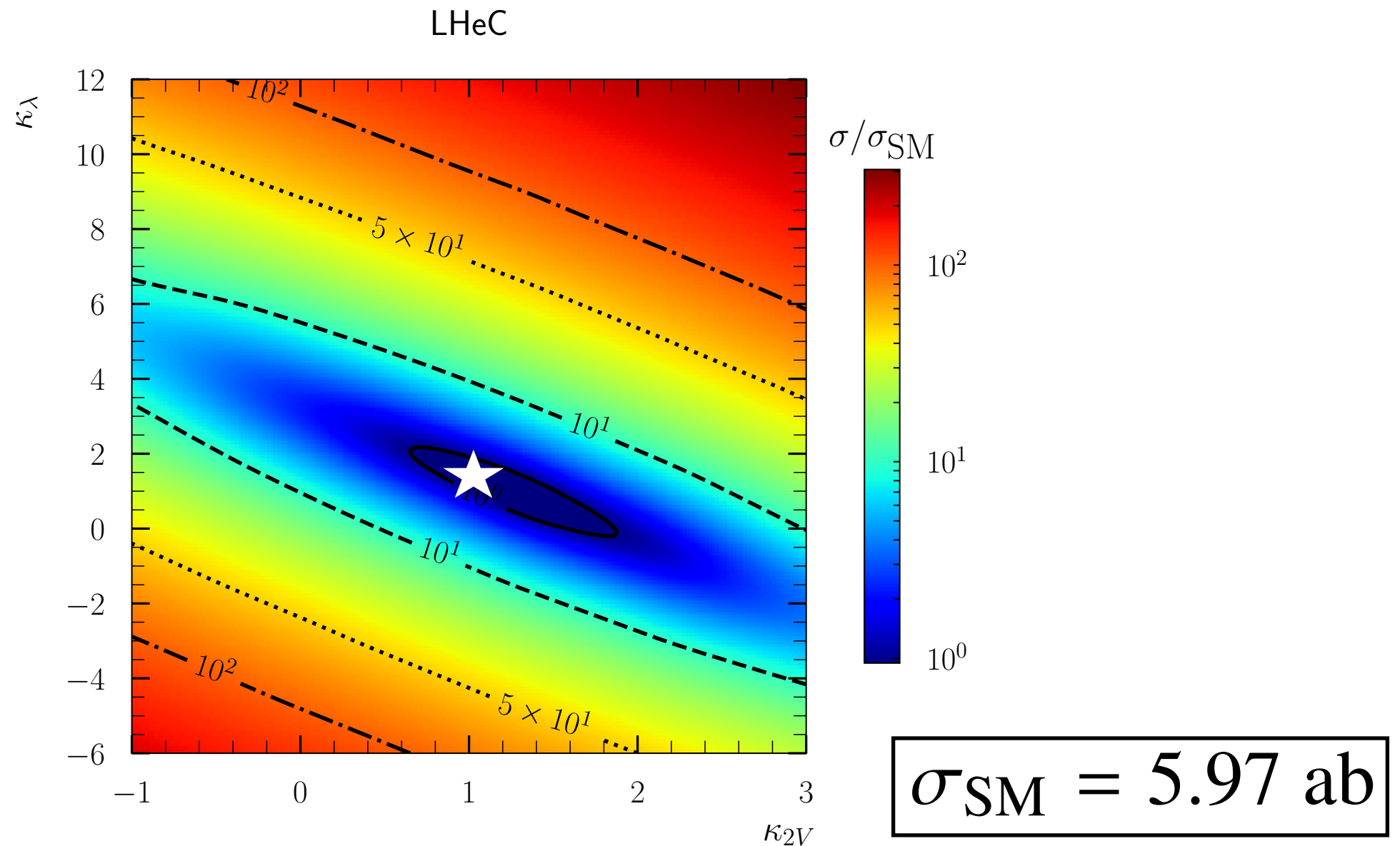
Zero in the SM

$$\frac{1}{g^2} \mathcal{M}(W_L^+ W_L^- \rightarrow HH) = \left(\kappa_{2V} - \kappa_V^2 \right) \frac{s}{4m_W^2} + \kappa_\lambda \frac{3m_H^2}{4m_W^2} + \kappa_V^2 \left[1 - \frac{m_H^2}{2m_W^2} - \frac{2}{\sin^2 \theta^*} \right] - \frac{\kappa_{2V}}{2} + \mathcal{O}\left(\frac{m_{W,H}^2}{s}\right),$$

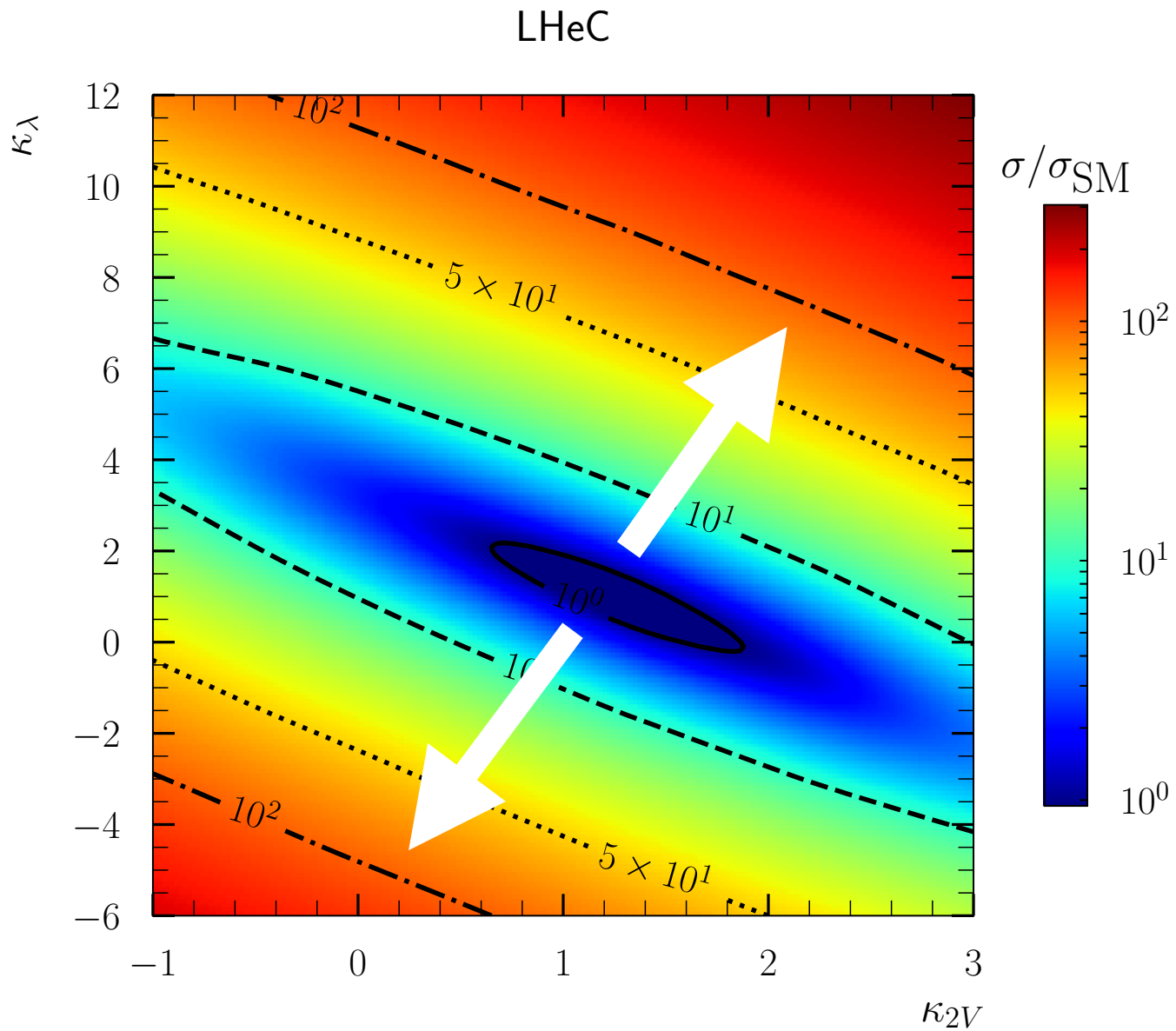
VBF HH PRODUCTION



Signal cross sections at the parton level



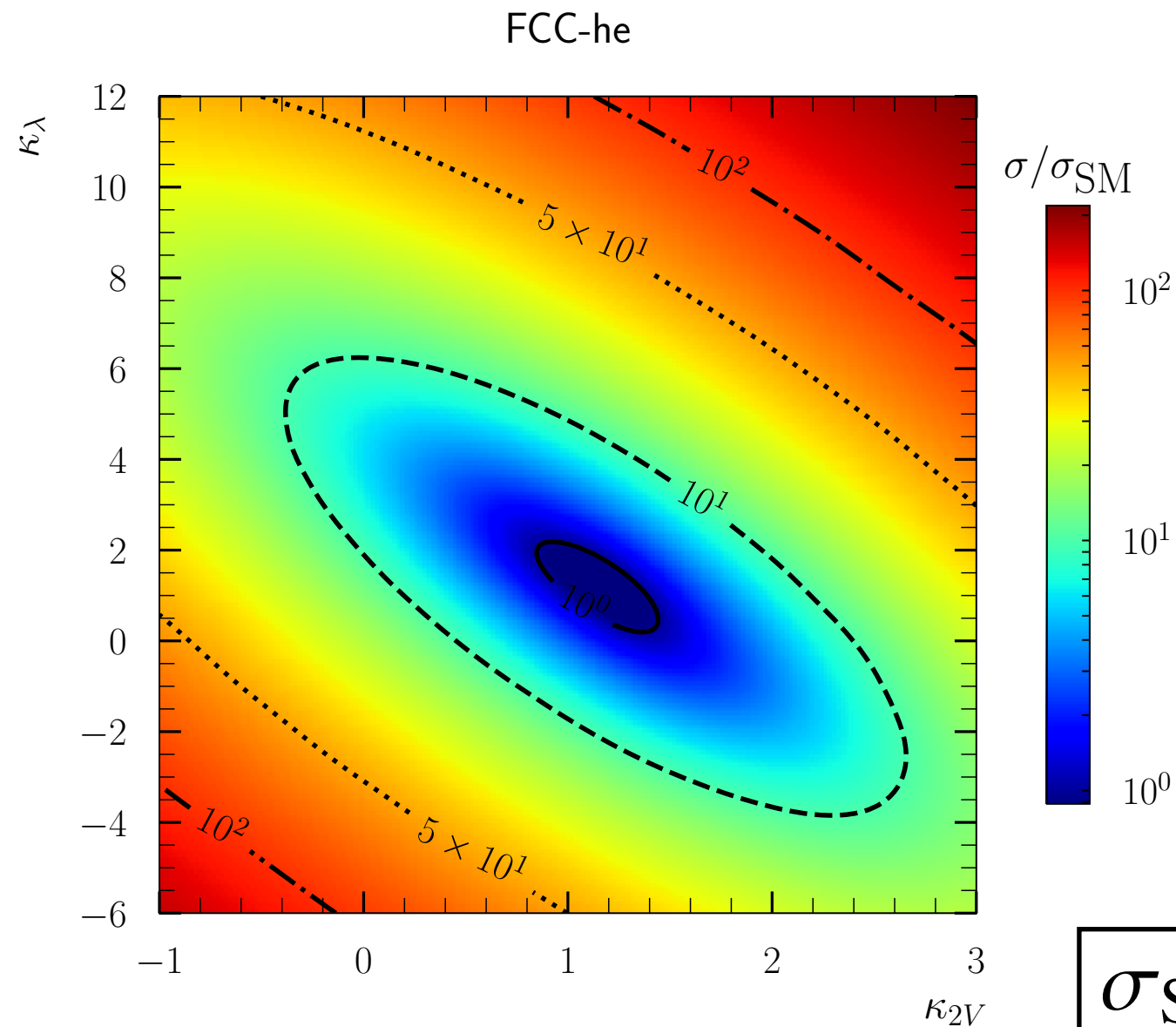
- SM (star mark): almost minimize the signal rate.
- Rapidly increasing with non-SM κ_λ and κ_{2V}



$$\mathcal{M} \sim \left(\kappa_{2V} - \kappa_V^2 \right) \frac{s}{4m_W^2} + \kappa_\lambda \frac{3m_H^2}{4m_W^2}$$

- Same-sign κ_λ and κ_{2V} enhance the cross section.

Signal cross sections at the parton level



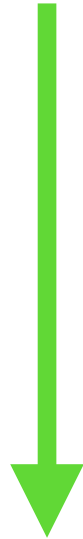
- FCC-ep is more sensitive to κ_{2V}

LO cross-sections for the backgrounds

Process	σ_{CC} [ab]	
	LHeC	FCC-he
$b\bar{b}jj + j_f\nu_e$	1.00×10^5 $^{+57.9\%}_{-33.9\%}$	7.18×10^5 $^{+51.7\%}_{-31.6\%}$
$ZZ + j_f\nu_e$	9.37×10^2 $^{+6.95\%}_{-5.45\%}$	2.24×10^4 $^{+3.65\%}_{-3.26\%}$
$Zb\bar{b} + j_f\nu_e$	5.38×10^2 $^{+27.5\%}_{-19.9\%}$	4.77×10^3 $^{+22.6\%}_{-17.1\%}$
$ZH + j_f\nu_e$	1.23×10^2 $^{+7.29\%}_{-6.27\%}$	3.45×10^3 $^{+3.99\%}_{-3.58\%}$
$b\bar{b}b\bar{b} + j_f\nu_e$	1.82×10^2 $^{+53.8\%}_{-32.4\%}$	7.11×10^2 $^{+50.9\%}_{-31.4\%}$
$Hb\bar{b} + j_f\nu_e$	4.53×10 $^{+28.4\%}_{-20.4\%}$	4.77×10^2 $^{+23.7\%}_{-17.8\%}$
$t\bar{t} + j_f\nu_e$	2.00×10 $^{+29.6\%}_{-21.2\%}$	7.49×10^2 $^{+22.9\%}_{-17.4\%}$

- Uncertainties are from the renormalization and factorization scale variation.

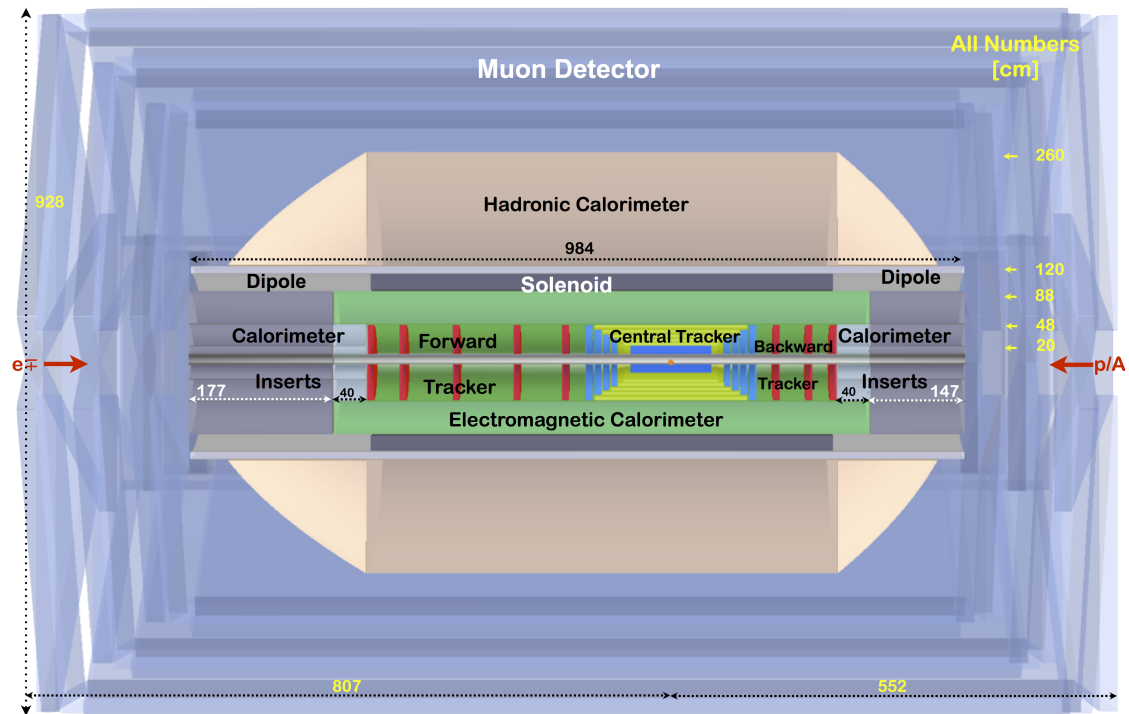
For 4b+(forward j)+nu



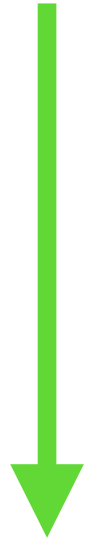
Initial
 4b-tag
 Forward jet
 Lepton veto
 $E_T^{\text{miss}} > 40 \text{ GeV}$
 Minimum D_{HH}
 $X_{HH} < 3.0$

Different forward jet definition

$$p_T^{j_f} > 20 \text{ GeV}, \quad 1.5 < \eta^{j_f} < 7$$



For 4b+(forward j)+nu



Initial
4b-tag

Forward jet

Lepton veto

$E_T^{\text{miss}} > 40 \text{ GeV}$

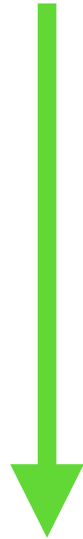
Minimum D_{HH}

$X_{HH} < 3.0$

$$D_{HH} = \sqrt{(M_{\text{dijet}}^{\text{lead}})^2 + (M_{\text{dijet}}^{\text{slead}})^2} \\ \times \left| \sin \left(\tan^{-1} \frac{M_{\text{dijet}}^{\text{slead}}}{M_{\text{dijet}}^{\text{lead}}} - \tan^{-1} \frac{116.5 \text{ GeV}}{123.7 \text{ GeV}} \right) \right|$$

To pick up HH

For 4b+(forward j)+nu



Initial

4b-tag

Forward jet

Lepton veto

$E_T^{\text{miss}} > 40 \text{ GeV}$

Minimum D_{HH}

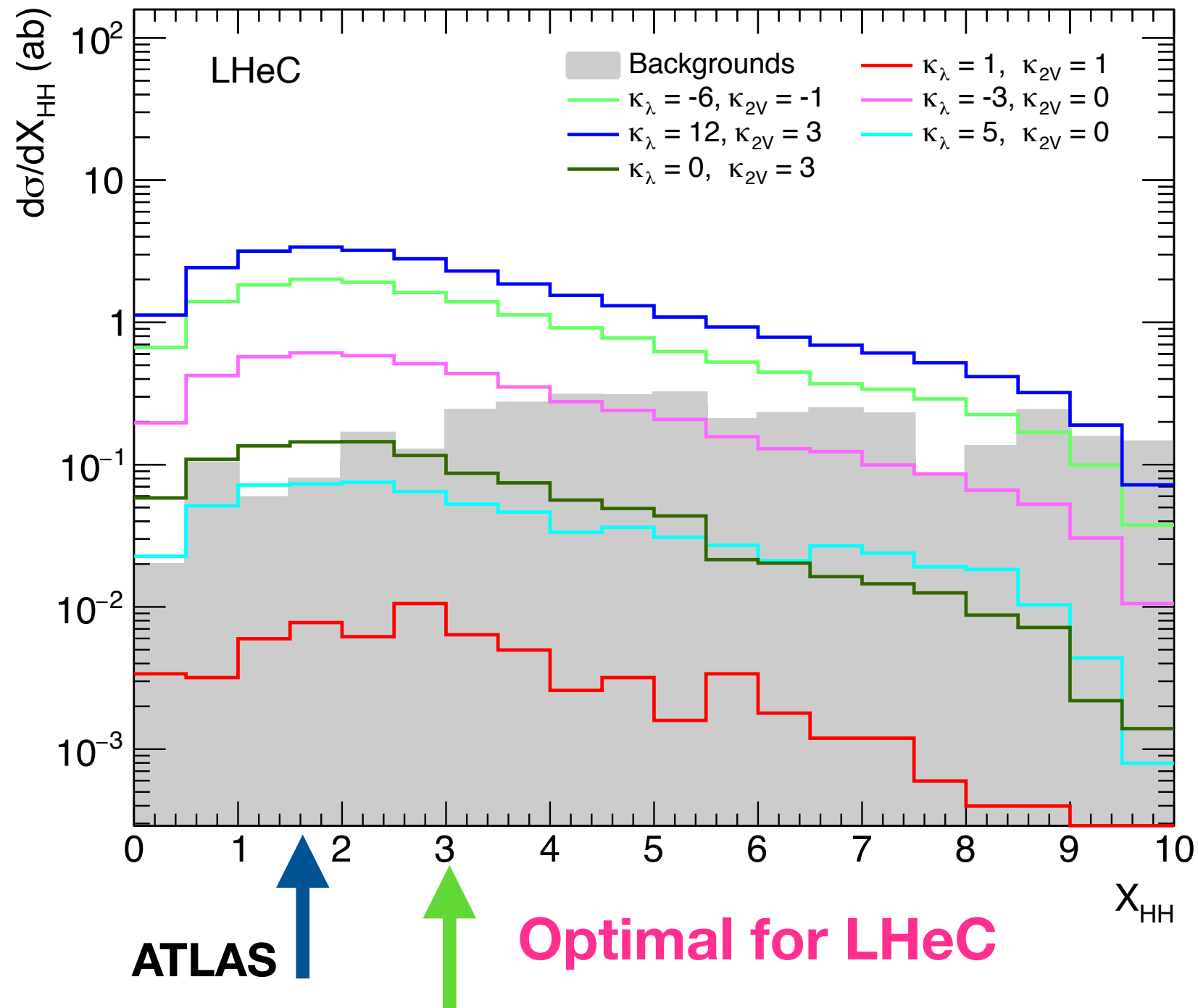
$X_{HH} < 3.0$

X_{HH}

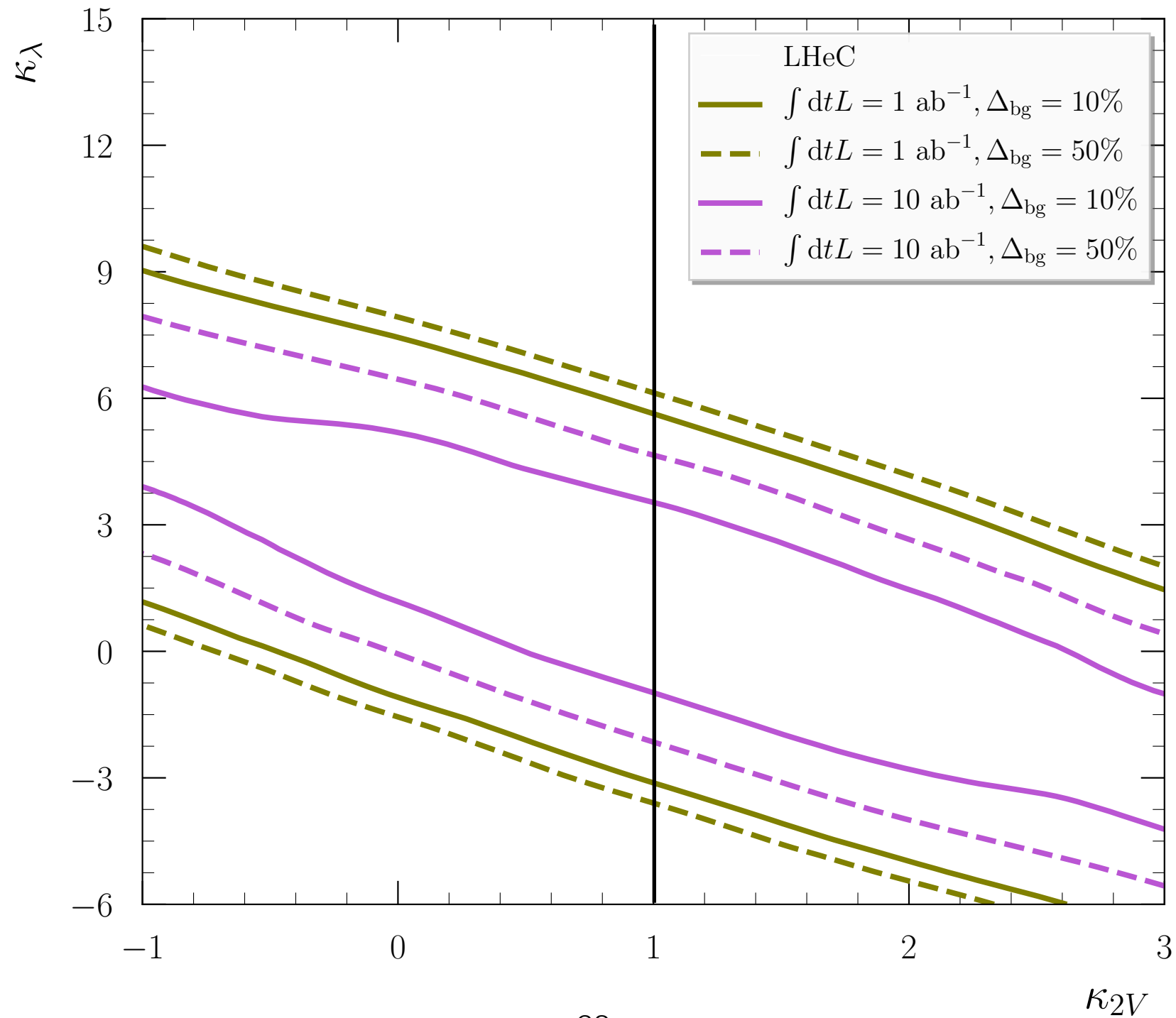
$$\equiv \sqrt{\left(\frac{M_{\text{dijet}}^{\text{lead}} - 123.7 \text{ GeV}}{11.6 \text{ GeV}}\right)^2 + \left(\frac{M_{\text{dijet}}^{\text{slead}} - 116.5 \text{ GeV}}{18.1 \text{ GeV}}\right)^2}$$

To guarantee bb from H

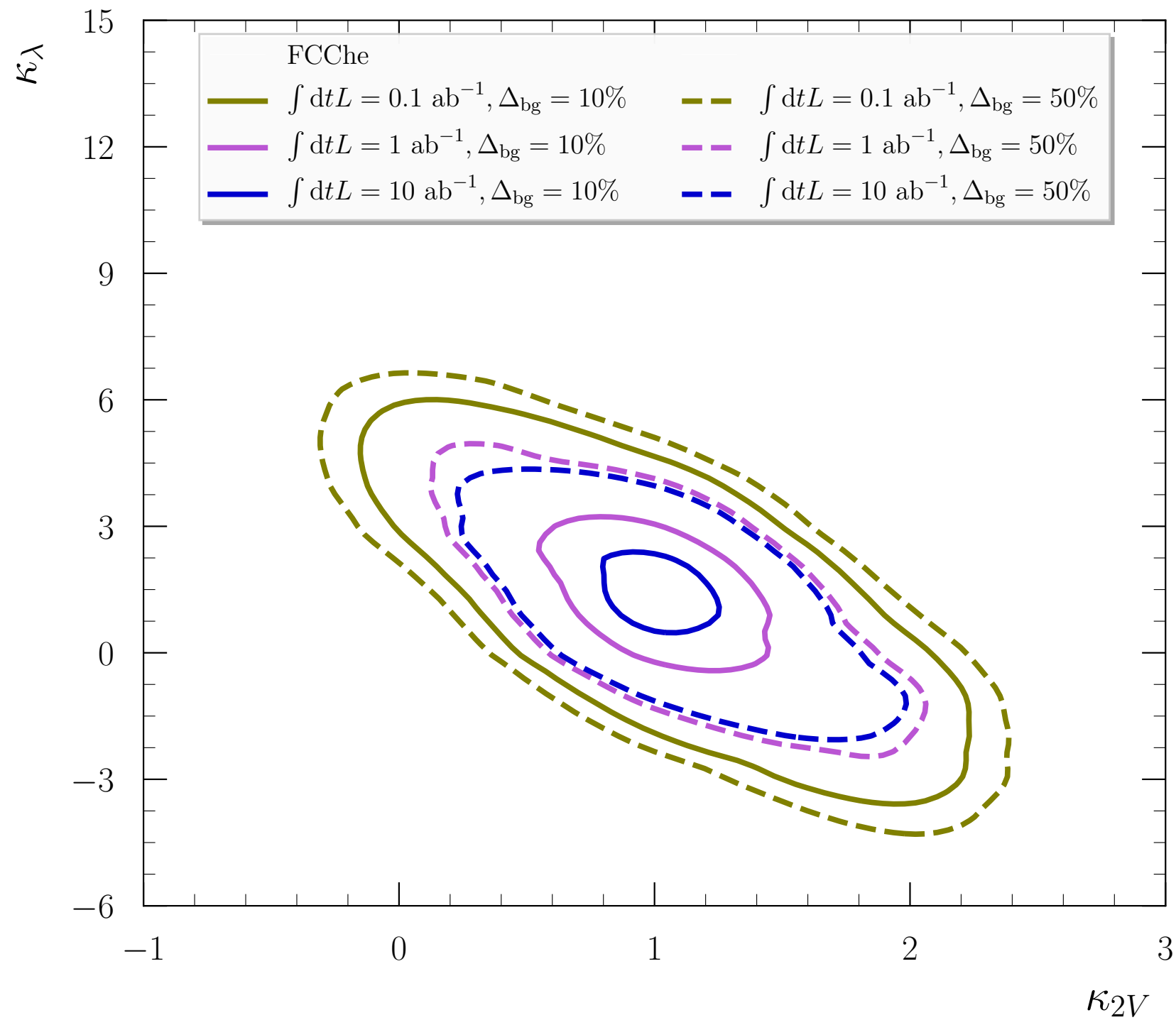
For 4b+(forward j)+nu



The expected exclusions at the LHeC



The expected exclusions at the FCC-he



Conclusions

- HHVV coupling is challenging to probe at the LHC, because of the unknown HHH coupling and the gluon fusion pollution.
- The future electron-proton colliders can be better to probe the HHVV vertex.
- Full detector simulations show that $|\kappa_{2V}| > 0.2$ can be excluded at the FCC-he.